Graz University of Technology

MASTER THESIS

Eva Maria Rechberger, BSc

Production of *mcl*-PHA by *Pseudomonas citronellolis*, *Pseudomonas chlororaphis* and *Pseudomonas putida* GPo1 on biodiesel from slaughterhouse waste

Project: ANIMPOL ("Biotechnological conversion of carbon containing wastes for eco-efficient production of high added value products"); 7th Framework Programme of the European Union

Submitted to
Institute of Biotechnology and Biochemical Engineering

Supervisors
Univ.-Prof. Dipl.-Ing. Dr. techn. Bernd Nidetzky
Dipl.-Ing. Dr. techn. Martin Koller

Graz, 4th December 2012

Deutsche Fassung:
Beschluss der Curricula-Kommission für Bachelor-, Master- und Diplomstudien vom 10.11.2008
Genehmigung des Senates am 1.12.2008

EIDESSTATTLICHE ERKLÄRUNG

Ich erkläre an Eides statt, dass ich die vorliegende Arbeit selbstständig verfasst, andere als die angegebenen Quellen/Hilfsmittel nicht benutzt, und die den benutzten Quellen wörtlich und inhaltlich entnommenen Stellen als solche kenntlich gemacht habe.

Graz, am …… ……..
(Unterschrift)

Englische Fassung:

STATUTORY DECLARATION

I declare that I have authored this thesis independently, that I have not used other than the declared sources / resources, and that I have explicitly marked all material which has been quoted either literally or by content from the used sources.

…… ……..
date (signature)

Danksagung

An dieser Stelle möchte ich mich bei Herrn Univ.-Prof. Dipl.-Ing. Dr. techn. Bernd Nidetzky bedanken, dass er mir die Möglichkeit gegeben hat meine Masterarbeit in der Arbeitsgruppe von Herrn Dipl.-Ing. Dr. techn. Martin Koller zu verfassen. Herrn Dr. Martin Koller und der ganzen Arbeitsgruppe danke ich für die tatkräftige Unterstützung, der stetigen Bereitschaft mir sämtliche Fragen zu beantworten und den vielen aufmunternden Worten.

Ein ganz besonderer Dank gebührt meinen Eltern, die mich nicht nur während meines Studiums immer unterschütz haben.

Index

Abbreviations

μ_{max}	maximum specific growth rate
CDM	Cell dry mass
FAME	Fatty acid methyl ester
FID	Flame ionization detector
GC	Gas chromatography
lcl-PHA	Long-chain-length polyhydroxyalkanoate
mcl-PHA	Medium-chain-length polyhydroxyalkanoate
OD_{420}	Optical density; λ=420nm
PHA	Polyhydroxyalkanoate
PHB	Polyhydroxybutyrate
$q_{Xr/P/CDM/C6-C12}$	specific production rate of biomass (X_r), product, cell dry mass (CDM), PHA composition (C6-C12)
$r_{Xr/P/CDM/C6-C12}$	volumetric production rate of biomass (X_r), product, cell dry mass (CDM), PHA composition (C6-C12)
scl-PHA	Short-chain-length polyhydroxyalkanoate
X_r	Biomass

Abstract

mcl-PHAs are polyhydroxyalkanoates with a monomer chain length of C6 to C14. They are produced by Pseudomonads of rRNA homology group I as intracellular storage material. *Pseudomonas citronellolis*, *Pseudomonas chlororaphis* and *Pseudomonas putida* GPo1 are able to accumulate PHA using biodiesel produced from slaughterhouse waste as sole carbon source. *Pseudomonas citronellolis* accumulated *mcl*-PHAs non growth associated during fermentation with 5 g/L and 10 g/L biodiesel. The main components in both fermentations were 3-hydroxyoctanoate with an average of about 38 % of total PHA and 3-hydroxydecanoate (average about 35 %). Additionally, 3-hydroxyhexanoate, 3-hydroxyheptanoate, 3-hydroxynonanoate and 3-hydroxydodecanoate were detected. The maximum specific growth rate was 0.08 h^{-1} during growth on 5 g/L biodiesel and 0.10 h^{-1} on 10 g/L biodiesel; the formation rate of PHA was 0.04 g/Lh and 0.05 g/Lh, respectively. *Pseudomonas chlororaphis* accumulated *mcl*-PHAs growth associated during cultivation on 5 g/L biodiesel with a maximum specific growth rate of 0.13 h^{-1} and a formation rate of PHA of 0.07 g/Lh. The main components were 3-hydroxyoctanoate (average about 44 % of total PHA) and 3-hydroxydecanoate (average about 25 % of total PHA); 3-hydroxyhexanoate, 3-hydroxyheptanoate, 3-hydroxynonanoate and 3-hydroxydodecanoate were also present. In comparison to these two strains, *Pseudomonas putida* GPo1 showed less PHA accumulation during growth on 5 g/L biodiesel as carbon source (μmax: 0.02 h^{-1}), whereby 3-hydroxynonanoate (average about 31 % of total PHA) and 3-hydroxydecanoate (average about 28 % of total PHA) were detected as the main components.

Zusammenfassung

mcl-PHAs sind Polyhydroxyalkanoate mit einer Kettenlänge der Monomereinheiten von C6 bis C14. Diese PHAs werden von Pseudomonaden der rRNA homology Gruppe I akkumuliert und fungieren dort als intrazelluläres Speichermaterial. *Pseudomonas citronellolis*, *Pseudomonas chlororaphis* and *Pseudomonas putida* GPo1 sind in der Lage, PHA auf Basis Biodiesel als Kohlenstoffquelle zu akkumulieren. Im Laufe zweier Fermentationen mit 5 g/L und 10 g/L Biodiesel akkumulierte *Pseudomonas citronellolis* PHA nicht wachstumsassoziiert. Die Hauptbestandteile des produzierten PHAs waren 3-Hydroxyoctanoat mit einem durchschnittlichen Anteil von 38 % am gesamten PHA und 3-Hydroxydecanoat (Anteil ca. 35 %). Zusätzlich wurden Anteile von 3-Hydroxyhexanoat, 3-Hydroxyheptanoat, 3-Hydroxynonanoat und 3-Hydroxydodecanoat detektiert. Die maximale spezifische Wachstumsrate betrug 0.08 h^{-1} bei 5 g/L Biodiesel als Kohlenstoffquelle und 0.10 h^{-1} bei 10 g/L Biodiesel. Die PHA-Bildungsraten betrugen 0.04 g/Lh bzw. 0.05 g/Lh. Im Gegensatz dazu produziert *Pseudomonas chlororaphis* bei der Fermentation mit 5 g/L Biodiesel *mcl*-PHAs wachstumsassoziiert. Die maximale spezifische Wachstumsrate betrug 0.13 h^{-1} und die Produktbildungsrate 0.07 g/Lh. Die Hauptbestandteile waren ebenfalls 3-Hydroxyoctanoat (Anteil ca. 44 % am gesamten PHA) und 3-Hydroxydecanoat (Anteil ca. 25 % am gesamten PHA), 3-Hydroxyhexanoat, 3-Hydroxyheptanoat, 3-Hydroxynonanoat und 3-Hydroxydodecanoat wurden ebenfalls nachgewiesen. Im Vergleich zu den anderen Teststämmen akkumulierte *Pseudomonas putida* GPo1 wenig PHA während der Fermentation mit 5 g/L Biodiesel (μ_{max}: 0.02 h^{-1}). Die Hauptbestandteile des produzierten PHAs waren 3-Hydroxynonanoat (Anteil ca. 31 % am gesamten PHA) und 3-Hhydroxydecanoat (Anteil ca. 28 % am gesamten PHA).

Part A: Introduction

After decades of using fossil resources, the motivation to use renewable resources has become stronger and stronger. Not only are fossil resources leading to a high CO_2 emission and the corresponding greenhouse effect, but also the restricted access and the imbalance of demand and discharging of fossil resources has an influence on political and economic aspects. (De Almeida & Silva, 2009; Endres & Sieberts-Raths, 2009) Further petrol based plastics, about 250 million tons annually (European Commission: Bio-Economy Press Release, 2012) lead to environmental pollution due to their non-biodegradability. All these facts lead to an increasing interest in ecologically and ethically sustainable products. In this context, biopolymers are well promising alternatives for petrol based plastics.

Biopolymers can be classified into (Endres & Sieberts-Raths, 2009)

- Non-biodegradable, based on renewable resources (e.g. gummi elasticum, cellulose acetate, bio-based poly(ethylene))
- Biodegradable, based on renewable resources (e.g. PHA, PLA)
- Biodegradable, based on fossil resources (e.g. Polycaprolactone)

In the year 2007 about 600 000 to 700 000 tons of biodegradable plastics were produced in Western Europe, which amounts to a market share of less than 1 % of the entire plastic market. Only 5 % of this niche market amounts to polyhydroxyalkanoates (PHAs) (Gahle *et al.*, 2008). Starch blends, with the main share of 40 %, are already established but not suitable for several applications. PHAs are promising materials due to their versatile properties from elastomers to thermoplastics.

Because of their promising future as alternative to fossil based plastics, also community institutions are interested in supporting further research work (European Commission: Bio-Economy Press Release, 2012).
This thesis was performed in the framework of the ANIMPOL Project. ANIMPOL is the acronym or "Biotechnological conversion of carbon containing wastes for eco-efficient production of high added value products", it is fundraised by the 7th Framework Programme of the European Union (start date: 2010/01/01; duration: 36 months).
The aim of the project is to use waste streams from slaughterhouses, the animal rendering industry and waste fractions of biodiesel manufactures to produce high value products.

Annually about 500 000 tons of animal lipids, contained by tallow, bones, etc., are discarded in Europe and 300 000 tons of waste are produced by biodiesel production. This waste streams are used for improved biodiesel production since only the unsaturated fatty acid methyl esters (FAME) of biodiesel can be used as fuel. The unused parts like saturated FAME and glycerol can be used for the production of PHA which is an important alternative to fossil based plastics. With the assumed 50 000 tons of saturated FAMEs, part of the biodiesel production waste, it is predicted that 35 000 tons of PHAs can be produced. (European commission, 2010) (European Commission: Research and Innovation, n.d. [online])

Due to recent public opinions that only edible resources are being used for the production of biopolymers like PHAs and also biofuel, it has to be stated again that only waste streams, in the case of ANIMPOL slaughterhouse wastes, are used for this process.

Part B: Theoretical background

1. Strain description

1.1. *Pseudomonas* spp.

In 1894 the genus *Pseudomonas* was proposed by Migula. Since then, this genus has undergone several reclassifications. Palleroni *et al.* (1973) divided them into five rRNA homology groups *via* rRNA-DNA hybridization. Whereby rRNA homology group I corresponds to fluorescent *Pseudomonas* strains like *Pseudomonas fluorescens*, but also to non-fluorescents strains like *Pseudomonas stuzeri*. (Palleroni, 2010; Palleroni *et al.*, 1973) Further *Pseudomonas* were arranged in α-, β- and γ-proteobacteria (Kersters *et al.*, 1996). The rRNA homogy group I can be divided in two lineage clusters: *Pseudomonas aeruginosa* and *Pseudomonas fluorescens*, *Pseudomonas citronellolis* belongs to the intrageneric cluster of *Pseudomonas aeruginosa*, whereby *Pseudomonas chlororaphis* and *Pseudomonas putida* belongs to the intrageneric cluster of *Pseudomonas fluorescens*. (Moore *et al.*, 1996)

Pseudomonas ssp. are aerobic, chemoorganotrophic, gram negative bacteria and occur rod-shaped. Further, they are non-sporulating and are motile with one or more polar flagella. They are non-fermentative and use the respiratory pathway with oxygen as terminal oxidant, some are able to use nitrate as final electron acceptor (Stanier *et al.*, 1966). Furthermore, they use the Entner-Doudoroff pathway instead of glycolysis for sugar catabolism (Fuhrer *et al.*, 2005). Because of their wide diversity several pathogenic species occurs. In general they have an important role in the natural carbon cycle, because of their ability to degrade several low molecular weight organic compounds (Kersters *et al.*, 1996).

1.2. Pseudomonas citronellolis

Pseudomonas citronellolis was discovered by Seubert (1960) during a study of degradation of isoprenoid compounds. The organism was collected from soil under pine trees in northern Virginia. It is described as a gram-negative rod with a single polar flagellum. It occurs mainly single, but sometimes in pairs. The optimal growth temperature is 31 °C. *Ps. citronellolis* also grows anaerobically but only in the presence of nitrate. (Seubert, 1960)

This morphology was confirmed by the picture visible in the microscope. Additionally, the shape changes to longer rods under stress conditions like a lack of carbon source or excess of metabolites. Also the strong motility under the microscope confirmes the flagellation.

1.2.1. Citronellol

Citronellol (Figure 1) consist of two isoprene units and is functionalised with a hydroxyl group. It can be classified as acyclic monoterpene. It occurs in several citrus plants. (Förster-Fromme & Jendrossek, 2010).

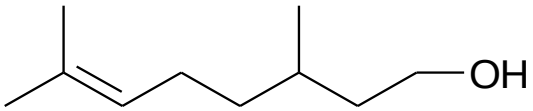

Figure 1. Chemical structure of citronellol.

Pseudomonas citronellolis is able to degrade citronellol and related compounds as sole carbon source. (Förster-Fromme & Jendrossek, 2010)

1.2.2. Biosurfactans

Further *Pseudomonas citronellolis* 222A, isolated from a petrochemical sludge land farming site, is able to grow on PAHs (polycyclic aromatic hydrocarbon) like anthracenes, phenanthrenes, pyrene, and on gasoline and diesel oil. To increase degradation, surfactants of low molecular mass are produced but no high mass surfactants like emulsifiers.(Jacques *et al.*, 2005)

These biosurfactans are a mixture of surface active substances. Microorganisms produce several substances like rhamolipids, lipopeptides, fatty acids, peptides and antibiotics. Pseudomonas spp. produces mainly rhamolipids, which vary with the carbon source. But a mass spectrometry analysis of surfactant produced by *Ps. citronellolis* showed that the surfactant is not identical to the one produced by *Ps. aeruginosa,* but there are indices that the surfactant is a dirhamolipid. (Déziel *et al.*, 1999; Jacques *et al.*, 2005, 2008)

1.3. Pseudomonas chlororaphis

Pseudomonas chlororaphis, formerly known as *Bacillus chlororaphis* (Tobie, 1945), was isolated 1894 by Gignard & Savegeou from worm carcase. Formations of a green crystal compound, chlororaphin, were proposed. Here, the proposed compound released by *Pseudomonas chlororaphis* was named xanthoraphin, a soluble yellow complex, which is reduced to chlororaphin. Chlororaphin can be further oxidised to oxychlororaphin (Kögl & Postowshy, 1930), as displayed in Figure 2. Whereas chlororaphin is a complex of reduced and oxidised phenanzine-1-carboxyamids (Kanner *et al.*, 1978), the proposed xanthoraphin seems to be only the reduced form.

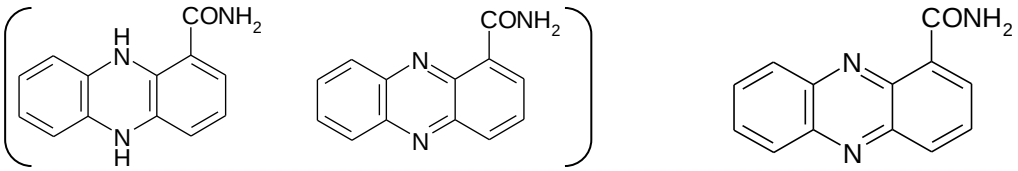

Chlororaphin Oxychlororaphin

(Complex of reduced and oxidised phenanzine-1-carboxyamids)

Figure 2. Chemical structure of chlororaphin and oxychlororaphin. (Kanner *et al.*, 1978)

The green insoluble chlororaphin can be produced by the subspecies *chlororaphis* (Figure 3) and *aurantiaca* (Peix *et al.*, 2007). Phenanzines are nitrogen-containing heterocyclic secondary metabolites, produced mainly by Pseudomonas and Streptomyces (Laursen & Nielsen, 2004; Mavrodi *et al.*, 2010). Phenanzines are acting as antibiotics, electron shuttle, influence growth in plants and can influence the cellular response. (Laursen & Nielsen, 2004; Mavrodi *et al.*, 2010; Pierson & Pierson, 2010).

Figure 3. *Ps. chlororaphis*, *Ps. citronellolis* and *Ps. putida* GPo1 on 3 g/L biodiesel after 25 days and continuous feeding (feeding every 3-4 days with 3 g/L). *Ps. chlororaphis* showed a slightly green culture broth.

Further investigations showed that *Pseudomonas chlororaphis* is not able to grow at 42 °C but at 5°C. In comparison to *Pseudomonas aeruginosa*, which possesses one flagellum, *Ps. chlororaphis* possess at least four flagella (Haynes & Rhodes, 1962). A publication by Timm & Steinbüchel (1990) proposed a formation of PHA with the major compound of 3-hydroxydecanoate during growth on gluconoate.

Pseudomonas chlororaphis can be divided into three subspecies: *Pseudomonas chlororaphis* subsp. *chlororaphis* DSM 50083, *Pseudomonas chlororaphis* subsp. *aurantiaca* NCIMB 10068 and *Pseudomonas chlororaphis* subsp. *aurefaciens* DSM 6698. (Peix *et al.*, 2007)

1.3.3. *Ps. putida* GPo1

Pseudomonas putida GPo1 ATCC 29347 formerly known as *Pseudmonas oleovorans* GPo1 (TF4-1L) was described by Baptist *et al.* (1963) as an Pseudomonad growing on pentane to dodecane (Schwartz, 1973). *Ps. putida* GPo1 is an improved strain to produce epoxides on 1-octene (Schwartz & McCoy, 1973; Schwartz & Mccoy, 1976; Schwartz, 1973).
Futhermore, DeSmet *et al.* (1983) proposed the formation of 3-hydroxyoctanoate during growth on octane. *Ps. putida* GPo1 is harbouring an OCT plasmid which contains alkane degradation genes in two gene clusters. The encoded enzymes, including an alkane hydroxylase, are responsible for the degradation of alkanes to acyl-CoAs, which are finally entering the ß-oxidation cycle. Several *Pseudomonas* strains contain an homologous chromosomal alkane hydroxylase (Van Beilen *et al.*, 1994, 2001; Smits *et al.*, 1999), whereby investigations with an OCT^- strain showed that the genes involved in PHA synthesis are located chromosomally (Huisman *et al.*, 1989).

Ps. putida GPo1 is not able to grow on gluconate, because of the lack of a transferase enzyme needed for the conversion of (R)-3-hydroxyacyl-ACP to (R)-3-hydroxyacyl-CoA derivatives, which is the precursor for the PHA synthases for structurally unrelated PHA substrates (Rehm *et al.*, 1998)

2. Polyhydroxyalkanoates

2.1. Definition

The monomers of polyhydroxyalkanoates are chiral aliphatic hydroxyl acids (Figure 4). The polymerisation to the polyester takes place *via* condensation. (Endres & Sieberts-Raths, 2009)
PHAs can be classified into three groups concerning their monomeric carbon numbers, short chain length PHA (*scl*-PHA) with C3 to C5, medium chain length PHA (*mcl*-PHA) with C6 to C14 and long chain length PHA (*lcl*-PHA) with carbon atoms more than 14. Additionally, the monomers can be saturated, unsaturated, straight, branched and aromatic. (Zinn *et al.*, 2001)

Further the hydroxyl group can be on the 3, 4, 5 or 6 position, or the backbone contains an unsaturated carbon bound (Steinbüchel & Valentin, 1995). Because of this high number of monomers, several co- or terpolymers are possible (Endres & Sieberts-Raths, 2009)

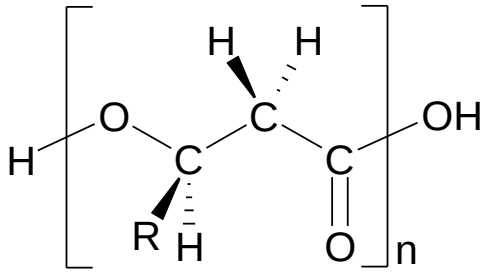

Figure 4. 3-hydroxy acid – building block for PHAs. R-unit contains C3 to C5 for *scl*-PHA and C6 to C14 for *mcl*-PHA. (Zinn *et al.*, 2001)

The first PHA was discovered by Lemoigne (1926), the isolated polyester was poly-3-hydroxybutyrate (PHB) discovered from *Bacillus megaterium* and is well investigated today. The next landmark was the identification of poly-ß-hydroxyoctanoate and poly-ß-hydroxyhexanoate which was accumulated by *Pseudomonas oleovorans* growing on n-octane (DeSmet *et al.*, 1983; Lageveen *et al.*, 1988). *lcl*-PHAs are part of the interest since *Pseudomonas aeruginosa* MTCC 7925 was found in the year 2008 to produce *scl-lcl*-PHAs (Singh & Mallick, 2008).

PHAs are carbon storage components in the cells which are built up during a lack of nutrient, for example nitrogen or phosphorous, and an excess of carbon. Under changed conditions with a lack of carbon the inclusion bodies are degraded as energy source. PHAs also can be degraded extracellular by other microorganisms as carbon source. (Khanna & Srivastava, 2005) Another reason for accumulating PHA is the detoxification of compounds in the environment of the organisms (Kranz *et al.*, 1997).

The PHAs are stored in granules, whose structure is different between *scl*- and *mcl*-PHA. *scl*-PHA granules have a lipid monolayer with protein on the outside, whereby *mcl*-PHA granules are lager and a phospholipid layer separates a two crystalline protein layers. The associated proteins are PHA synthase, PHA depolymerase and phasins. Phasins are important for the build-up and degradation of the granules and further for their quantity and size (Zinn *et al.*, 2001).

2.2. *mcl*-Polyhydroxyalkanoates

2.2.1. Synthesis

Fluorescent Pseudomonas of rRNA homology group I are not able to accumulate PHB (Huisman *et al.*, 1989), because they lack the enzymes which are needed for the conversion of acetyl-CoA to 3-hydroxybutyrate-CoA. Instead they are accumulating *mcl*-PHAs consisting of several different building blocks (Kessler & Palleroni, 2000). In general, PHA synthases are divided into 4 classes concerning there substrate specificity and subunits. *mcl*-PHA synthases belonging to class II have 2 subunits (*phaC1* and *phaC2*) and accept CoA thioesters of fatty acids with 6 to 14 carbon atoms as substrate (Rehm, 2003).

Huisman *et al.* (1991) already proposed two PHA synthases in *Pseudomonas oleovorans*, which are homologous to the PHB-synthase in *Ralstonia eutropha*. These two open reading frames are interrupted by a PHA depolymerase gene (*phaZ*). Investigations with *Pseudomonas corrugata* and *Pseudomonas stutzeri* showed that both PHA synthases (*phaC1*, *phaC2*) are expressed independently, their activities vary with the substrate and further influence the monomer composition.(Chen *et al.*, 2006; Conte *et al.*, 2006) During growth of *Pseudomonas corrugate* on oleic acid, only phaC1 was expressed, whereas during growth on glucose both synthases were expressed but at different rates (Conte *et al.*, 2006). The molecular masses of PHA are determined by the activity of the synthase. High activity results in low molecular mass PHAs and low activity in high molecular mass PHAs (Sudesh *et al.*, 2000). The activity can be controlled by the amount of the substrate, i.e. much substrate generally leads to high activity of PHA synthase. Furthermore, the molecular mass of PHAs can be influenced for example by the cultivation stage, the process conditions (pH-value, temperature) (Koller, 2001), the medium composition and downstream processing (Rai *et al.*, 2011).

The pathway for *mcl*-PHA formation depends on the carbon source. During growth on related substrates like for example n-alkane acids or n-alkanes, the formation takes place via the ß-oxidation pathway (Lageveen *et al.*, 1988). When non-related substrates, like glucose or gluconate, are used as carbon source, the formation takes place via fatty acid *de novo* synthesis. Further, a combination of both pathways was proposed for the case of cultivation on hexanoate (Huijberts *et al.*, 1994). The pathways are displayed in figure 5.

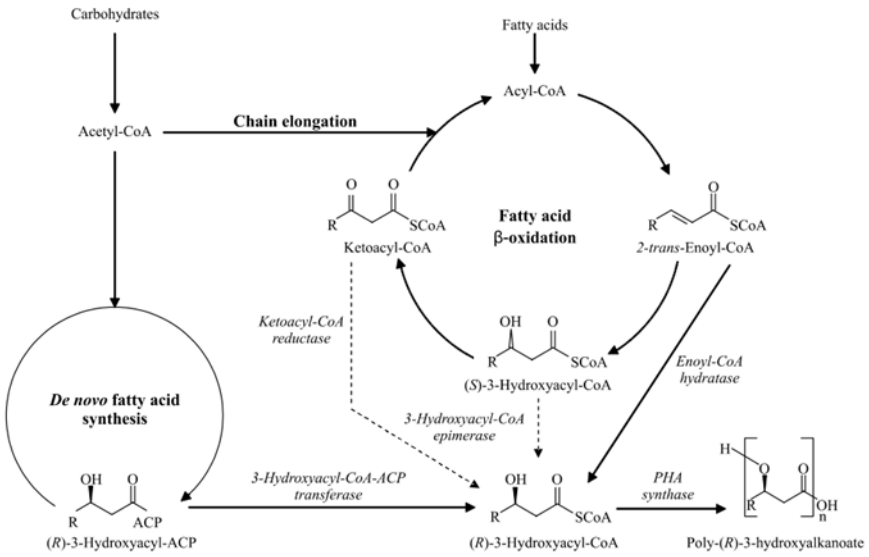

Figure 5. *mcl*-PHA synthesis pathways. (Kim *et al.*, 2007)

In case of this thesis, fatty acid methyl esters (FAMEs; biodiesel) were used as substrate. Thereby the methyl-group has to be hydrolysed by unspecific esterases *in vivo* before entering the PHA synthesis pathway. The released methane leads to toxic effects *in vivo*, and this is responsible for the strong inhibition effect of biodiesel as substrate.

2.2.2. Beta-Oxidation

By this pathway the building blocks are used directly from the substrate or *via* intermediates produced by ß-oxidation. The building blocks are related to the carbon source and the *mcl*-PHA production can be affected by it (Huisman *et al.*, 1989; Lageveen *et al.*, 1988).

ß-oxidation is the degradation pathway of fatty acids *via* cyclic elimination of C2 units. Several pathways are possible how the monomer units (R)-3-hydroxyacyl-CoA are derived from the ß-oxidation cycle. 2-trans-enoyl-CoA could act as precursor and is converted to the building block *via* the enzyme (R)-enoyl-CoA hydratase. Another precursor might be 3-ketoacyl-CoA which is reduced *via* 3-ketoacyl-CoA reductase to (R)-3-hydroxyacyl-CoA. The polymerisation enzyme PHA synthase is stereospecific and recognises only (R)-configurations. If 3-hydroxyacyl-CoA epimerase is present, (S)-3-hydroxyacyl-CoA can also act as precursor (Fiedler *et al.*, 2002; Rehm *et al.*, 1998).

2.2.3. *De novo* fatty acid pathway

This pathway is used if structurally non-related carbon source like glucose are provided as carbon source. The PHA formation takes place *via* the fatty acid *de novo* synthesis pathway.

The carbon source is degraded to acetyl-CoA, which is the starting compound of the fatty acid *de novo* synthesis pathway (Huijberts *et al.*, 1992, 1994). During this pathway C2 units are condensed to fatty acids by releasing of one molecule of free CoA per chain elongation step. Hoffmann *et al.* (2000) proposed a (R)-3-hydroxyacyl-CoA-ACP transacylase, which connects the de novo fatty acid cycle with the PHA synthesis.

2.2.4. Chain elongation

Another pathway was proposed during growth on hexanoate. Acetyl-CoA compounds can be condensed to 3-hydroxyacyl-CoA. (Rehm *et al.*, 1998) Furthermore, high activity of this pathway, characterized by a high intracellular pool of acetyl-CoA seems to terminate the breakdown of long fatty acids *via* the ß-oxidation pathway.

2.2.5. *mcl*-PHA Degradation

The degradation of PHA can take place intracellular to create an accessible carbon source during a lack of extracellular carbon source. In addition, PHA, which is released to the environment after cell death, is degraded by extracellular depolymerases as present at many different microbes. However, intracellular PHA-depolymerases are only able to degrade PHA *in vivo* and no exogenous PHAs. *Vice versa*, extracellular PHA-depolymerases are only able to degrade released PHA from death cells. The reason for this fact is the different morphology of PHA granules. Intracellular granules are amorphous and during release of PHA the granules become crystalline (Jendrossek *et al.*, 1996).

Intracellular PHB (Polyhydroxybutyrate) degradation has been part of several studies (Kobayashi *et al.*, 2003; Merrick & Doudoroff, 1964; Uchino *et al.*, 2007; York *et al.*, 2003). In contrast, *mcl*-PHA degradation is still under investigation. As already mentioned the *mcl*-PHA-depolymerase (*phaZ*) is flanked by two PHA synthases in *Pseudomonas putida* GPo1 (Huisman *et al.*, 1991). It was proposed that, firstly, PHA depolymerases are repressed by soluble carbon sources, and, secondly, that PHA-depolymerase is expressed constitutively and synthesis and depolymerisation of PHA works simultaneously, meaning that the intracellular degradation and build-up of PHA is a highly dynamic process (Kessler & Witholt, 2001). Investigating *Pseudomonas putida* KT2442, De Eugenio *et al.* (2007) showed that the PHA-depolymerase, encoded by *phaZ*, mechanistically acts like a serine hydrolase. During investigations with *Pseudomonas putida* GPo1 an acyl-CoA synthetase, attached to the PHA

granules, was identified, which activates the monomer units of the hydrolysed PHA for further utilisation (Ruth *et al.*, 2008) (Figure 6).

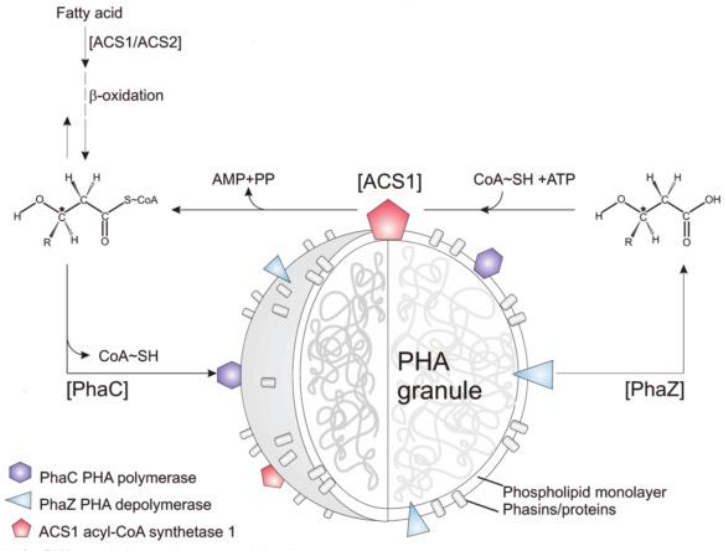

Figure 6. PHA degradation pathway investigated with *Pseudomonas putida* GPo1 (Ruth *et al.*, 2008)**.**

Exogenous PHA is hydrolysed by secreted PHA-depolymerases to oligo- or monomers and absorbed through the cell wall (Philip *et al.*, 2007). Most extracellular PHA degraders are degrading only *scl*-PHAs; because of the more common appearance of *scl*-PHA, these organisms are simply not adapted to utilize *mcl*-PHA as substrate (Mergaert and Swings, 1996; Jendrossek, 2001; Kim and Rhee, 2003). Only few bacteria, mainly *Pseudomonas* and *Stenotrophomonas*, are able to degrade *mcl*-PHA, while no fungi, well-known degraders of *scl*-PHA, are known to catabolize *mcl*-PHA (Kim *et al.*, 2007).

Kim *et al.* (2007) proposed that, due to horizontal gene transfer, all currently known extracellular *mcl*-PHA-depolymerases show similarities in their amino acids sequence, hence their primary structure, and furthermore in their catalytic activities.

2.2.6. *mcl*-PHA properties

PHAs have several properties similar to synthetic plastics. These properties vary with the monomer composition of the PHA. Although PHA inclusion bodies occur as amorphous granula *in vivo*, they crystallise immediately after isolation (Khanna & Srivastava, 2005). The degree of crystallinity, which is also varying with the monomer composition, determines the mechanical properties. Exceptions among *scl*-PHAs like poly-(4-hydroxybutyrate) [P(4HB)] are elastomers with a melting point of 60 °C and grass transition temperature at -51 °C; especially the high elongation to break (about 1000%) distinguished P(4HB) from classical

scl-PHAs. The thermoplastic poly-(3-hydroxybutyrate) (PHB) with the same monomer chain length but with a shorter backbone has a melting temperature of 170 - 180 °C and a glass transition temperature of around 1 °C (Martin & Williams, 2003). In comparison, *mcl*-PHAs are defined as elastomers or semi-crystalline material with low melting points (42-54 °C), low glass transition temperature (-25 to -40 °C) and low crystallinity (Gross *et al.*, 1989; Khanna & Srivastava, 2005; Koller *et al.*, 2010). Because of the longer monomer chains, *mcl*-PHAs are more suitable for post-synthetic modifications with functional groups, which also lead to varying and improved properties. (Hazer & Steinbüchel, 2007)

Because of the material properties, the production process without utilizing fossil resources and the biodegradability, PHA is relevant to many industrial fields. PHA is already applied as: package materials in the food industry, everyday products like disposable razors, parts of car armatures and paper coatings (Khanna & Srivastava, 2005). Because of the chiral nature of the building blocks and biocompatibility, PHA is an interesting material for medical applications like heart valves, vascular grafts, carrier of long-term drugs, etc. (Khanna & Srivastava, 2005; Martin & Williams, 2003). For these applications, the attention has to be directed on the purity of the PHA, because contaminations by endotoxins (lipopolysaccharides produced by gram-negative microbes) (Furrer *et al.*, 2007) can seriously harm humans.

3. Biodiesel

3.1. General

Biodiesel is composed of fatty acid methyl esters derived from vegetable oils, waste oils, non-edible oils or animal fats and oils.

The main feedstock for the biodiesel production is rapeseed oil with a share of about 85 %. Such oils are preferable for the production of biodiesel, because of high amount of unsaturated fatty acids (Mittelbach & Remschmidt, 2004). However, an alternative source for biodiesel production can be animal fats and oil. As already mentioned, about 500 000 tons of slaughterhouse waste are disposed of annually. Such a waste stream, which is not in competition with edible resources, has a high potential for application as a lipid-rich feed stock. Unfortunately, animal fats and oils contain a high amount of saturated FAMEs (Mittelbach & Remschmidt, 2004).

Due to their linear chemical structure, unsaturated fatty acids have better cold-temperature behaviour and are less clogging than saturated fatty acids and are therefore better suitable for fuel usage. For example rapeseed oil has a cloud point temperature (point where the first crystals are visible) of -2 °C and tallow of 14 °C. Hence, at the one hand, a high amount of saturated fatty acids causes disadvantages in respect of their high crystallisation temperature. But, on the other hand, long-chain saturated fatty acids decrease the flash point and increase the cetane number (Mittelbach & Remschmidt, 2004).

3.2. Transesterification

Biodiesel is produced *via* transesterification. During this process, also known as alcoholysis, triglyceride reacts with alcohol in a molar ration of 1:3. During a three step hydrolysis (tri-, di- and monoglyderide), glycerol and three fatty acid alkyl esters are formed (Figure 7). Methanol is the preferable alcohol reactant, because both occurring phases (biodiesel, glycerol phase) are easily separated with lower alcohols (Ma & Hanna, 1999; Mittelbach & Remschmidt, 2004).

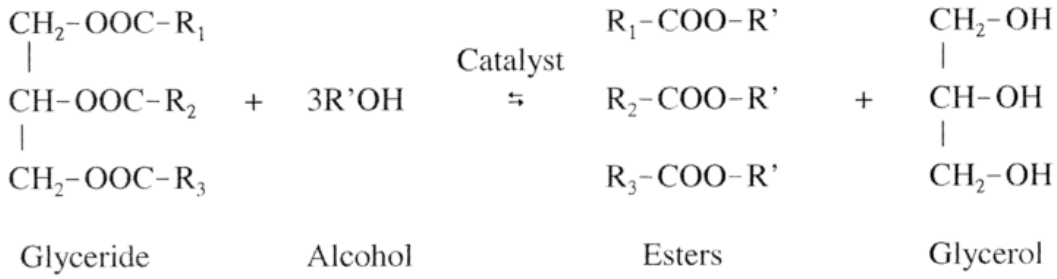

Figure 7. Mechanism of the transesterification (Ma & Hanna, 1999)**.**

Both phases have to be purified for further use. Especially the ester phase contains undesirable by-products like free fatty acids. To remove these acids, a distillation is done (Mittelbach & Remschmidt, 2004).

The by-product glycerol is used for cosmetic industry and several other industrial sectors. Glycerol also can be used for energy generation and as carbon source for PHA production. The biodiesel with lower quality, saturated FAMES as already mentioned, is also used as carbon source and not as fuel.

Part C: Experimental part

4. Material and methods

4.1. Strains

The three following Pseudomonas strains, belonging to the RNA-homology group I, were used for the experimental part.

Pseudomonas putida GPo1 ATCC 29347 obtained from Prof. Manfred Zinn, Institute of Life Technologies, University of Applied Sciences Western Switzerland

Pseudomonas citronellolis DSM 50332 obtained from DSMZ – German Collection of Microorganisms and Cell cultures

Pseudomonas chlororaphis DSM 50083 obtained from strain collection of University of Technology Graz.

4.2. Cultivation

The strains were maintained in DSMZ liquid media and on DSMZ agar plates (Table 3). Furthermore, they were adapted to biodiesel as carbon source. This was done by inoculation from liquid complete media to adapted Kueng mineral media (Kueng Walter, 1982; Marsalek Lukas, 2011) containing 1 g/L biodiesel. After adaption, the concentration was increased to 3 g/L and further to 5 and 7.5 g/L biodiesel for *Ps. citronellolis* and *Ps. chlororaphis*. *Ps. putida* GPo1 was kept at 5 g/L.

The adapted Kueng medium differs from the original Kueng medium (Kueng Walter, 1982) due to a higher concentration of phosphate buffer. The media consists of four sterilisation groups as shown in Table 1, whereby group III also contains trace elements (Table 2). The pH-value was adjusted to 7.0. The four fractions of the medium were prepared separately and united after steam autoclaving (20 min, 121°C).

For all experiments the adapted Kueng medium was used. The cultivation took place at 30 °C for all experiments.

Double distilled biodiesel from slaughterhouse waste, provided by Univ.-Prof. Martin Mittelbach, Institute of Chemistry, Karl-Franzens-University Graz, was used as carbon source for cultivation in all experiments, only the concentration of biodiesel varied between the different experimental set-ups. Grindsted CITREM SP 70 was determined as the favourable emulsifier after shaking flask experiment 5.1.

Table 1. Kueng-Media			
I)	Na_2HPO_4	7,17	g/L
	KH_2PO_4	3	g/L
	Agar, if necessary		
II)	$(NH_4)_2SO_4$	1	g/L
	$MgSO_4.7H_2O$	0,2	g/L
III)	$CaCl_2.2H_2O$	0,02	g/L
	$NH_4Fe(III)Citrate$	0,05	g/L
	SL6 [mL]	1	mL
IV)	Biofuel + Grindsted CITREM SP 70		

Table 2. SL6 composition		
$ZnSO_4.7H2O$	100	mg/L
H_3BO_3	300	mg/L
$CoCl_2.6H_2O$	200	mg/L
$CuSO_4$	6	mg/L
$NiCl_2.6H2O$	20	mg/L
$Na_2MoO_4.2H_2O$	30	mg/L
$MnCl_2.2H_2O$	25	mg/L

Table 3. DSMZ-Complete Media		
Peptone	5	g/L
Meat extract	3	g/L
Agar, if necessary	15	g/L

4.3. Optical density

Bacterial growth was monitored *via* optical density at 420 nm (OD_{420nm}) with Genesys 10S UV-VIS Spectrophotometer (*Thermo Scientific*) and deionized water as zero reference.

4.4. Determination of cell dry mass

For determination of the cell dry mass (CDM), 5 mL fermentation broth were put into pre-weight glass tubes (16x100, *Wheaton*) twice. These tubes were centrifuged at 4 000 rpm for 10 min (Megafuge 1.0R, *Heraeus Sepatech*). The supernatants were united and used for ammonium determination. In case of remaining biodiesel or emulsifier the biomass pellets were washed with 5 mL H_2O:EtOH (1:1) solution, vortexed and centrifuged. The remaining pellets were frozen and lyophilised (Christ Alpha 1-4, B. *Braun Biotech International*). Afterwards the full tubes were weighted again and the difference to the empty tubes amounts to the CDM in a 5 mL sample.

4.5. Determination of Ammonium

4.5.7. Ammonium fast test

During the fermentation the ammonium concentration was determined using a visual semi quantitative test (*Co. Merck*, Merckoquant, 1.10024.0001). With Neßler's reagent, the ammonium ions form a yellow-brown compound. By comparison of the resulting compound of the test strip with a colour scale, the approximate concentration of ammonium can be determined.

After the centrifugation of the tubes for CDM and PHA determination (see 1.4), 1 mL of the supernatant was mixed with 2 drops of reagent NH_4-1. A test stripe was immersed into the sample for 3 sec. After 10 sec the reaction zone of the test stripe was compared with the colour scale.

4.5.8. Ammonium accurate test

A more accurate test (*Co. Merck*, Spectroquant, 1.00683.0001) is needed in order to get exact data for the kinetic analysis. The principle of this test is the reaction of ammonia with hypochlorite ions to monochloramine, which subsequently reacts with substituted phenol to form a blue indophenol derivative. This complex can be determined photometrically at λ=690 nm. The measuring range of the test for ammonium is 6 – 193 mg/L. Ammonium sulphate was used as reference.

First, 0.1 mL of filtrated supernatant (deionized water as zero reference) was added to 5 mL of NH_4-1 reagent and incubated for 15 min. Second, 1 level blue microspoon NH_4-2 was added and the solution was mixed until the reagent was dissolved. The solution was measured in a 10-mm cell at 690 nm.

4.6. Bioreactor equipment

For the fermentations Labfors 3 (*Infors*, CH) reactors were used with total volumes of 7.5 litres and 5 litres. The reactor with a total volume of 7.5 litres (Figure 8), were equipped with a two impeller stirrer, a Hamilton Visiferm DO 425 optical pO_2 electrode and a Hamilton Easyferm Plus K8 425 pH electrode.

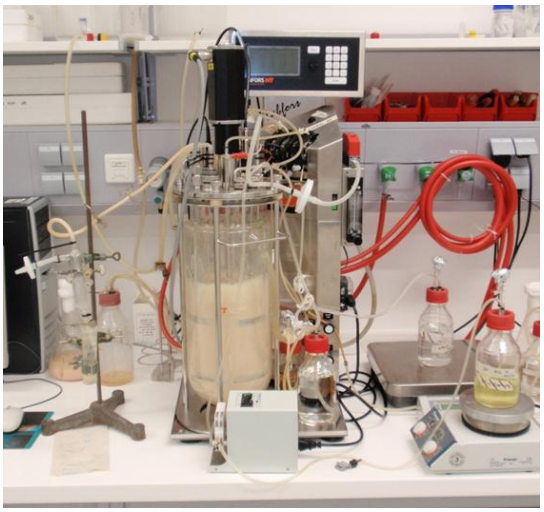

Figure 8. Labfors 3 (Infors, CH) with a total volume of 7.5 litres during fermentation with *Pseudomonas citronellolis* on biofuel.

One impeller was used as stirrer in both small reactors with a total volume of 5 litres (Figure 9). Furthermore, both reactor sizes were equipped with Hamilton Oxyferm VP 225 amperometric pO_2 electrodes and Hamilton Easyferm Plus K8 200 pH electrodes.

Figure 9. Labors 3 (Infors, CH) with a total volume of 5 litres during fermentation with *Psuedomonas putida* GPo1 on biofuel.

4.7. PHA-Analysis

4.7.1. Pretreatment for GC

It is not possible to analyse a polymeric material directly *via* gas chromatography (GC). Intracellular PHA has to be transesterificated to create volatile methyl esters. This happens *via* the well-known method of acidic methanolysis (Braunegg *et al.*, 1978).

$$Polyester + Methanol \xrightarrow{Sulfuric\ acid} Methylester + H_2O$$

For the transesterification 2 mL transesterification solution were transferred into the tubes containing the lyophilised biomass as obtained according to 1.4. Afterwards 2 mL of chloroform were added in order to bring the intracellular PHA in solution.

The transesterification solution was composed of methanol 91.15 % (v/v), sulfuric acid 4.75 % (v/v) and hexanoic acid 0.10 % (v/v), which was used as internal standard for gas chromatography.

After addition of the chloroform, the tubes were tightly closed to avoid evaporation. The tubes were shaken continuously in a water bath (GFL 1083) at 95 °C for 1.5 hours. Afterwards the tubes were vortexed to dissolve the pellets. Subsequently, they were put again into the water bath for 1.5 hours.

After the hot water bath, the tubes were cooled at 4 °C for at least 30 min before further use to avoid evaporation.

After the transesterification 1 mL of cooled 10 % $NaHCO_3$ was added and the tubes were vigorously vortexed in order to achieve an excellent distribution of the dissolved components between the organic and the aqueous phase. Subsequently, the tubes were centrifuged at 4 000 rpm for 5 min (Megafuge 1.0R, *Heraeus Sepatech*) to separate the organic and aqueous phase. The lower organic phase, which contains the major part of the methyl esters of the PHA building blocks, was transferred into gas chromatographic vials.

4.7.2. GC

The gas chromatographic analysis was performed with 6850 Network GC System, *Agilent Technologies*, equipped with a 25m x 0.32mm x 0.52µm HP5 capillary column and a flame ionization detector (FID). Furthermore, Helium (*Linde*; purity = 4.6) was used as mobile phase with a flow rate of 1.3 mL/min and split ratio of 1:5. Hydrogen (*Linde*; purity = 5.0) and synthetic air (*Linde*; purity = "free of hydrocarbons") were used as detector gases and

nitrogen (*Linde*; purity = 5.0) as auxiliary gas. The injection volume was 2 µl. The temperature program for the *mcl*-PHA determination is shown in Table 4.

Table 4. Temperature program for *mcl*-PHA determination

Initial temperature: 50 °C		
Rate 1: 15 °C/min	Rate 2: 15 °C/min	-
Final temperature 1: 200 °	Final Temperature 2: 240 °C	Final temperature 3: 300 °C
Final time 1: 10 min	Final time 2: 4 min	Final time 3: 5 min

The references for the *mcl*-PHA determination *via* gas chromatography are listed in Table 5.

Table 5. References for GC

Company	Composition	Percentage	
Metabolix	C6	11.9	%
	C8	54.4	%
	C10	28.3	%
	C12	5.4	%
Polyferm	C7	30	%
	C9	70	%

4.8. Kinetic analysis and fermentation parameters

4.8.1. Mass balances

A bioreactor system can be closed or open, with several intermediate stages. A closed system does not allow entering mass through the system boundaries, for example batching process. An open system, for example a continuous process, allows mass to flow in and out. A Fed-batch process is a semi-closed system, which allows input of matter but not output.

It is not possible to operate a closed process under steady state conditions, because a steady state implies that any variable will be unchanged at any time, provided that temperature, pressure, volume etc. do not vary with time.

During a fed-batch process mass will increase or decrease with time and also during a batch process changes occur within the system, which leads to changed variables. Such a process is called unsteady-state. Nevertheless, steady state assumptions are important for analysis (Doran, 2012).

General mass balance equation for a process:

Mass in through system boundaries	-	Mass out through system boundaries	+	Mass generated within system	-	Mass consumed within system	=	Mass accumulated within system

$$\frac{dM}{dt} = \widehat{M}_i - \widehat{M}_o + R_G - R_c \quad \textbf{(1)}$$

dM/dt is the rate of change of mass with time, $\widehat{M}_i$ is the mass flow rate in, $\widehat{M}_o$ is the mass flow rate out and R_G is the mass generated and R_c is the mass consumed. During steaty state dM/dt must be zero.

For application of mass balance, the volume balance is required where F conforms to the flow rate:

$$\frac{dV}{dt} = \sum_i F_i = \sum_m F_{m,in} - \sum_n F_{n,out} \quad \textbf{(2)}$$

With the assumption that M is equal to the flow rate F multiplied by the concentration C, the general mass balance can be written as followed:

$$\frac{d(c * V)}{dt} = Flow_{in} \times Conc._{in} - Flow_{out} \times Conc._{out} \pm r_c \times V \quad \textbf{(3)}$$

The term "$r_c \times V$" corresponds to the kinetic term.

For a fed-batch process the following general mass balance equation takes effect, because $Flow_{out} = 0$:

$$\frac{d(c * V)}{dt} = Flow_{in} \times Conc._{in} \pm r_c \times V \quad \textbf{(4)}$$

For a fed process volume V is not constant and the equation is:

$$\frac{dc}{dt} = \frac{Flow}{Volume} \times (Conc._{Flow} - Conc.) \pm r_c \quad \textbf{(5)}$$

4.8.2. Reaction kinetic

The specific growth rate (μ) can be calculated with the volumetric rate of biomass production (r_x) as followed:

$$r_X = \mu \times X \quad \textbf{(6)}$$

$$r_X = \frac{dX}{dt} = \mu \times X \quad \textbf{(7)}$$

$$\int \frac{dX}{x} = \int \mu \times dt \quad \textbf{(8)}$$

$$\frac{\ln X_t - \ln X_0}{t - t_0} = \mu \quad \textbf{(9)}$$

$$X = X_0 \times e^{\mu t} \quad \textbf{(10)}$$

During the exponential phase $\mu = \mu_{max}$ which was used to calculate the doubling time:

$$t_d = \frac{\ln(2)}{\mu_{max}} \quad \textbf{(11)}$$

The volumetric production rate of product formation (r_P), biomass (r_X), cell dry mass (r_{CDM}) and PHA-composition ($r_{C6\text{-}C12}$) was calculated with the following general formula:

$$r_A \left[\frac{g}{Lh}\right] = \frac{dA\ [g]}{dt\ [h]} \times \frac{1}{V\ [L]} \quad \textbf{(12)}$$

The specific production rate of product formation (q_P), biomass (q_X), cell dry mass (q_{CDM}) and PHA-composition ($q_{C6\text{-}C12}$) was calculated using the general formula:

$$q_A \left[\frac{1}{h}\right] = r_A\left[\frac{g}{Lh}\right] \times \frac{1}{\bar{X}\ \left[\frac{g}{L}\right]} \quad \textbf{(13)}$$

The volumetric production rate and specific production rate were calculated for the entire process, the accumulation phase and for each measurement time.

Following yield coefficients were calculated:

$$Y_{CDM/Biodiesel} = \frac{CDM_{end} - CDM_0}{Biodiesel_{\ added}} \quad \textbf{(14)}$$

$$Y_{PHA/Biodiesel} = \frac{PHA_{end} - PHA_0}{Biodiesel_{\ added}} \quad \textbf{(15)}$$

4.9. PHA-isolation

There are several methods to isolate PHA.

- Direct extraction with solvent-anti-solvent
- Chemical or enzymatic digestion of the non-PHA cellular material
- Osmotic disruption of microbes.

Due to the better extraction yields and product purity direct extraction was used for the experiments (Koller *et al.*, 2010). Further the isolation method and the applied solvents can influence the molecular mass of PHAs (Rai *et al.*, 2011).

Direct extraction can be done by batch extraction and/or with a soxhlet apparatus, which allows several cycles of PHA extraction. The extraction involves three steps: degreasing of the biomass using a PHA anti-solvent, isolation of PHA using a PHA solvent, and precipitation of PHA from the solution using a PHA anti-solvent. The first two steps can be performed as batch extraction or/and with a soxhlet apparatus. For all experiments only the first step was performed as batch extraction, because *mcl*-PHA gets dissolved in ethanol at 40 °C during the soxhlet extraction and consequently lost during the degreasing step.

For the batch process of degreasing, the frozen and lyophilised biomass was homogenised and stirred with the 5-fold quantity of ethanol (96 %) overnight. Afterwards, the mixture was vacuum filtrated and the filter cakes were dried on air. In case of inefficient degreasing, visible by the lipid rich filtrate, further cycles of degreasing were needed. The isolation of the PHA with chloroform was done with a soxhlet apparatus. Chloroform is needed as solvent reagent to dissolve the surrounded membrane of the PHA granules and finally to bring the PHA in solution. In the third step the PHA remaining in the filtrate was precipitated by adding the 10-fold amount of ice cold ethanol (96 %). The precipitated PHA was separated from the liquid phase by evaporation of the chloroform-ethanol solution using a rotary evaporator (Rotavapor: Büchi RE111; Water bath: Büchi 451).

5. Shaking Flask Experiments

5.1. Evaluation of the suitable emulsifier

5.1.3. Aim of the experiment

Because of its chemical structure (fatty acid methyl ester) biodiesel forms micelles in aqueous media. This condition influences the conversion of the carbon source by bacteria.

Emulsifiers are surface-active substances with a hydrophobic tail and hydrophilic head, which enhance the distribution of the lipophilic substrate in aqueous surroundings making biodiesel better available for organisms.

The aim of this experiment was to screen different commercial emulsifiers (Table 6) for the best conversion of biodiesel by *Ps. citronellolis, Ps. chlororaphis and Ps. putida* GPo1.

Table 6. Emulsifier

Emulsifier	Company
Grindsted PGE 0 80	Danisco
1 Oleoyl-rac-glycerol	Sigma-Aldric, Inc.
Struktol SB 2121	Schill + Seilacher “Struktol” GmbH
Struktol SB 2228	Schill + Seilacher “Struktol” GmbH
Struktol SB 2020	Schill + Seilacher “Struktol” GmbH
Struktol SB 2226	Schill + Seilacher “Struktol” GmbH
Struktrol SB 2071	Schill + Seilacher “Struktol” GmbH
Grindsted CITREM SP 70	Danisco
KFO 673	LUBRIZOL
KFO 770	LUBRIZOL
Glanapon 2000 Konz.	Bussetti
No Emulsifier	-

5.1.4. Experimental setup

The experiment was done for each strain separately and according to the same protocol. For the main cultures 24 small shaking flasks (300 mL) were filled with 150 mL adapted Kueng medium, 450 µL biodiesel dest. (3 g/L) and 120 µL of the respective emulsifier (Table 6). A double set-up for each emulsifier was performed.

The main cultures were inoculated with 2 mL of liquid culture on complete media. The incubation was done at 30 °C. As sterility control, media with 3 g/L biodiesel dest. without emulsifier and microbes was used.

About every 24 hours a sample was taken and the values for OD_{420} were determined. At the end, the pH-value was determined. Furthermore, 5 mL were taken twice for CDM determination. The biomass pellets of the samples were washed once with 5 mL of H_20:EtOH solution to remove remaining biodiesel and emulsifier.

5.1.5. Discussion and results

5.1.5.1. Pseudomonas citronellolis

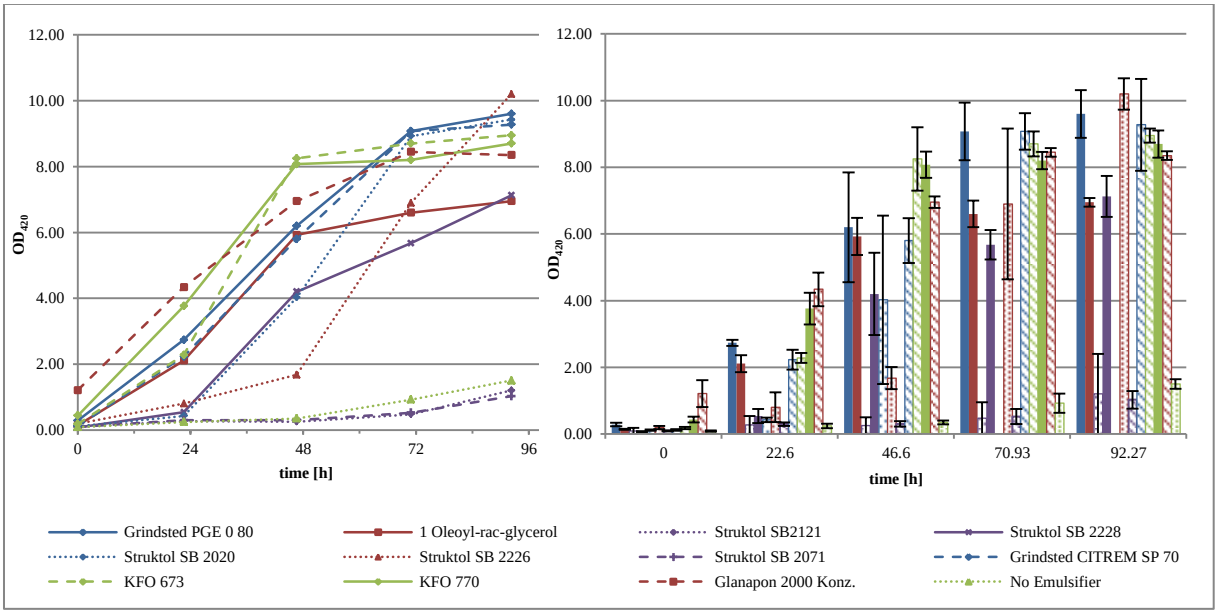

Figure 10. Time scheme of OD_{420} of *Ps. citronellolis* with different emulsifiers.

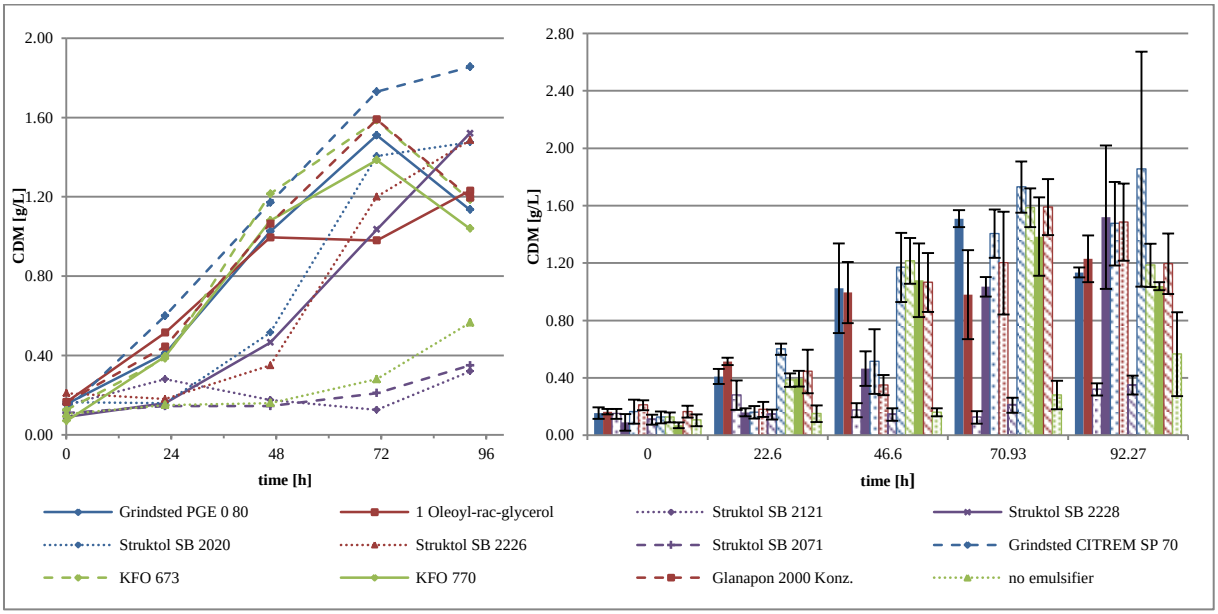

Figure 11. Time scheme of CDM of *Ps. citronellolis* with different emulsifiers.

The shaking flask experiment showed that *Ps. citronellolis* was able to grow on biodiesel best with emulsifier Grindsted CITREM SP 70. With Struktol SB2121 and Struktol SB 2071 the growth on biodiesel was worst. As shown by the OD_{420} analysis during the experiment Grindsted PGE 0 80, KFO 673 and several other emulsifiers performed as well as Grindsted CITREM SP 70 (Figure 10). Regarding the final CDM analysis (Figure 11) the growth seemed to be better with Grindsted CITREM SP 70. This difference resulted from light scattering of biodiesel in the OD_{420} analysis. The OD_{420} curve Figure 10 shows a classical run with exponential and stationary phase. With Glanapon 2000 conc. and KFO 770 there seemed to be no lag phase, but in comparison to the cell dry mass curve there was a significant lag phase visible. This difference also results from the light scattering in the OD_{420} analysis. Struktol SB 2226 showed an increasing and ongoing growth after 45 hours in both curves. Nevertheless it was not chosen as the preferred emulsifiers for the further experiments because the adaption time to exponential growth took too long. The pH-values were measured at the end using a pH meter and were about 6.70 to 7.09 for all emulsifiers, showing no significant changes in the pH-values.

5.1.5.2. Pseudomonas chlororaphis

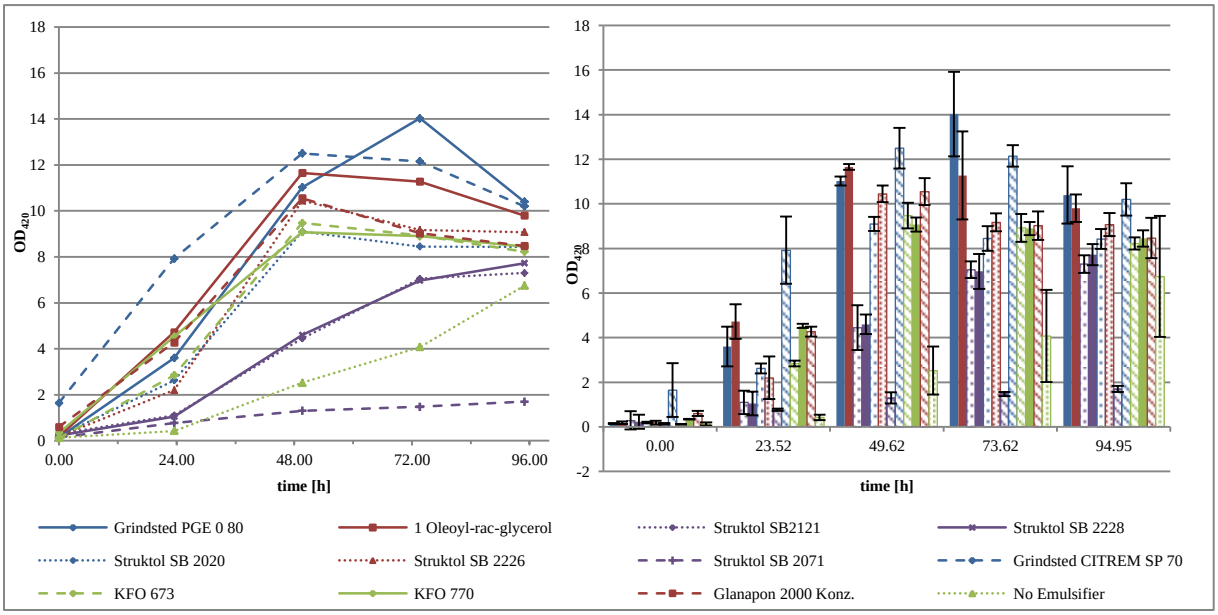

Figure 12. Time scheme of OD_{420} of *Ps. chlororaphis* with different emulsifiers.

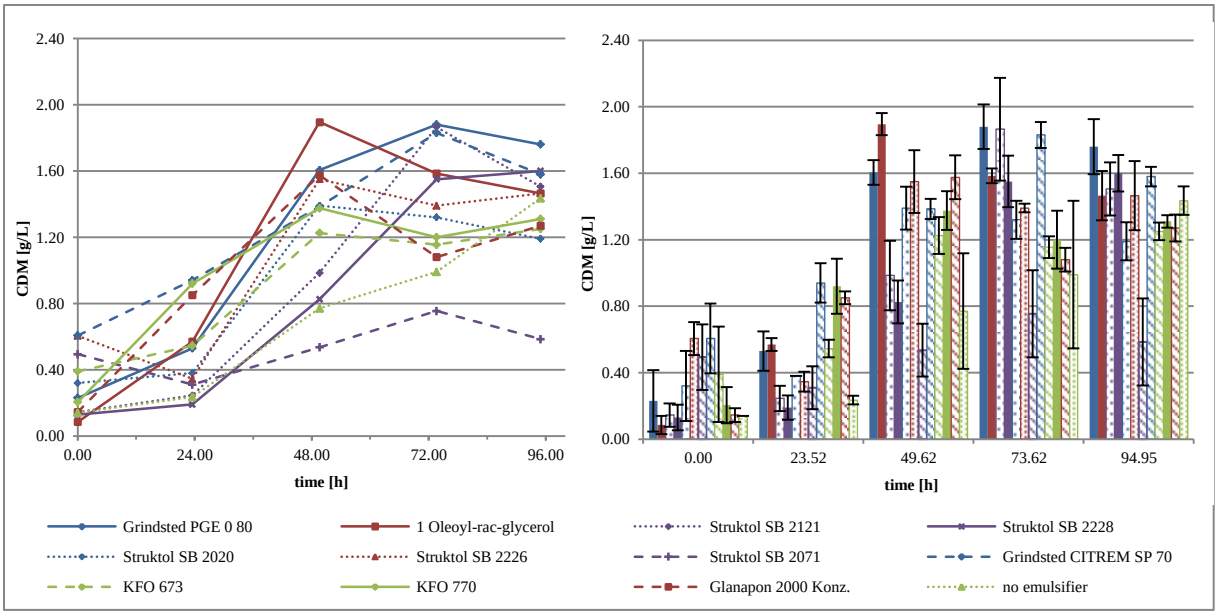

Figure 13. Time scheme of CDM of *Ps. chlororaphis* with different emulsifiers.

Ps. chlororaphis was cultivated best on biodiesel with 1 Oleoyl-*rac*-glycerol, Grindsted PGE 0 80 and Grindsted CITREM SP 70. As shown by the OD_{420} analysis *Ps. chlororaphis* reached the highest values with Grindsted PGE 0 80, but with Grindsted CITREM SP 70 high values were reached already during the lag and exponential phase (Figure 12), whereby Grindsted CITREM SP 70 already started with a high OD_{420} because of light scattering caused by the emulsifier.

Regarding the final cell dry mass analysis (Figure 13) Grindsted CITREM SP 70 and 1 Oleoyl-*rac* glycerol performed as well as Grindsted PGE 0 80. 1 Oleoyl-*rac*- glycerol showed a significant decrease after 48 hours which made it unsuitable for usage.

Comparing the results from OD_{420} analysis and CDM analysis the values vary a lot. These differences resulted from light scattering of biodiesel and emulsifier in the OD_{420} analysis, the remaining biodiesel and emulsifier in the CDM determination or the loss of biomass because of cell disruption during cultivation, caused by a lack of biodiesel or acidification.

The pH-values were measured at the end using a pH meter and were about 6.5 to 6.8 for all emulsifiers. These changes in the pH-values together with the cell dry mass analysis and optical density analysis shows that *Ps. chlororaphis* is able to grow on biodiesel with several different emulsifiers. Nevertheless Grindsted CITREM SP 70 was chosen as emulsifier for the further experiments because of the accomplished results and the simple handling.

5.1.5.3. *Pseudomonas putida* GPo1

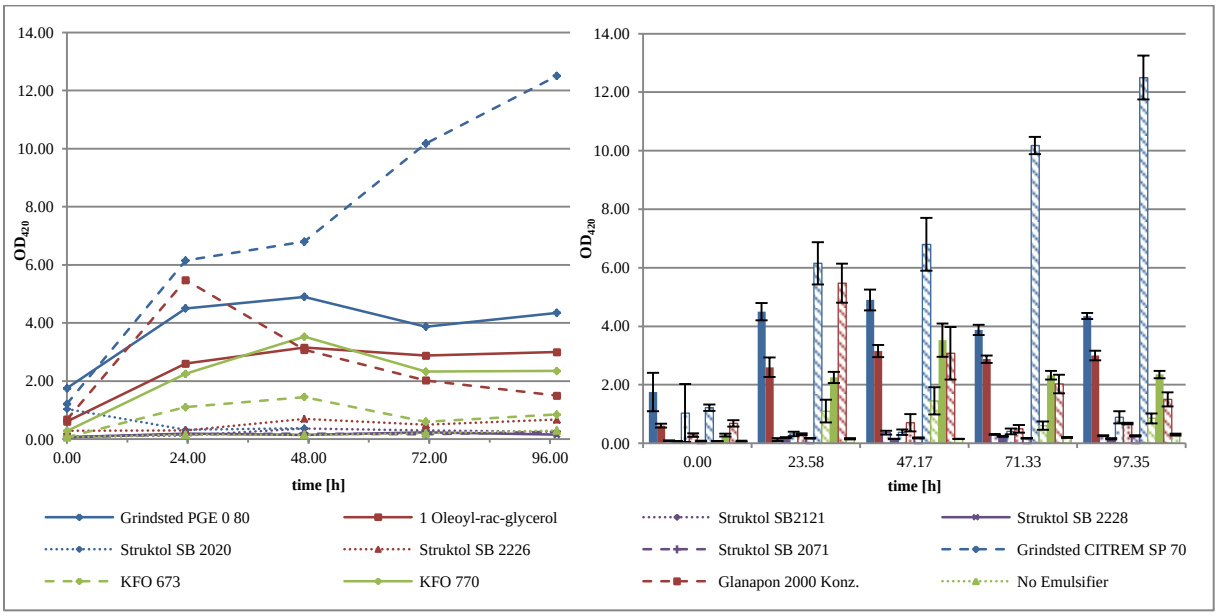

Figure 14. Time scheme of OD_{420} of *Ps. putida* GPo1 with different emulsifiers.

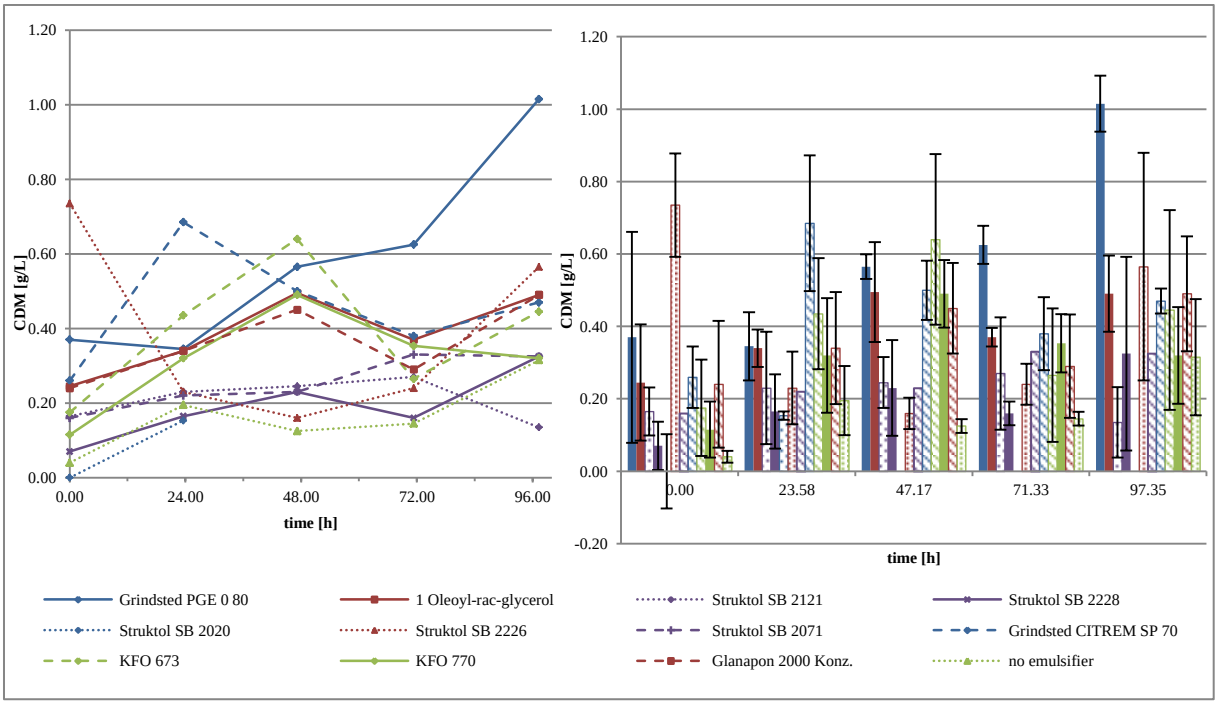

Figure 15. Time scheme of CDM of *Ps. putida* GPo1 with different emulsifiers.

The OD_{420} analysis (Figure 14) during the experiment showed that *Ps. putida* GPo1 was cultivated best on Grindsted CITREM SP 70. By contrast, the analysis of the CDM determination let assume that the optical density values were not reliable. In the final CDM analysis (Figure 15) Grindsted PGE 0 80 showed the best growth.

The pH-values were measured at the end with a pH meter and were about 6.8 to 6.9 for all emulsifiers. Despite the OD_{420} and CDM values, the culture with Grindsted CITREM SP 70 had the lowest pH-value of 6.8, which indicated a lot of acid metabolites resulting from growth.

5.1.6. Conclusion

As the main result of this experiment it can be concluded that Grindsted CITREM SP 70 is the preferred emulsifier for *Ps. citronellolis* and *Ps. chlororaphis* cultivation on biodiesel. For *Ps. putida* GPo1, Grindsted PGE 0 80 turned out to be more suitable, nevertheless, due to the more convenient handling and the comparability Grindsted CITREM SP 70 was used. The concentration of the emulsifier for the subsequent experiments was 4 g per 100 mL pure biodiesel for all experiments.

5.2. Evaluation of inhibiting biodiesel concentration

5.2.1. Aim of the experiment

Because biodiesel has a strong inhibiting effect on the growth of microorganisms, the aim of this experiment was to determine the upper concentration limit of biodiesel for *Ps. citronellolis*, *Ps. chlororaphis* and *Ps. putida* GPo1, which shows no growth inhibition.

5.2.2. Experimental setup

The experiment was done for each strain separately and in the same manner. For the main cultures small shaking flasks (300 mL) were filled with 150 mL adapted Kueng media and with the corresponding biodiesel volume (emulsifier Grindsted CITREM SP 70) of 1 g/L, 3 g/L, 5 g/L, 8 g/L, 10 g/L and 15 g/L. A single determination for each biodiesel concentration was performed, except 5 g/L was done with a double determination because of additional kinetic studies (see chapter 5.3).

The cultures were inoculated with 2 mL of a liquid culture on complete media. Medium with 1 g/L biodiesel (emulsifier Grindsted CITREM SP 70) and without microbes was used as sterility control. Samples were taken about every 24 hours. OD_{420} and pH-value were measured and a sample of 5 mL was taken from each concentration twice for cell dry mass determination. The biomass pellets of the samples were washed once with 5 mL of H_20:EtOH solution to remove remaining biodiesel and emulsifier.

5.2.3. Discussion and results

5.2.3.1. Pseudomonas citronellolis

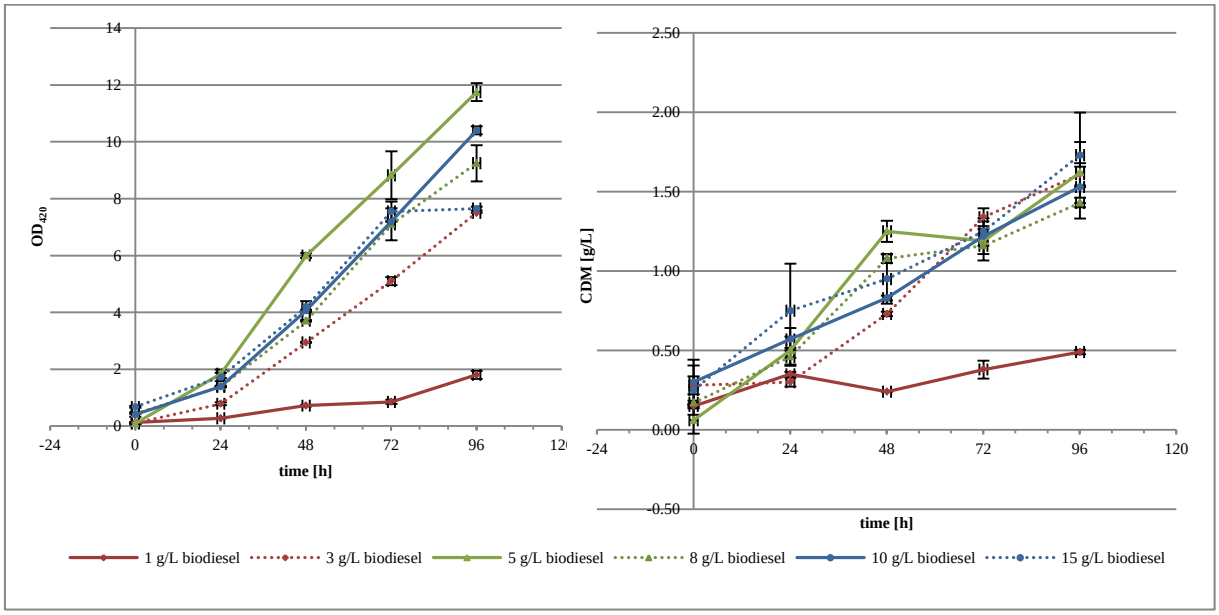

Figure 16. Time scheme of OD_{420} and CDM of *Ps. citronellolis* with different biodiesel concentrations.

As shown in Figure 16, no substrate inhibition occurs until the concentration of 15 g/L. The trend of 15 g/L showed a stationary phase in the OD_{420} analysis after 72 hours but this trend is not reliable because there is no similar trend determinable in the CDM analysis. The best growth was obtained with 15 g/L during CDM analysis. 1 g/L biodiesel is a too small amount of carbon source to ensure reasonable growth. The CDM values vary because of remaining biodiesel or emulsifier in the sample tubes.

5.2.3.2. *Pseudomonas chlororaphis*

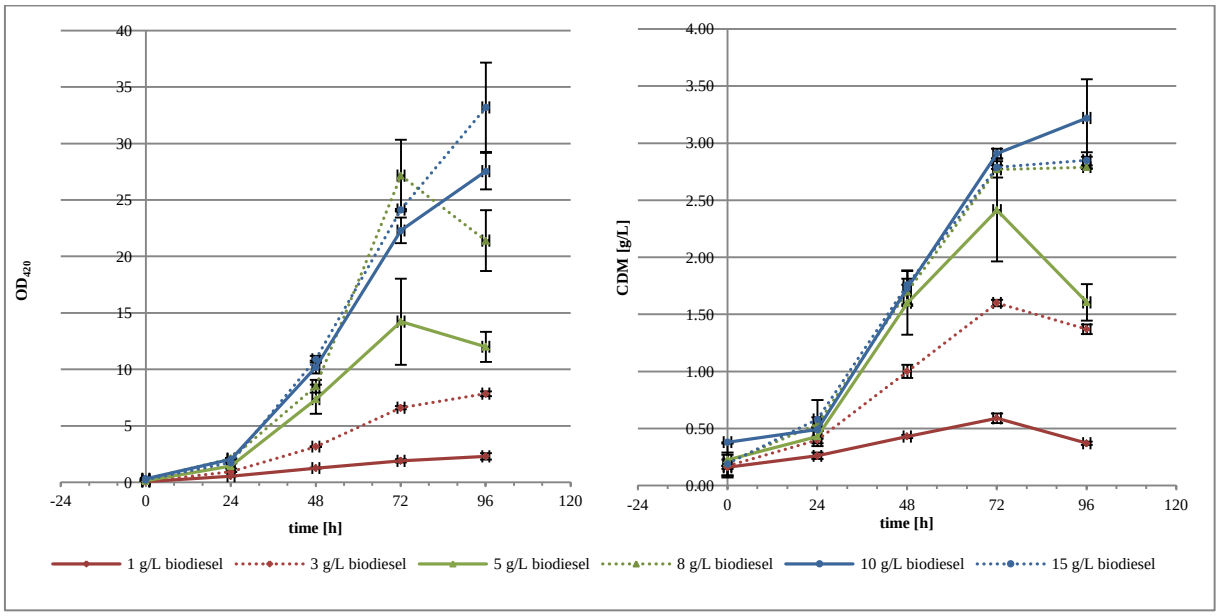

Figure 17. Time scheme of OD_{420} and CDM of *Ps. chlororaphis* with different biodiesel concentrations.

There is no inhibition effect until 15 g/L biodiesel. 1 g/L and 3 g/L biodiesel are again too small amounts of carbon source to obtain reasonable growth. The stationary phase was reached for all concentrations after 72 hours because of nutrient limitation in the media.

5.2.3.3. *Pseudomonas putida* GPo1

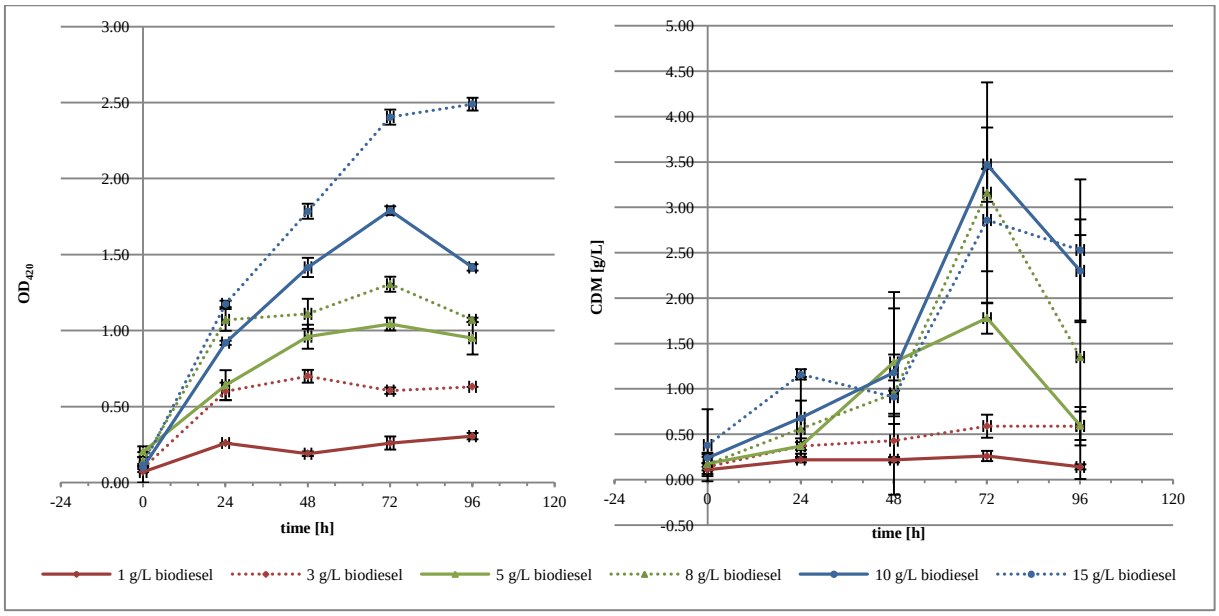

Figure 18. Time scheme of OD_{420} and CDM of *Ps. putida* GPo1 with different biodiesel concentrations.

The best result was obtained with 15 g/L biodiesel (Figure 18) based on OD_{420} determination. Nevertheless, the CDM analysis is more reliable. Regarding these data, *Ps. putida* GPo1 grew best with 10 g/L biodiesel according to the CDM analysis. After 72 hours there was a strong loss of biomass at 15 g/L, 10 g/L, 8 g/L and 5 g/L which may results from a nutrient depletion.

5.2.4. Conclusion

1 g/L biodiesel was a too low concentration of carbon source to obtain reasonable growth for all three strains. Furthermore, they grew well with 15 g/L biodiesel and no substrate inhibition was observed. Comparing all three strains, *Ps. chlororaphis* grew best and achieved 3.2 g/L CDM with 15 g/L biodiesel. *Ps. putida* GPo1 grew slowest with 2.5 g/L CDM at 15 g/L biodiesel. In view of these results, application of 15 g/L biodiesel causes no major problems.

5.3. Kinetical analysis

5.3.1. Aim of the experiment

During the experiment "Evaluation of inhibiting biodiesel concentration" (see chapter 5.2) kinetic analysis with 5 g/L biodiesel was accomplished to determine growth behaviour, the max. specific growth rate and duplication time.

5.3.2. Experimental setup

The experiment was done for each strain separately and in the same manner. For the liquid cultures small shaking flasks (300 mL) were filled with 150 mL adapted Kueng media and with a biodiesel volume (with emulsifier Grindsted CITREM SP 70) of 5 g/L. A double determination was performed.

The cultures were inoculated with 2 mL of liquid culture cultivated on complete media. About every 8 hours (alternatively every 16 hours) a sample was taken. The OD_{420} and the pH-value were measured for each culture and a sample volume of 5 mL was taken twice for CDM determination. The biomass pellets of the samples were washed once with 5 mL of H_20:EtOH to remove remaining biodiesel and emulsifier.

5.3.3. Discussion and results

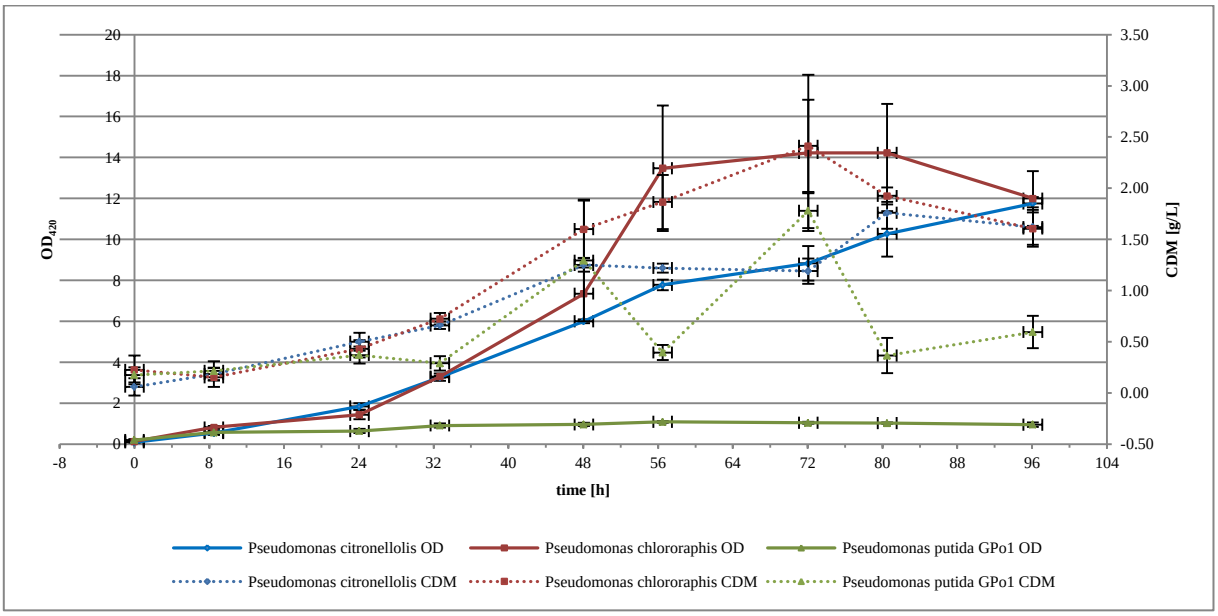

Figure 19. Kinetic diagram of cultivation at 5 g/L biodiesel.

As shown in Figure 19 *Ps. chlororaphis* showed classical growth behaviour with a well visible lag phase, exponential phase and stationary phase after 56 hours. This was confirmed by OD_{420} and CDM analysis. During the experiment no stationary phase of *Ps. citronellolis* was obtained. Also by CDM analysis no plain stationary phase was observed. *Ps. putida* GPo1 displayed slowest growth. Although CDM analysis is more reliable than optical density analysis, the data of CDM of *Ps. putida* GPo1 seems to be not reliable because of strong aberration. If there was a loss of biomass, the max. specific growth rate was comparable to the other investigated strains. But if there was remaining biodiesel or emulsifier the growth was worst and the assumption of the OD_{420} analysis is confirmed.

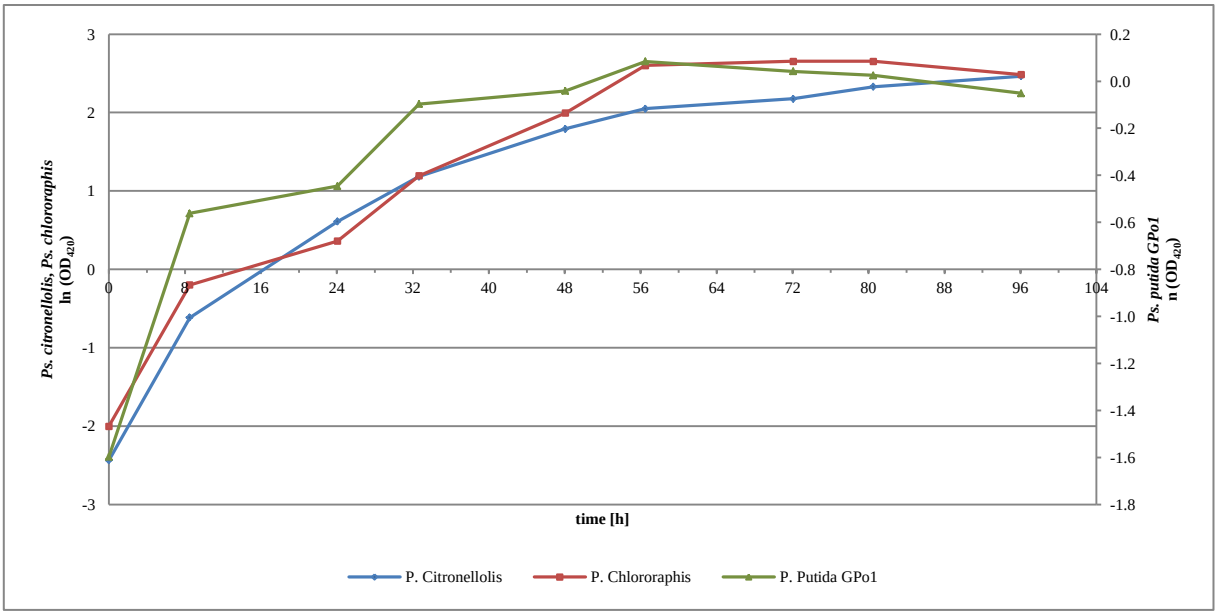

Figure 20. Logarithmic graphs of OD_{420} with 5 g/L biodiesel.

Table 7. Growth parameters

	Ps. citronellolis	*Ps. chlororaphis*	*Ps. putida* GPo1
Specific growth rate [h^{-1}]	0.07	0.07	0.02
Double time [h]	9.30	10.18	36.02

The max. specific growth rate listed in Table 7 was evaluated from the natural logarithmic plot of OD_{420} *vs.* time (Figure 20). For the calculation the exponential phase was used in Eq.(9). *Ps. citronellolis* grew as fast as *Ps. chlororaphis*. Both displayed a max. specific growth rate of 0.07 h^{-1} and an average duplication time of about 10 hours. *Ps. putida* GPo1 displayed a max. specific growth rate of 0.02 h^{-1} and a duplication time of 36 hours.

5.4. PHA accumulation

5.4.4. Aim of the experiment

Ps. citronellolis, *Ps. chlororaphis* and *Ps. putida* GPo1 are known as PHA producing microorganisms (Bear *et al.*, 1999; Rai *et al.*, 2011; Timm & Steinbüchel, 1990; Zinn *et al.*, 2011). No literature is available about PHA accumulation on biodiesel, only about degradation of diesel oil and formation of PHAs by *Pseudomonas citronellolis* (Sadouk *et al.*, 2009). This experiment was a preliminary test before fermentation on bioreactor scale in order to examine PHA accumulation and PHA composition.

5.4.5. Experimental setup

To trigger PHA accumulation in adapted Kueng medium (Table 1) without $(NH_4)SO_4$ was used for the main cultures. 5 g/L biodiesel was used as carbon source. The main cultures (250 mL) were inoculated with 10 mL of the corresponding adapted strain on 5 g/L biodiesel. A double determination for each strain was done. Sampling and determination of OD_{420} was done every 3 hours during daytime. Every 24 hours 5 mL of each culture were taken as a sample to determine CDM. After about 24 hours all strains were fed again with 2.5 g/L biodiesel to avoid degradation of PHA. *Ps. chlororaphis* was fed one more time after about 73 hours.

Depending on the OD_{420} and after microscopic surveillance of the cultures, the end of the experiment was determined individually for each strain. The cultures were pasteurized at approximately 65 °C for about 30 min. Afterwards the broth was centrifuged at 5 000 rpm for 20 min at 4°C (Sorvall RC-5B, F10S-6x500, *Thermo Scientific*). The supernatant was rejected and the pellet was resolved in 40 mL H_2O:EtOH solution. Afterwards the resolved biomass was concentrated in two tubes by repeated cycles of centrifugation at 4 000 rpm for 10 min (Megafuge 1.0R, *Heraeus Sepatech*). Finally, the biomass pellets were frozen and lyophilised for CDM determination and transesterificated for the GC analysis. This procedure was done separately for each strain. The washing steps were accomplished in order to remove the remaining biodiesel and degrease the biomass.

5.4.6. Discussion and results

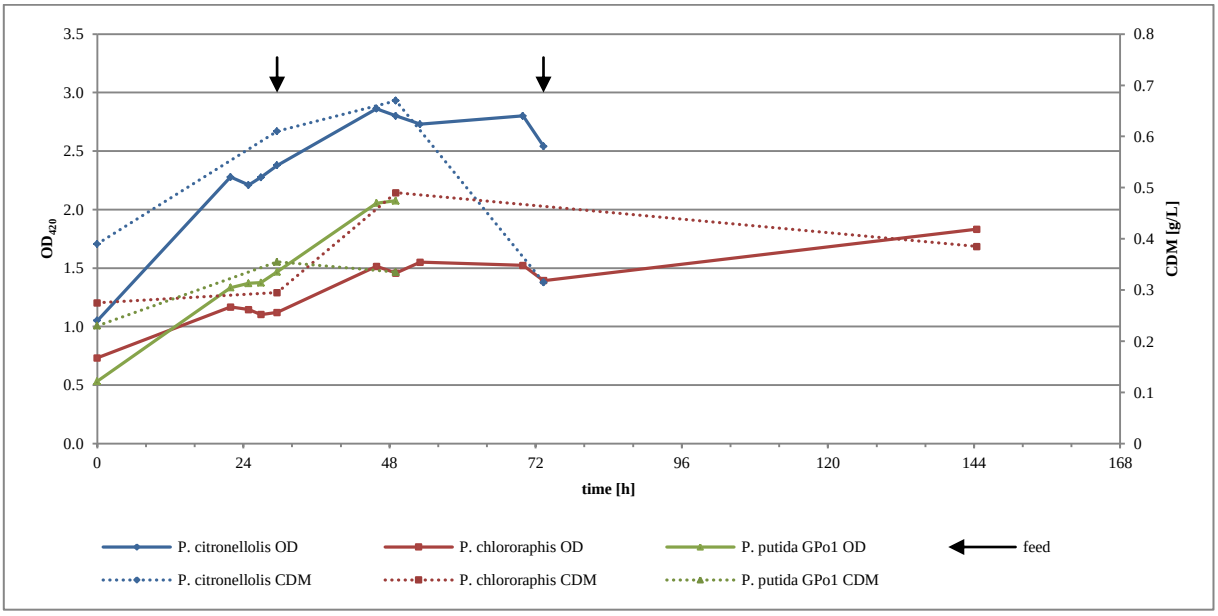

Figure 21. Time diagram of OD_{420} and CDM.

Ps. putida GPo1 cultures were shut down after 49 hours after visible PHA inclusions in the microscope and a steady OD_{420} were obtained. *Ps. citronellolis* also showed a steady OD_{420} but fewer inclusions than *Ps. putida*, therefore the cultures of *Ps. citronellolis* were kept for another 24 hours and were shut down after 73.3 hours of cultivation. *Ps. chlororaphis* showed the lowest amount of inclusions of all set-ups. The cultures were fed after 73.3 hours and the experiment was shut down after 144.27 hours. (Figure 21)

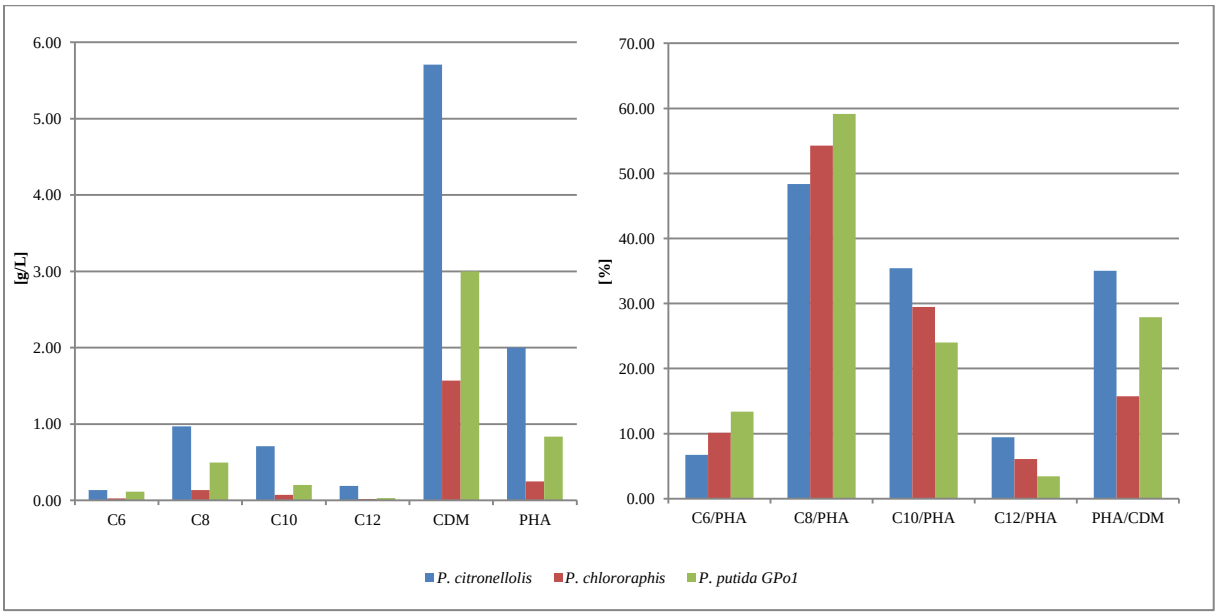

Figure 22. Composition and shares of *mcl*-PHA.

As shown in Figure 22 *Ps. putida* reached 3 g/L CDM with a percentage of 27.88 PHA per CDM after 49 hours. *Ps. citronellolis* showed 5.71 g/L CDM and 35.02 % PHA per CDM after 49 hours. *Ps. chlororaphis* showed 1.57 g/L CDM and a percentage of 15.73 PHA per CDM. The pre-dominant component of PHA of all strains was C8. The percentage of C8 from total PHA was 48.38 % for *Ps. citronellolis*, 54.26 % for *Ps. chlororapis* and 59.15 % for *Ps. putida* GPo1. The second most amount consistet of C10. *Ps. citronellolis* showed the biggest amount of C10 with 35.44 %, followed by *Ps. chlororaphis* with 29.46 % and *Ps. putida* GP01 with 24.01 %. The components C6 (6 to 13 %) and C12 (3 to 10 %) showed the lowest amounts, with*Ps. putida* GPo1 accumulating most C6 (13.39 %) and least C12 (3.44 %). The amounts of C6 and C12 in *Ps. citronellolis* are reverse. It has the highest share of C12 (9.44 %) and the smallest of C6 (6.74 %). The contents in *Ps. chlororaphis* are between the previous strains with 10.16 % for C6 and 6.12 % for C12.

6. Fermentations

6.1. *Pseudomonas citronellolis* as production strain – 1st Fermentation

6.1.7. Aim of the experiment

Ps. citronellolis showed good growth behaviour and *mcl*-PHA accumulation during the preliminary experiments. The fermentation was done in order to repeat PHA accumulation on a laboratory bioreactor scale under controlled conditions in regard to future industrial relevance.

6.1.8. Experimental setup

The fermentation was performed with a total volume of 5 litres. First, the sterile reactor was filled with 2.5 litres of adapted Kueng media without biodiesel. Second, the inoculum of 2.5 litres was added. For the inoculum 10 x 250 mL adapted Kueng media with 5 g/L biodiesel was inoculated with 2 mL of a preculture (average OD_{420} of 9.2) and was incubated for 3 days at 30 °C. The average OD_{420} of the inoculum was 11.4. After inoculation a concentration of 5 g/L biodiesel as carbon source was added.

During fermentation, the fermentation broth was kept at 30 °C, the oxygen supply (40 % during growth phase and 20 % during accumulation phase) was regulated by the stirrer (initial 400 rpm). Because of high concentrations of extracellular material, the monitoring of oxygen supply could not be accomplished properly at the end of the fermentation. The first sample was taken immediately after inoculation. During lag-phase, no samples were taken; consequently the second sample was taken after 12 hours. Afterwards every 3 hours a sample was taken for OD_{420} measurement, CDM determination, ammonium fast test and accurate test. In addition the fermentation was monitored *via* microscope for monosepsis of the microbial culture. The decision to re-feed was made after a check for presence of biodiesel droplets under the microscope and according to the consumption of dissolved oxygen. After 33 hours an OD_{420} of 138 was reached and the growing phase was stopped by changing the base of the automated pH-control from NH_4OH to NaOH in order to limit the NH_4^+ supply and provoke the start of PHA accumulation. The fermentation was stopped after 72 hours when the average OD_{420} was 243.5. Because of extracellular material, the pasteurised broth (70°C, 1 h) was precipitated by addition of 0.05 L/L H_2SO_4 (10 %) and centrifuged for 20 min at 5 000 rpm (Sorvall RC-5B, F10S-6x500, *Thermo Scientific*). The supernatant was rejected away and the

biomass pellet was lyophilised. Afterwards the PHA content was isolated as described in chapter 4.9.

6.1.9. Discussion and results

The fermentation started with an average OD_{420} of 6.35. The OD trend (Figure 23) shows a lag phase, exponential phase but no stationary phase during growth phase was detectable. The NH_4^+ supply was stopped after 33 hours and an average OD_{420} of 138. The further increase of the optical density in the accumulation phase was induced by PHA formation and the related cell thickness. The maximum value of optical density amounted to 269 after 69 hours and the fermentation was stopped after 72 hours at OD_{420} 243.5 when the OD_{420} showed a slightly decrease and additionally the extracellular material produced by *Ps. citronellolis* limited the aeration. *Ps. citronellolis* had a max. specific growth rate (μ_{max}) of 0.08 h^{-1} and a duplication time of 8.45 h. The max. specific growth rate is equal to the slope of the linear regression shown in Figure 23.

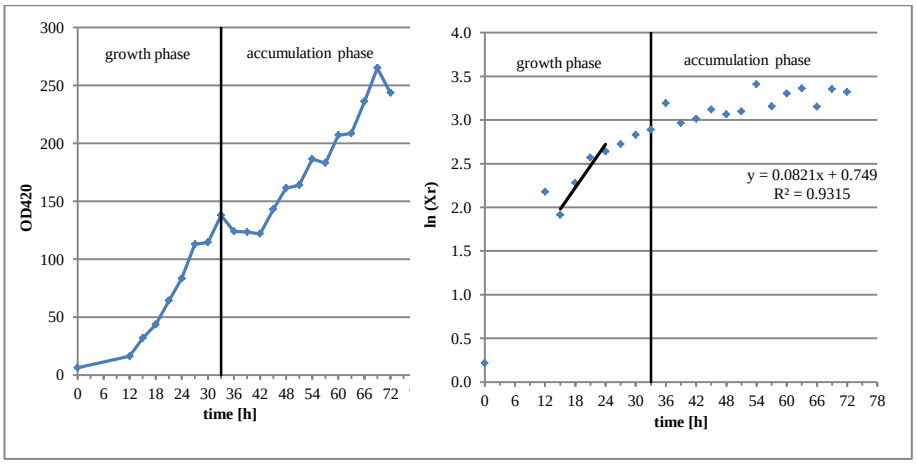

Figure 23. Growth scheme of *Pseudomonas citronellolis*.

As shown in Figure 24, the concentration of PHA remained constant during growth phase between 0.18 and 0.57 g/L and increased as expected during accumulation phase to a maximum value of 2.9 g/L after 72 hours. The CDM values increased constantly from 1.51 to 18.50 g/L during accumulation phase except one aberration at 15 hours. Biomass (X_r) showed the same trend with 1.24 to 17.94 g/L also with an aberration at 15 hours, which might be due to a shortage in carbon source after recovering from the lag phase. The maximum values of CDM and X_r were reached after 54 hours with 32.19 g/L and 30.24 g/L. The aberrations in the CDM graph and consequently in the X_r were natural fluctuations of cell death and subsequently cell division, because of the nitrogen limitation no optimal growth conditions

were guaranteed. Nevertheless, these fluctuations had no negative influence on the PHA accumulation. As expected, the NH_4^+ concentration (Figure 25) showed a distinct decrease after restriction of nitrogen supply at 33 hours from 0.43 to 0 g/L at 42 hours. In comparison, PHA concentration increased after stopping the growth phase.

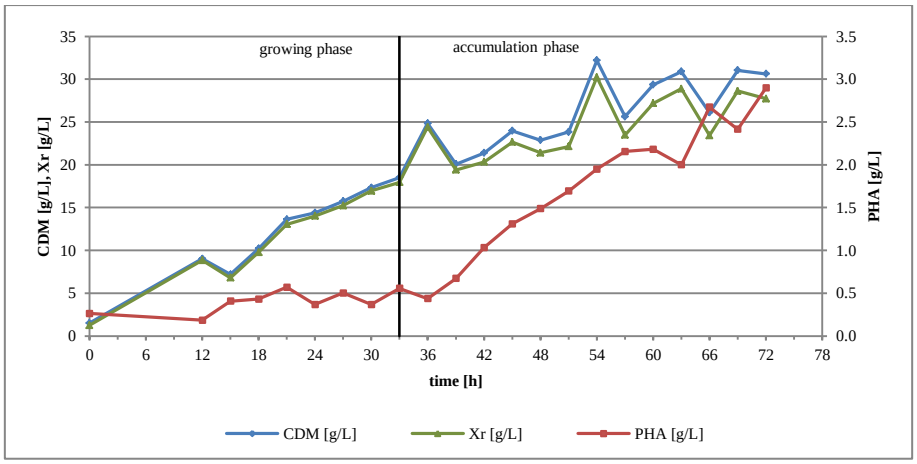

Figure 24. Correlation of CDM, X_r and PHA.

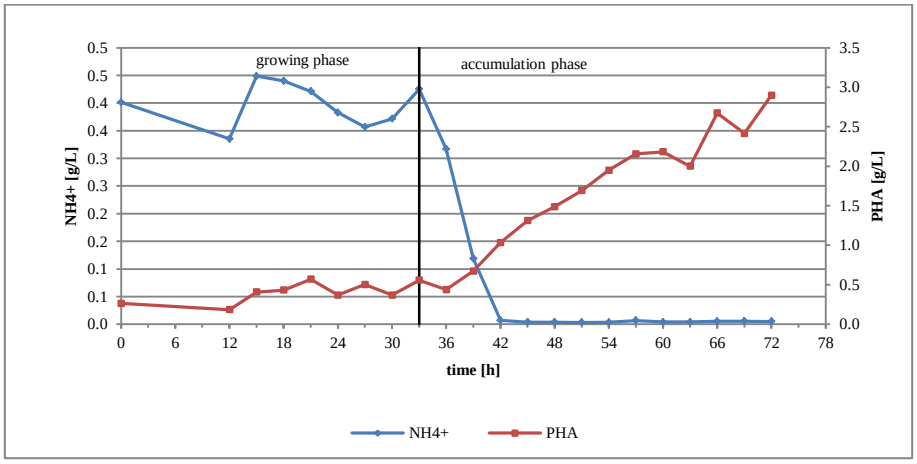

Figure 25. Depletion of nitrogen and accumulation of PHA.

After 54 hours the highest concentration of catalytically active biomass (X_r) was determined with 30.24 g/L. The highest CDM value of 32.19 g/L (Figure 24) with 6.06 % PHA content (1.95 g/L) was also measured at this time point. In contrast to this, the highest PHA content was determinated at the beginning of the fermentation with 17.38 % per CDM corresponding to 0.27 g/L. That was because the cells in the inoculum already accumulated PHA. At the end of the fermentation at 72 hours, the content was 9.46 % PHA of total CDM, respectively a PHA concentration of 2.9 g/L. Summarizing, there is an increase of PHA content after restriction of nitrogen source (0.44 g/L to 2.90 g/L), indicating that the application of this

nutritional stress factor is suitable for enhancing the PHA productivity by this production strain (Figure 26).

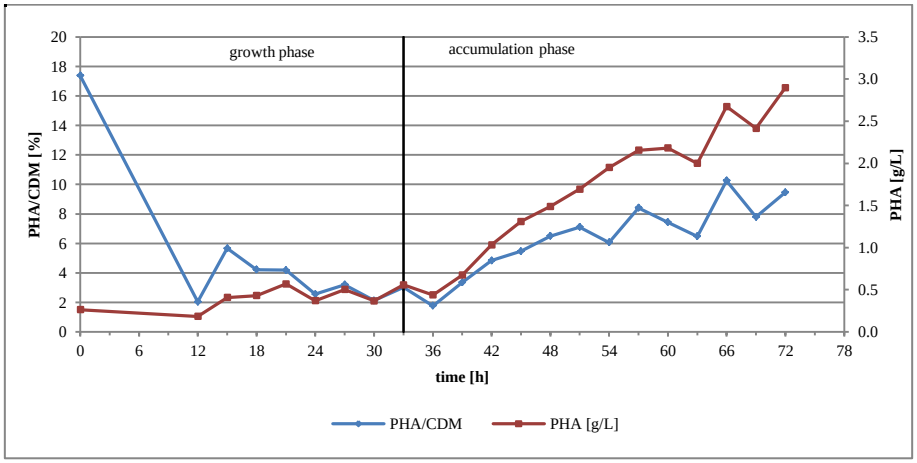

Figure 26. Shares diagram of PHA accumulation from total CDM of *Ps. citronellolis*.

As shown in Figure 27, the percentage of C6 of total PHA varies over the entire process between 5 and 7 %, although no C6 was detectable in the beginning of the fermentation. Also no C7 building blocks were detected until 15 hours of cultivation. At this measurement point a share of 8.26 % of PHA in cell dry mass was present. During late growth phase and early accumulation phase the percentage was subjected to variation of accumulation and degradation of C7. After 42 hours the percentage has become stable at about 3 to 1.5 %. C8 of total PHA showed also variation between 26 and 44 % during the first 39 hours. Afterwards, the share of C8 per PHA was stable at 38 to 39 % over the rest of accumulation time and finally had a concentration of 1.14 g/L at the end. The amount of C9 displayed a significant decrease from about 27 % at the beginning to 12 % at the end of the growth phase. During the accumulation phase a further decrease to 4.55 % was detected. The percentage of C10 of total PHA was between 21% and 30 % during the first 18 hours. Slight variations of this building block percentage were also detected during late growth phase and early accumulation phase. After 42 hours the share of C10 was between 36 to 38 % until the end of the process with a maximum concentration of 1.13 g/L at 72 hours. The amount of C12 building blocks increased from about 5 % to 11 % over the fermentation and has a concentration of 0.32 g/L at the end. Regarding the proportionate share of this building block in the entire *mcl*-PHA, no variations were detected.

The analysis of the composition shows that the mainly produced building blocks were C8 and C10. This implicates that the provided fatty acids were not degraded completely by the ß-oxidation pathway. The low percentage of C6 affirms this statement. The small amounts of

C9 and C7 components indicate that there is a low amount of odd-numbered fatty acids present in the biodiesel for example Pentadecanoic acid with 0.39 % (m/m) or Margaric acid with 1.18 % (m/m) (Mittelbach, unpublished data). During the ß-oxidation odd-numbered fatty acids end up in a C3 unit and not like saturated fatty acids in C2 units (see chapter 2.2.2). Choi & Yoon (1994) reported the biosynthesis of *mcl*-PHA on various carbon sources, including decanoate, with *Ps. citronellolis* ATCC 13674. The obtained composition during this study correlated with the PHA composition mentioned above. Choi and coworkers obtained 11 mol% of C6, 48 mol% C8 and 40 mol% C10 with decanoate as carbon source. It is also proposed that the length of the monomer units is equal to the carbon chain length in the carbon source or shorter than one or more C2 units (Brandl *et al.*, 1988; Huijberts *et al.*, 1992; Huisman *et al.*, 1989; Lageveen *et al.*, 1988).

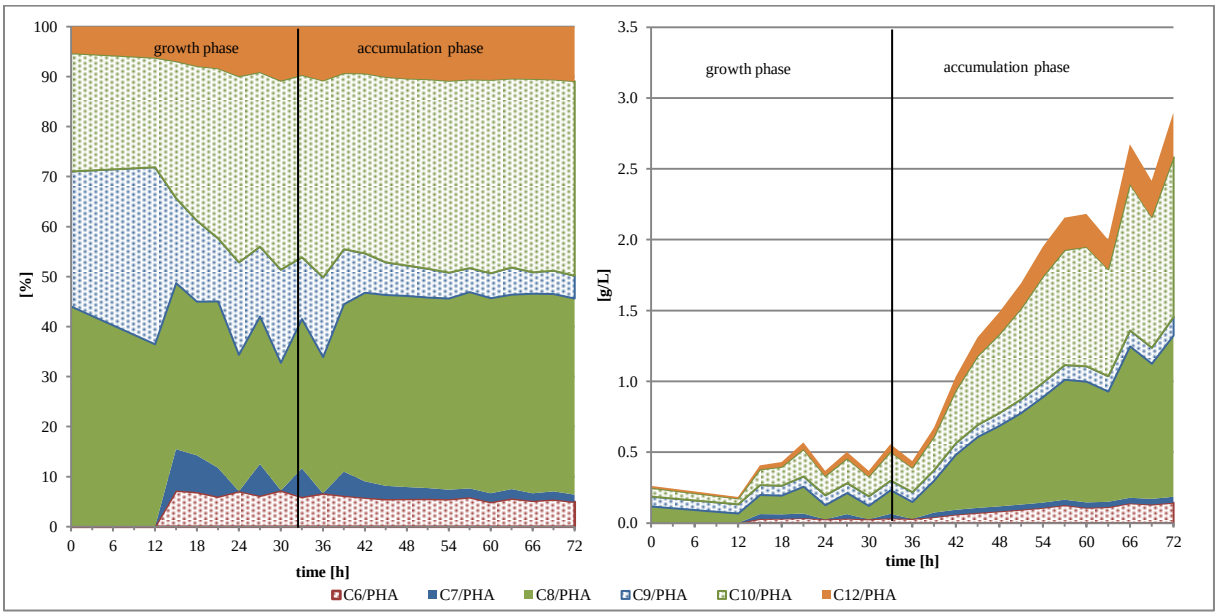

Figure 27. Concentration, composition and shares of *mcl*-PHA.

The feeding concentration of biodiesel was 5 g/L until 45 hours. Afterwards the biodiesel concentration was reduced to 3 g/L in order to avoid substrate inhibition as well as degradation of PHA.

The production rates (Figure 28) showed that accumulation of PHA (increasing rate) resulted in stagnant biomass concentration (decreasing rate).

In other words, increasing biomass rates and decreasing PHA rates indicate that the carbon source was used mainly for microbial growth, respiration and maintenance energy and not for PHA production.

The production rate of PHA was negative in the first 12 hours because PHA was degraded in the favour of biomass formation which is shown in positive production rates. During the next 21 hours there was a change between PHA accumulation and degradation as shown by the fluctuating production rates. After nitrogen restriction the product formation of PHA is increasing until 63 hours. At this time, a strong fluctuation in accumulation and degradation was observed, which may have resulted from insufficient supply with biodiesel.

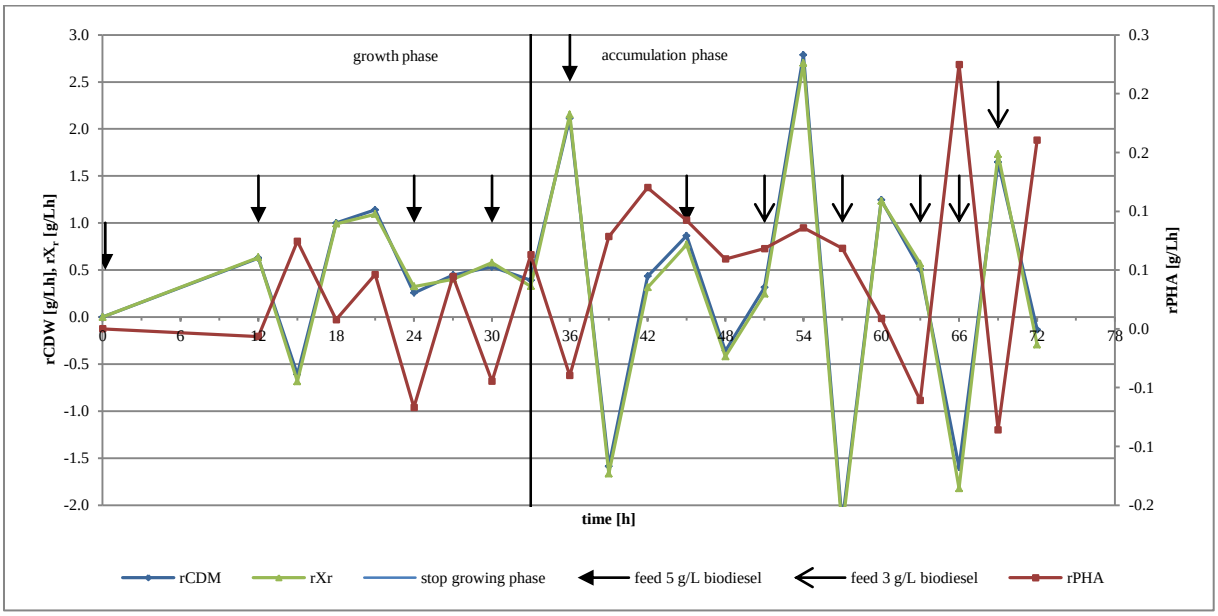

Figure 28. Production rates of CDW, X_r and PHA

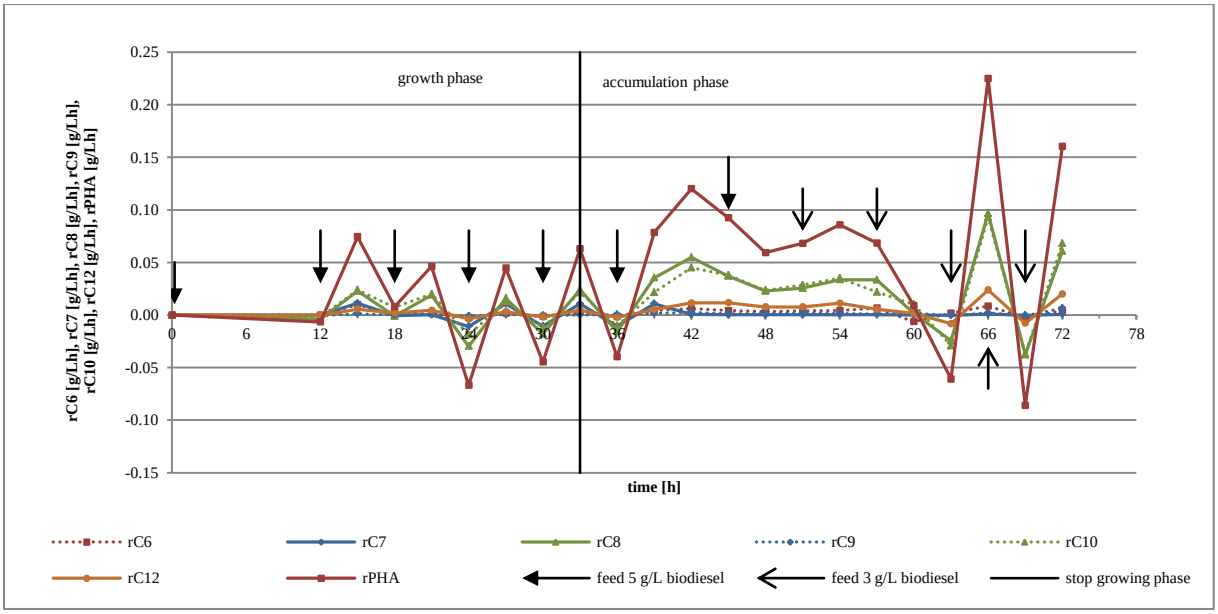

Figure 29. Production rates of C6, C7, C8, C9, C10, C12 and PHA.

The production rates of the PHA components (Figure 29) show the same trend as the PHA product formation. C8 and C10 show higher values than the other components, which confirmed that they were the main building blocks.

The specific production rates (Figure 30) were calculated according to Eq. (13). The trend of the PHA components is similar to the trend of PHA. The higher specific production rates of C8 and C10 confirm their role as main PHA components. The graph displaying the specific production rates of CDW, X_r and PHA (Figure 31) is similar to the production rates, except the difference of the values because they refer to the mean value of active biomass.

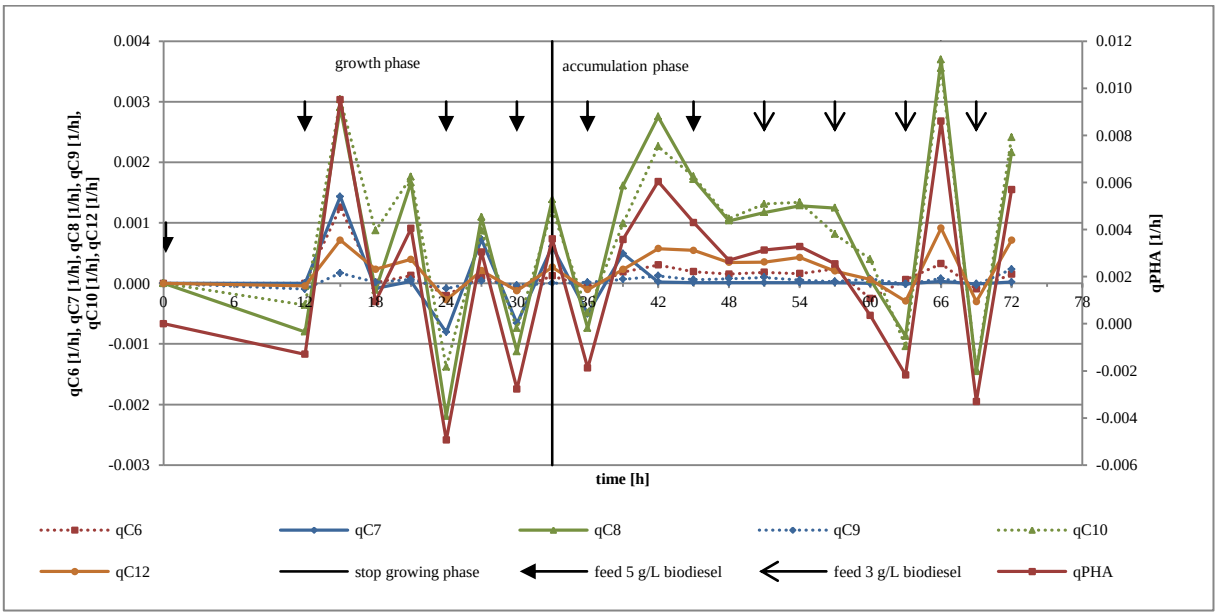

Figure 30. Specific production rates of C6, C7, C8, C9, C10, C12 and PHA.

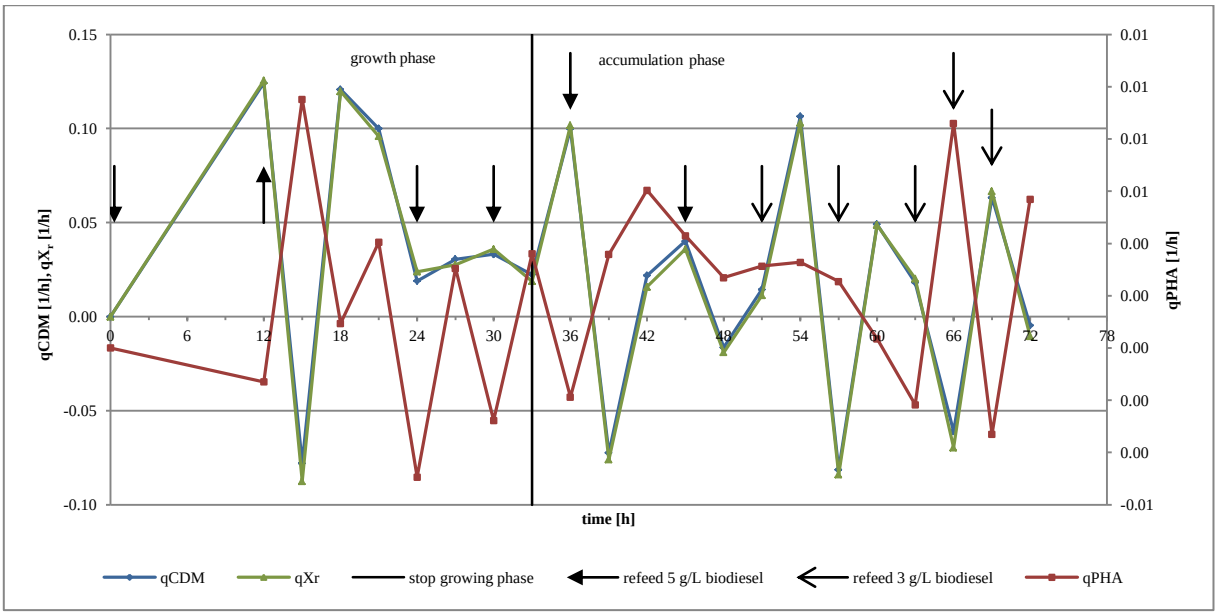

Figure 31. Specific production rates of CDM, X_r and PHA.

After the shutdown of the fermentation the fermentation broth was pasteurised and treated with H_2SO_4 as already described in the experimental set up (see chapter 6.1.8). Finally the lyophilised biomass was used for the PHA isolation as described in chapter 4.9. After all degreasing and isolation steps, 4.27 g/L PHA were obtained. In Figure 32 samples of the isolated *mcl*-PHA are shown. The texture was like latex.

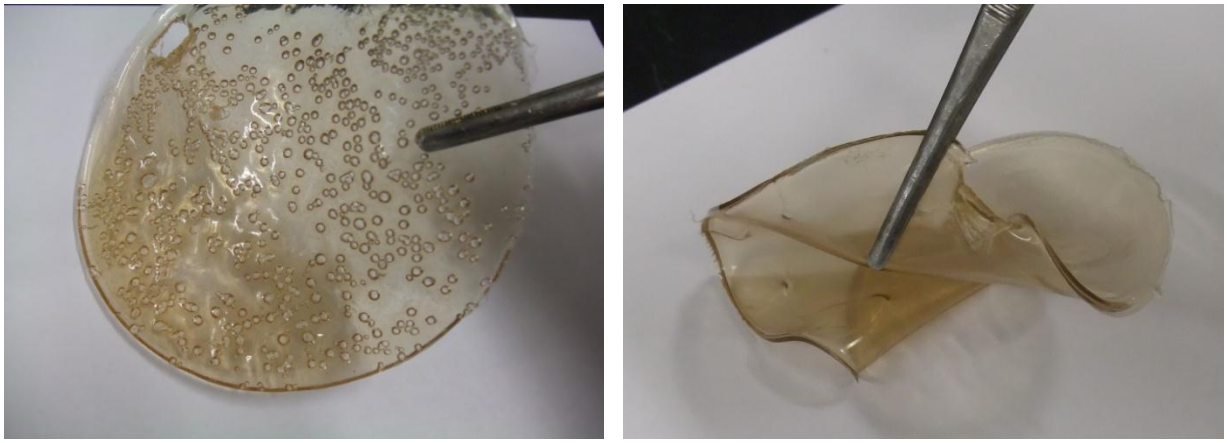

Figure 32. Examples of isolated *mcl*-PHA of *Ps. citronellolis*.

6.2. *Pseudomonas citronellolis* as production strain – 2nd Fermentation

6.2.1. Aim of the experiment

Because the 1st fermentation with *Ps. citronellolis* showed promising results, a 2nd fermentation was done as in order to confirm the obtained data and enhance the results. This experiment was done with an increased concentration of biodiesel to obtain higher amounts of product and to increase the industrial relevance. Due to the focus on production instead of kinetic analysis, the time intervals between sampling were longer.

6.2.2. Experimental setup

The setup for the 2nd fermentation with *Ps. citronellolis* was done like the first time with 5 litres total volume but with 10 g/L biodiesel except 5 g/L. The average OD_{420} of the inoculum (2.5 litres) was 27.49. The fermentation broth was kept at 30 °C, the oxygen supply (40 % during growth phase and 20 % during accumulation phase) was regulated by the stirrer (initially 400 rpm). In the end of the fermentation the oxygen supply could not be measured like during the first fermentation because of the extracellular material. The first sample was taken immediately after inoculation. After 3 hours, the second sample was taken during the lag phase. The next sampling was done after 12 hours and, from this point on, every 4 hours, except for an 8 hours break at 31 to 39 hours. The sample was used for OD measurement, CDM determination, ammonium fast test, ammonium accurate test and for monitoring the bacteria *via* microscope. The decision to feed was made after a check for presence of biodiesel droplets under the microscope. After 19 hours an OD_{420} of 98.5 was reached and the nitrogen source was restricted by changing the base form NH_4OH to NaOH. The fermentation was shut down after 43 hours at an OD_{420} of 312.

Although the pasteurized fermentation broth was precipitated with 0.05 % (v/v) H_2SO_4 (10 %) and centrifuged for 20 min at 5 000 rpm (Sorvall RC-5B, F10S-6x500, *Thermo Scientific*) similar to the first fermentation, no separation could be reached. As consequence, the entire broth was lyophilised.

6.2.3. Discussion and results

The fermentation was started with an OD_{420} of 19.55. In the first 14 hours a lag phase was detectable but no stationary phase (Figure 33). After 19 hours and an OD_{420} of 98.5 the supply of nitrogen source was restricted. After restriction the OD_{420} increased constant until the end of the fermentation at 45 hours and an OD_{420} of 312. The max. specific growth rate was

calculated with the natural logarithm of the catalytically active biomass. It is equal to the slop, thus 0.103 per hour (Figure 33). With this rate the duplicating time was calculated with Eq. (11) and resulted in 6.73 hours.

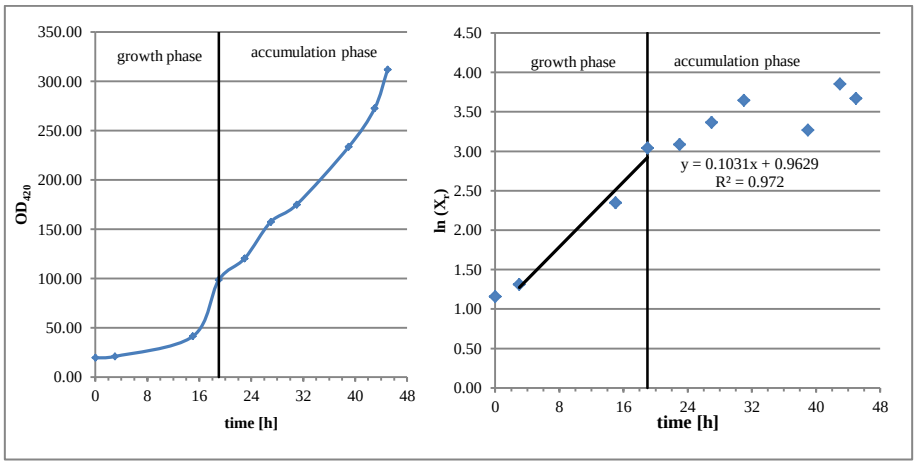

Figure 33. Growth scheme of *Ps. citronellolis* 2nd fermentation.

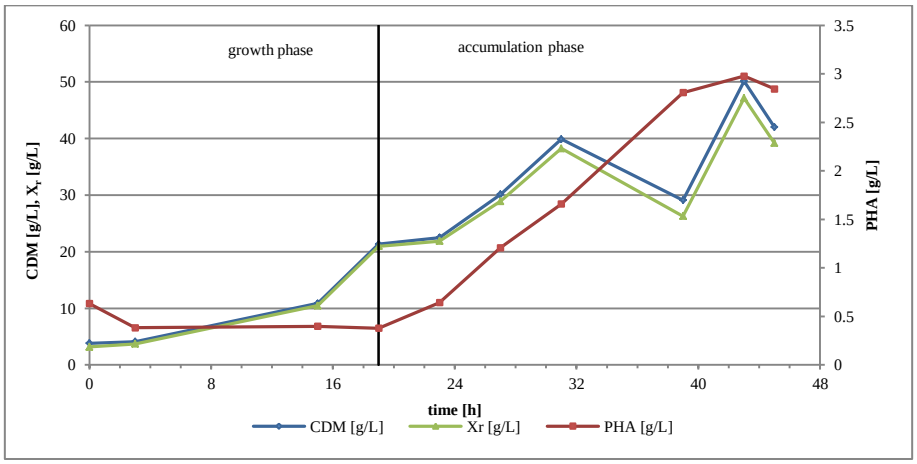

Figure 34. Correlation of CDM, X_r and PHA of *Pseudomonas citronellolis* 2nd fermentation.

The trend of CDM and X_r were similar (Figure 34) whereas they slightly separated after 27 because of the increasing PHA content and as a consequence a reduced biomass accumulation. The aberration at 39 had no influence on the accumulation of PHA. During the growth phase the PHA concentration was between 0.38 g/L and 0.63 g/L. After restriction of nitrogen source at 19 hours (Figure 35), ammonium was completely depleted at the next measurement point at 23 hours. In parallel to this depletion, the PHA accumulation increased significantly to a final concentration of 2.84 g/L.

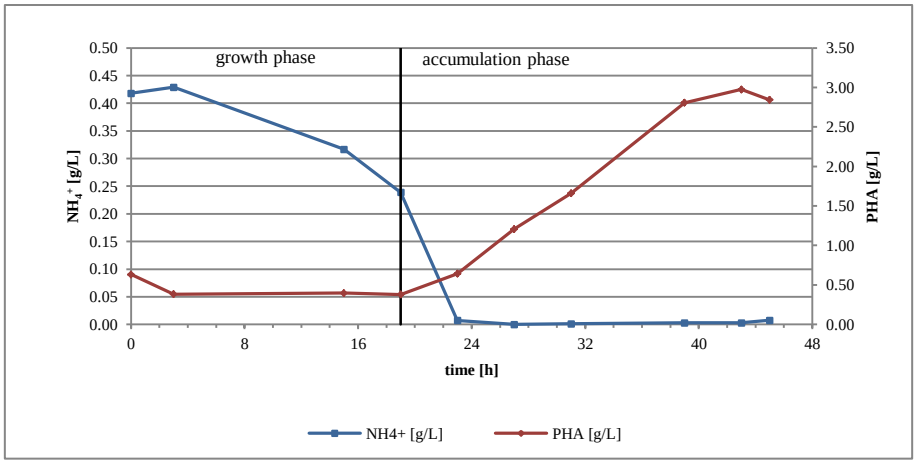

Figure 35. Depletion of NH_4^+ and accumulation of PHA

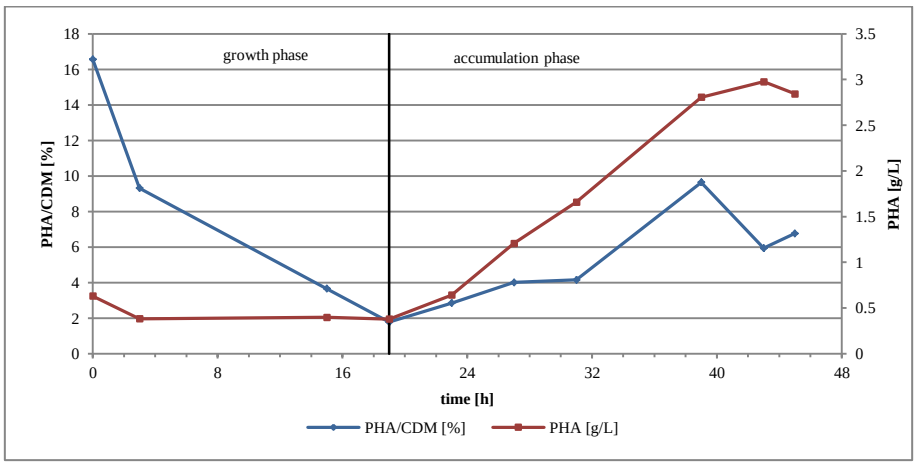

Figure 36. Share of PHA from total CDM and yield of total PHA of *Ps. citronellolis*.

As shown in Figure 36 the percentage of PHA reaches its highest value at the beginning of the fermentation, because PHA was already accumulated in the inoculation. The percentage of PHA from total CDM decreased until the restriction of nitrogen and increased afterwards to a maximum value of 9.654 % at 39 hours. The yield confirmed the data with low values during the growing phase ranging from 0.38 g/L to 0.63 g/L. After restriction of nitrogen source, the yield increased to 2.98 g/L at 43 hours. The composition of the *mcl*-PHA building blocks (Figure 37) kept constant over the entire process, except for C6 and C7, which were not detectable from 3 to 19 hours. Regarding the other measurement points, C7 had a percentage from 5.70 to 1.69 % and C6 from 11.17 to 6.32 %. The biggest fractions were C8 (32.40 to 46.47 %) and C10 (29.77 to 40.72 %). The percentage of C9 decreased during the fermentation from about 9 % to 2.62 %. C12 was between 6.90 and 15.48 % over the whole experiment. The maximum yield of C8 was 1.37 g/L and 1.07 g/L for C10 after 43 hours. The analysis of the composition showed that the main building blocks of PHA consist of C8 and

C10. This indicates that the provided fatty acids were not degraded completely by the ß-oxidation.

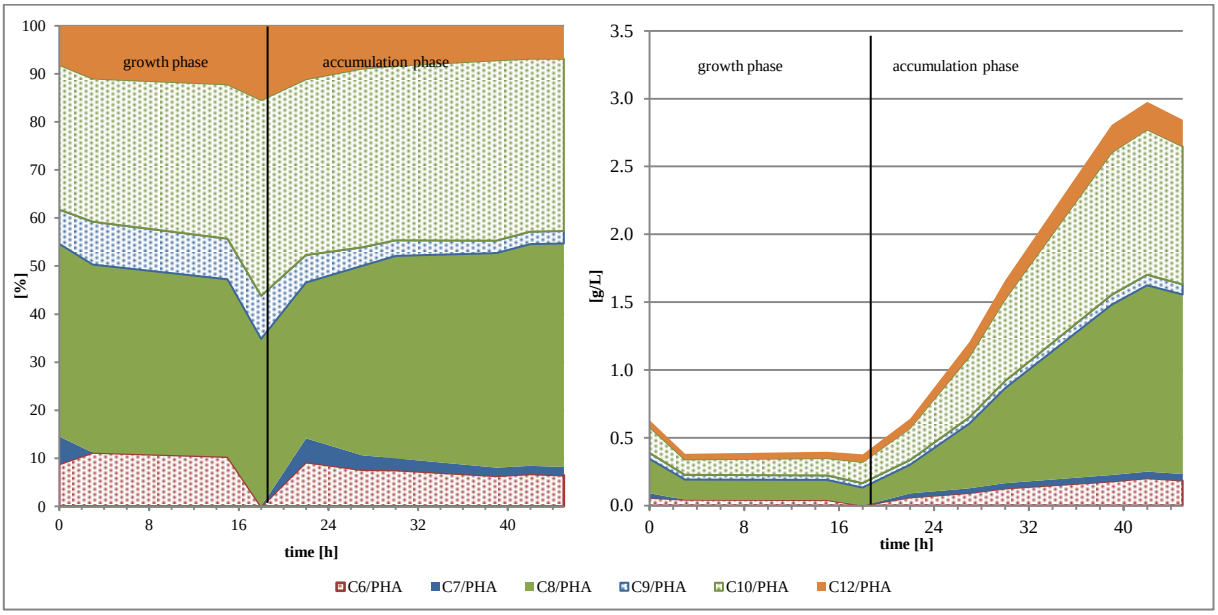

Figure 37. Concentration, composition and shares of *mcl*-PHA.

In the beginning the PHA production rates were negative, indicating that PHA was degraded, and biomass production was the predominant on-going during this phase. After restriction of the nitrogen source the PHA production rates were increasing until they drop again after 39 hours. The trend of PHA production rates (Figure 38) also correlated with the trend of PHA accumulation shown in Figure 34. The rates were negative at the beginning, when PHA was degraded and after nitrogen depletion, the productions rates became positive which means that PHA was accumulated. C8 and C10 showed the highest production rates (Figure 39) which correlates to the high amount of these building blocks. The production rates of PHA and its components were negative during the first 15 hours of the fermentation. The slightly increase of the CDM let assume that PHA was used for maintenance and growth. After 15 hours the CDM production rate started to increase as well as the production rates of the PHA components C8 and C10 (Figure 39). The production rate of the biomass was between 0.18 and 2.62 g/Lh during growth phase and drops to -1.49 g/Lh at 39 hours due to cell death. The following increase of biomass to 5.21 g/Lh correlated with the PHA production rate which decreased after 39 hours indicating that PHA was degraded in favour of biomass accumulation.

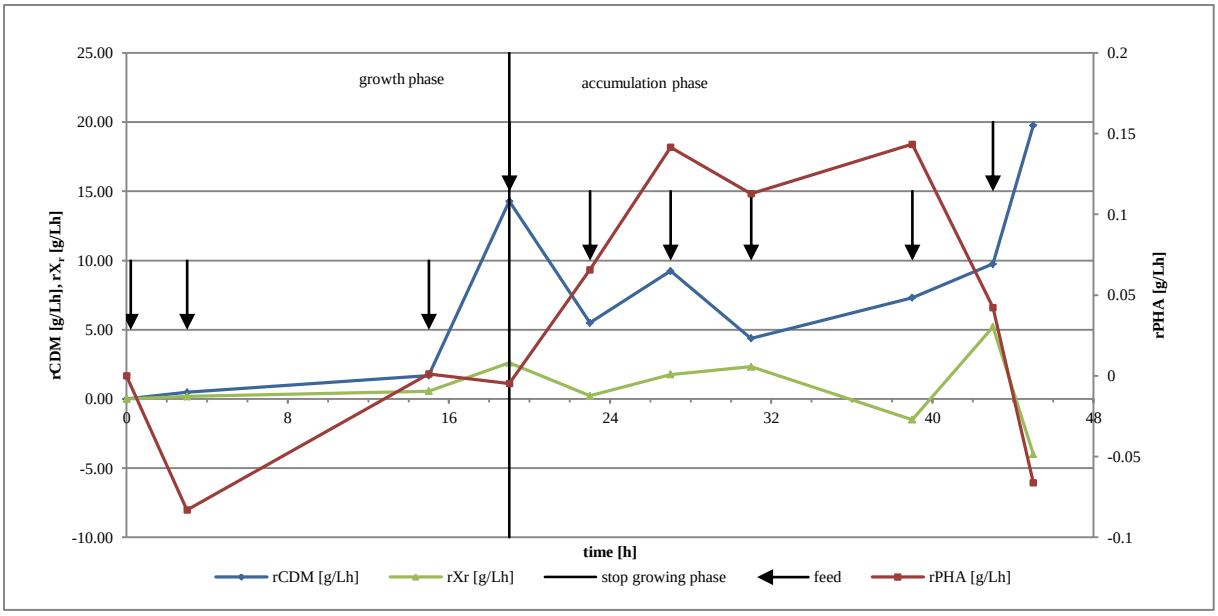

Figure 38. Production rates of CDM, Xr and PHA of *Ps. citronellolis* 2nd fermentation.

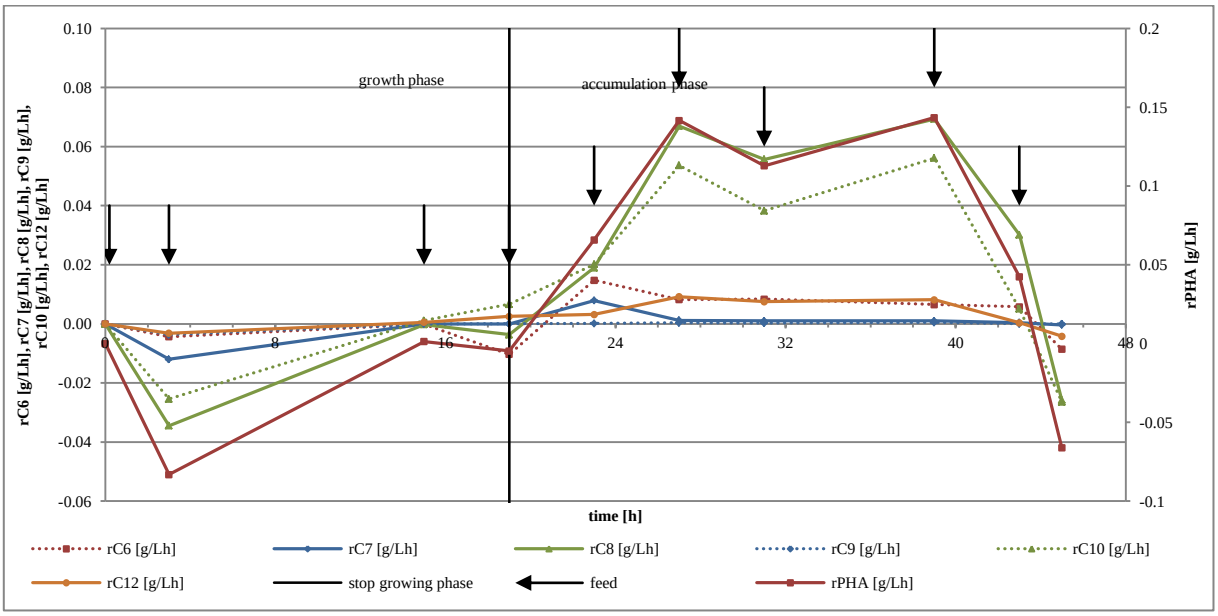

Figure 39. Production rates of components of PHA of *Ps. citronellolis* 2nd fermentation.

As shown in Figure 40 the trend of the specific production rates of the PHA components is similar to the trend of PHA formation. The higher specific production rates of C8 and C10 confirm that they are the main components. The graph of the specific production rates of CDM, X_r and PHA (Figure 31) is similar to the production rates. The values differ from the production rates because the specific production rate refers to the mean value of active biomass calculated with Eq. (13).

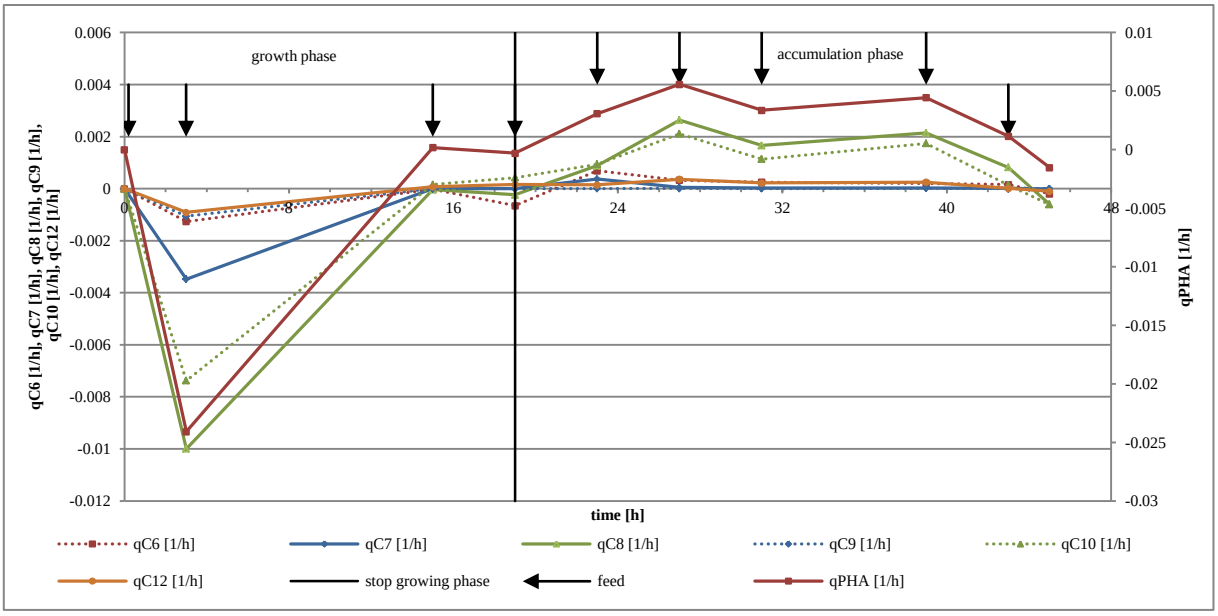

Figure 40. Specific production rates of components of PHA of *Ps. citronellolis* 2nd fermentation.

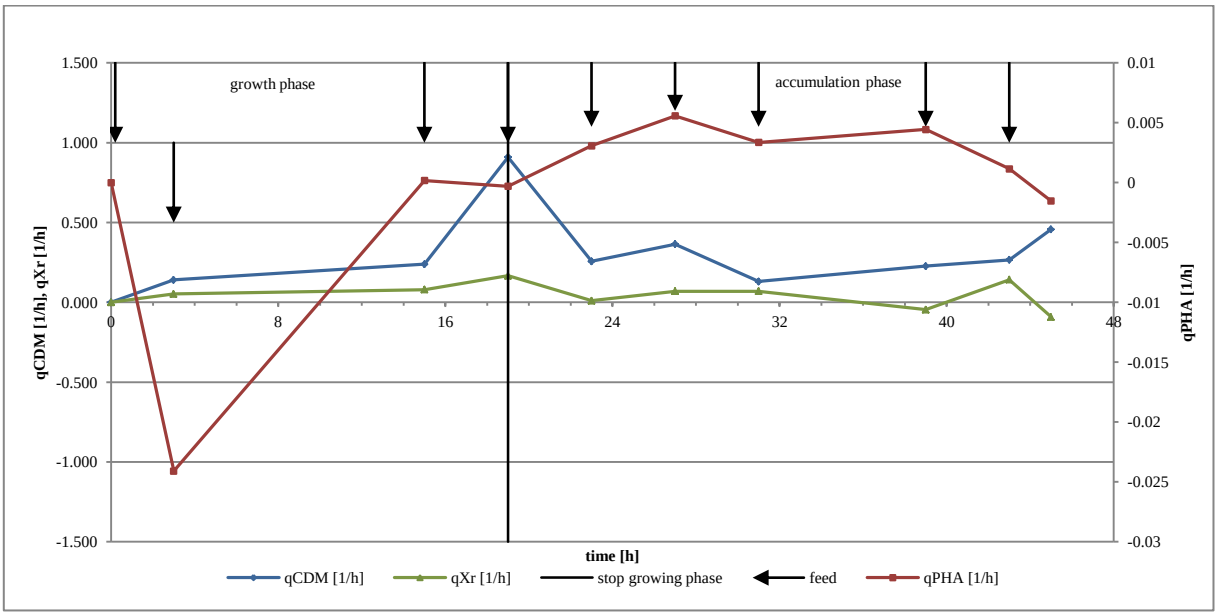

Figure 41. Specific production rates of CDM, Xr and PHA of *Ps. citronellolis* 2nd fermentation.

After the shutdown of the fermentation the fermentation broth was pasteurised and treated with H_2SO_4 as already mentioned in the experimental set up (see chapter 6.2.2). Finally the lyophilised biomass was used for the PHA isolation as described in chapter 4.9. After all degreasing and isolation steps, the *de facto* amount of PHA was 2.99 g/L.

6.3. *Pseudomonas chlororaphis* as production strain

6.3.4. Aim of the experiment

Ps. chlororaphis showed fast growth during preliminary experiments but rather modest PHA accumulation. Nevertheless, because growth behaviour is an important selection criterion for industrial use fermentation, laboratory bioreactor scale fermentation was done with this strain.

6.3.5. Experimental setup

The fermentation was performed with a total volume of 2 litres. First, the sterile reactor was filled with 1 litre of adapted Kueng medium without biodiesel. Second, the inoculum of 1 litre was added. For the inoculum 4 x 250 mL adapted Kueng media with 5 g/L biodiesel was inoculated with 2 mL of a preculture (average OD_{420} of 5.85) and incubated for 3 days at 30 °C. The average OD_{420} of the inoculum was 8.96. Finally, the biodiesel was added at a concentration of 5 g/L into the reactor.

During fermentation the broth was kept at 30 °C, the oxygen supply (40 % during growth phase and 20 % during accumulation phase) was regulated by the stirrer (initially 400 rpm). The first sample was taken immediately after inoculation. During lag phase no samples were taken. The second sample was taken after 12 hours and afterwards every 3 hours. The sample was used for OD_{420} and CDM determination, the ammonium fast and accurate tests. In addition the fermentation was monitored *via* microscope for cell behaviour and monosepsis. The decision for feeding was made after examining the presence of biofuel droplets under the microscope. After 27 hours an OD_{420} of 148.5 was reached and the nitrogen source was restricted by changing the base from NH_4OH to NaOH to induce the accumulation phase. The fermentation was shut down after 49 hours when the OD_{420} decreased. The broth was pasteurized (70 °C, 1h) and afterwards centrifuged for 20 min at 5 000 rpm (Sorvall RC-5B, F10S-6x500, *Thermo Scientific*). The supernatant was discarded and the pellet was lyophilised and used for PHA isolation.

6.3.6. Results and Discussion

The fermentation was started with an average OD_{420} of 7.25. As displayed in Figure 42 there was no distinct lag, exponential or stationary phase visible. The limitation of the nitrogen source was done at an average OD_{420} of 148.5 after 27 hours. The optical density increased during the accumulation phase, except an aberration at 36 hours, and reached a maximum value of 253 at 45 and 48 hours. After 49 hours and an OD_{420} of 223.5 the fermentation was

shut down. The slope of the linear regression (Figure 42) is equal to maximum specific growth rate of 0.131 h^{-1}. The doubling time of 5.37 hours was calculated with Eq. (11).

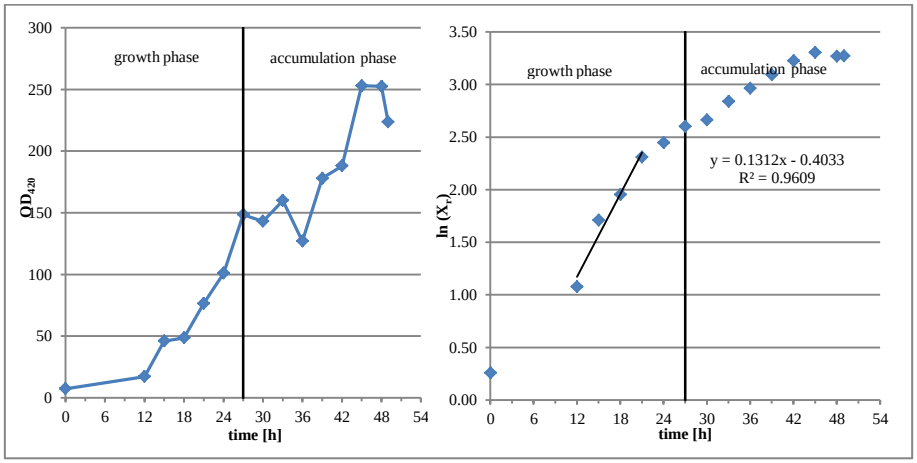

Figure 42. Growth scheme of *Ps. chlororaphis*.

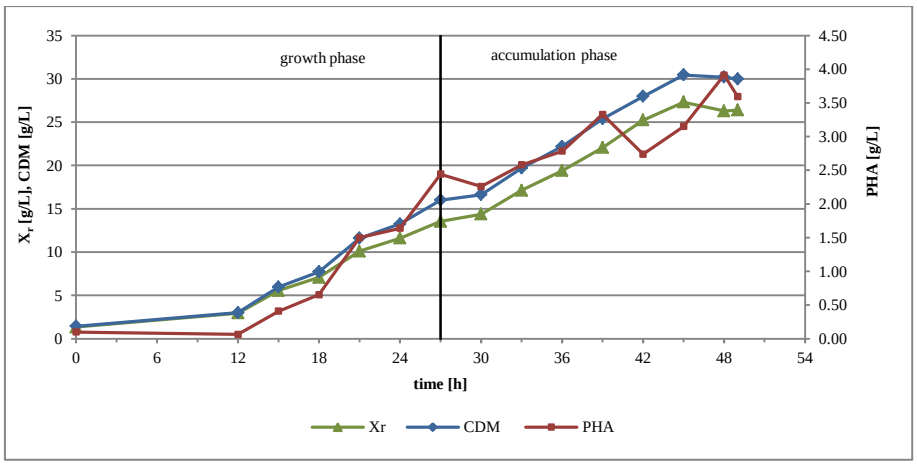

Figure 43. Correlation of CDM, X_r and PHA values from the fermentation with *Ps. chlororaphis*.

Cell dry mass, X_r and PHA showed an increasing trend during the entire process, except discrepancies of PHA during the first 12 hours and at the sampling point after 42 hours (Figure 43). CDM reached its maximum value of 30.45 g/L and X_r the value of 27.30 g/L after 45 hours. PHA content reached its maximum after 48 hours with 3.91 g/L. There is no difference visible between growing phase and accumulation phase concerning X_r, CDM and PHA accumulation. Since PHA was accumulated during the entire process, hence also during balanced microbial growth, it seemed that *Ps. chlororaphis* accumulates PHA in a growth associated way. Even though the nitrogen supply was restricted after 27 hours, there was no depletion until the fermentation shutdown (Figure 44). However, the ammonium concentration did decrease from 3.26 g/L at 27 hours to 0.89 g/L at 49 hours.

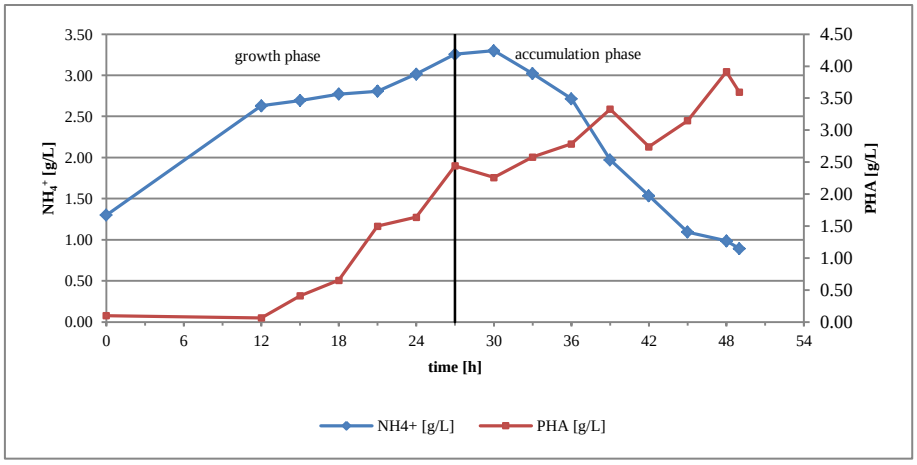

Figure 44. Graph of nitrogen depletion and PHA accumulation.

As shown in Figure 45, the PHA share of total CDM was 6.87 % in the beginning of the fermentation because of the low biomass concentration (1.34 g/L). During the first 12 hours the percentage decreased to 2.10 % and increased afterwards to a maximum of 15.27 % at 27 hours. From this sampling point on, the share slightly decreased and, at the end of the fermentation at 49 hours, the value was 11.99 % (3.59 g/L). No increase of PHA percentage in total CDM after the nitrogen limitation was detectable which again possibly indicates growth associated PHA accumulation.

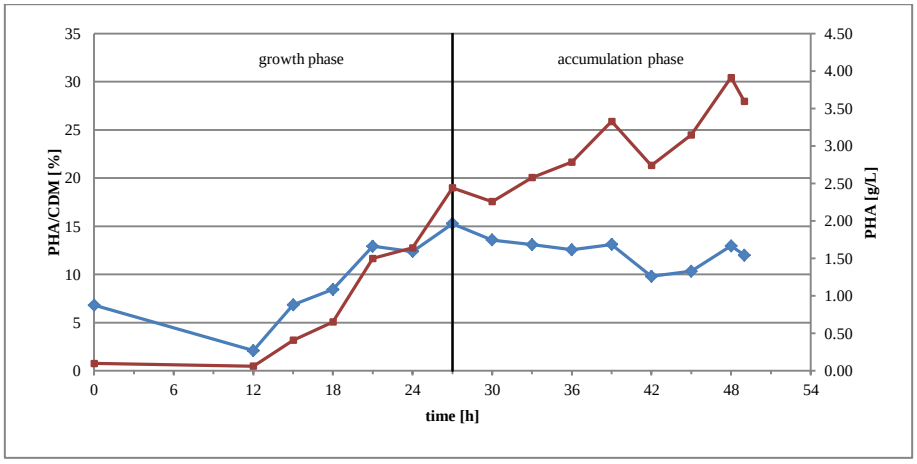

Figure 45. Shares of PHA from total CDM and PHA accumulation of *Ps. chlororaphis*.

The distribution of PHA building blocks (Figure 46) remained constant after 21 hours. The C6 share from total PHA increased from 5.35 % at the beginning to 14.32 % after 30 hours and remained constant for the remaining process at about 15 %. In the beginning of the fermentation C7 building blocks had a share of 24.22 % from total PHA, which decreased within 12 hours to 0 % and increased again to 4.03 % after 15 hours. The C7 share decreased

further until the end of the fermentation to 1.11 %. The main component was C8 with a steady percentage of 41% to approximately 51 % after the first 15 hours. Before this, the percentage was about 15 %. The maximum concentration of C8 was obtained at 42 hours with 2 g/L. The share of the C9 building blocks started with 48 % and afterwards from 7 to 2 % over the entire process. The percentage of C10 was constant between 24 and 28 % (0.02 to 0.98 g/L), except for the first measurement (7.49 %). The C12 building blocks also had a low share at the first measurement with 2.97 %. During the rest of the fermentation the share was between 6 and 10 %.

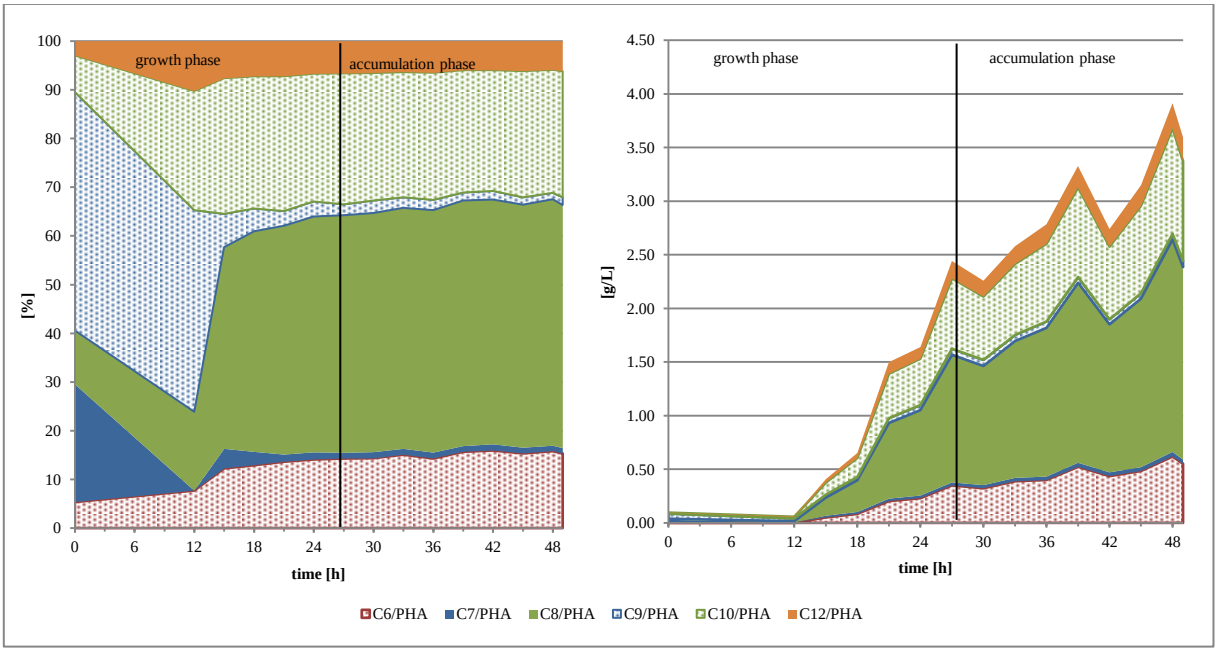

Figure 46. Concentration, composition and shares of *mcl*-PHA.

The production rates of PHA, C6, C8 and C10 (Figure 47) show a similar trend. The main component C8 had the highest product formation rate. In comparison the production rates of CDM, X_r and PHA (Figure 48) supported the assumption of growth associated *mcl*-PHA biosynthesis. With an increasing production rate of CDM and X_r, the PHA formation increased also. Only at the end of the fermentation, PHA formation showed an inverse trend. No difference was encountered concerning the production rates during the process except at the beginning and the end.

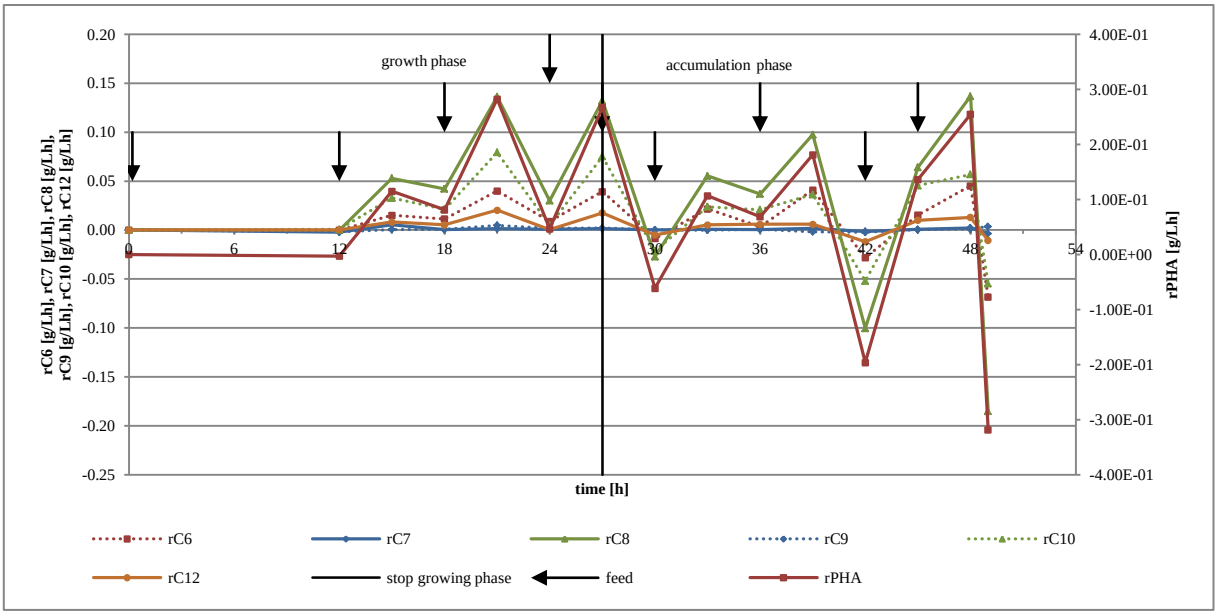

Figure 47. Production rates of C6, C7, C8, C9, C10, C12 and PHA of *Ps. chlororaphis*.

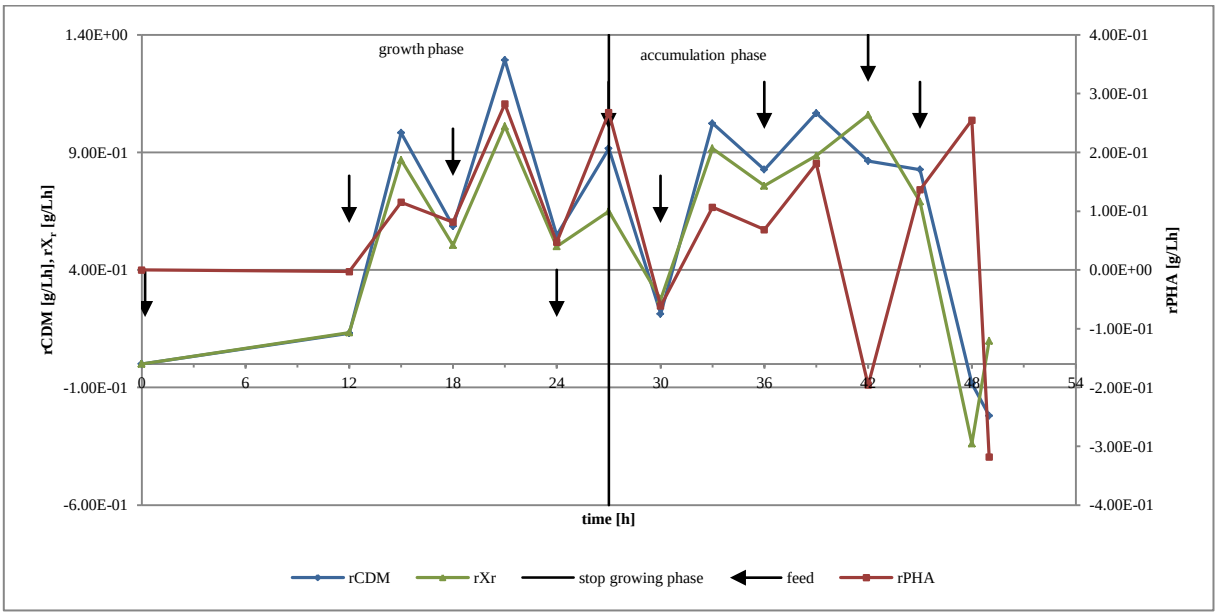

Figure 48. Production rates of CDM, X_r and PHA of *Ps. chlororaphis*.

During the accumulation phase the specific production rates were at a lower level than during growth phase (Figure 49 and Figure 50). Assuming growth associated *mcl*-PHA accumulation, the reduction of the biomass production due to nitrogen limitation also influences PHA formation.

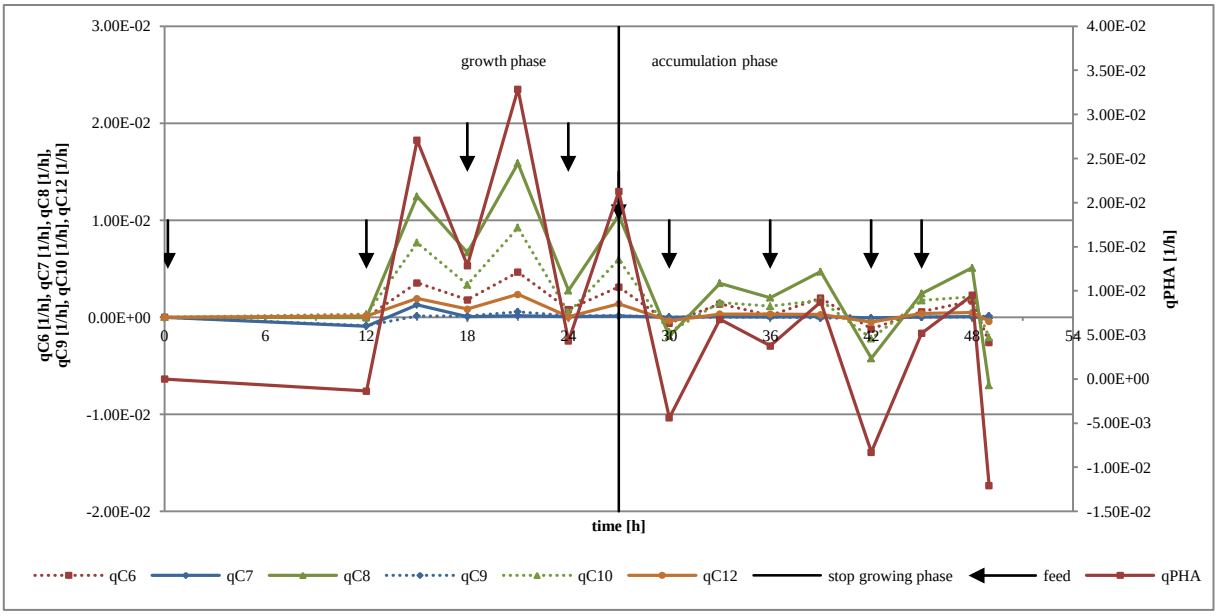

Figure 49. Specific production rates of C6, C7, C8, C9, C10, C12 and PHA of *Ps. chlororaphis*.

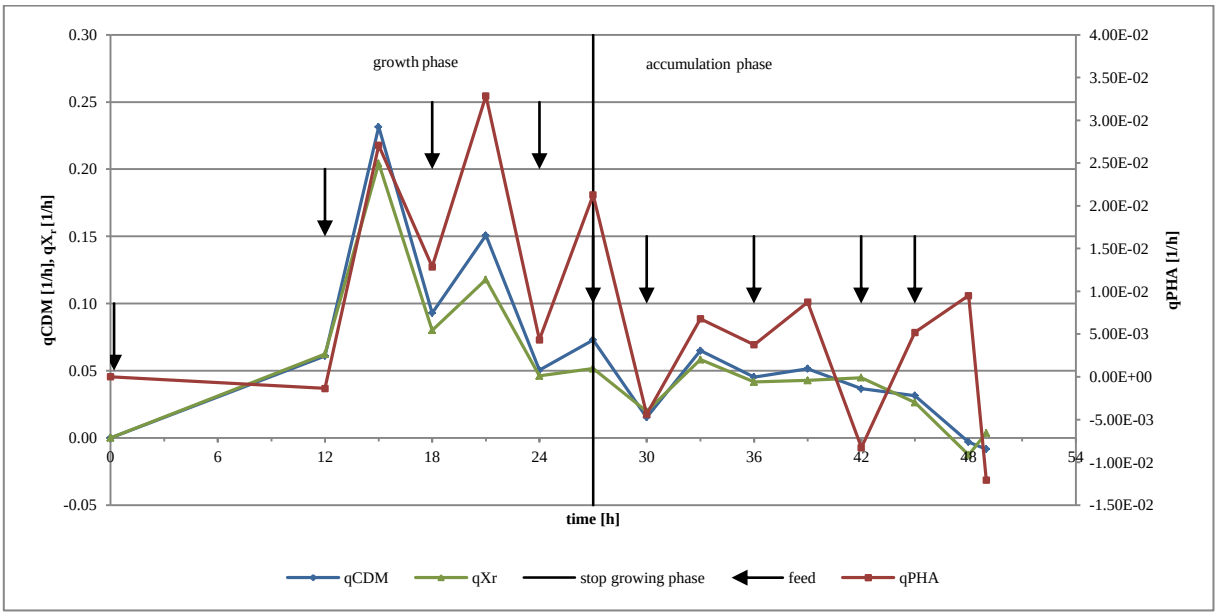

Figure 50. Specific production rates of cell dry mass, biomass and PHA of *Ps. chlororaphis*.

After 49 hours the fermentation was shut down and the fermentation broth was pasteurised and lyophilised. The lyophilised biomass was used for the PHA isolation as described in chapter 4.9. After all degreasing and isolation steps, 1.02 g/L PHA were obtained. The texture of the isolated PHA was resin-like (Figure 51).

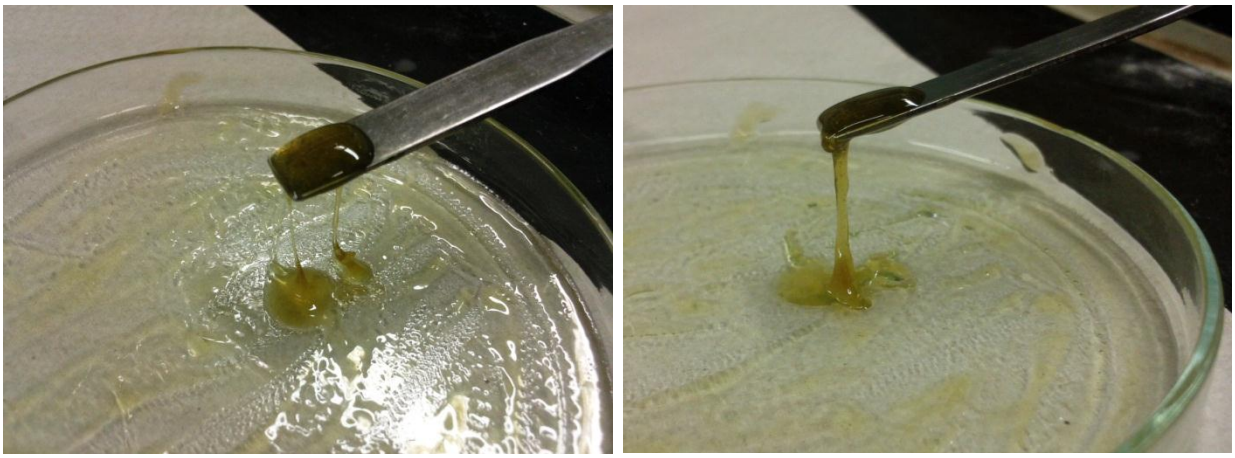

Figure 51. *mcl*-PHA accumulated by *Pseudomonas chlororaphis* during growth with 5 g/L biodiesel.

6.4. *Pseudomonas putida* GPo1 as production strain

6.4.1. Aim of the experiment

Ps. putida GPo1 is the only strain among the strains experimentally tested in this thesis which was already tested for PHA accumulation under controlled conditions (Durner *et al.*, 2000, 2001; Zinn *et al.*, 2011). In comparison to the other strains no adequate growth rate was achieved. However, good PHA accumulation during the preliminary experiments was encountered. Because of this fact and for use as a reference strain, laboratory scale fermentation was done with *Ps. putida* GPo1.

6.4.2. Experimental setup

The fermentation was conducted with a total volume of 2 litres. First, the sterile reactor was filled with 1 litre of adapted Kueng media without biodiesel. Second, the inoculum of 1 litre was added. For the inoculum 4 shaking flasks, each with 250 mL adapted Kueng media and 5 g/L biodiesel were inoculated with 5 mL of a preculture (average OD_{420} of 4.29) and incubated for 4 days at 30 °C. Afterwards the inoculum was added at an average OD_{420} of 7.4. Finally, biodiesel was added into the reactor at a concentration of 5 g/L.

During fermentation, the broth was kept at 30 °C, the oxygen supply (pO_2 40 % during growth phase and 20 % during accumulation phase) was regulated by the stirrer (initially 400 rpm). The first sample was taken immediately after inoculation. During lag phase no samples were taken. The second sample was taken after 12 hours and subsequently every 3 hours. The sample was used for OD_{420} and CDM determination as well as the ammonium fast test and the accurate test. In addition the fermentation was monitored *via* microscope for growth behaviour and monosepsis. The decision to feed was made after examining the presence of biofuel droplets under the microscope. After 60 hours an OD_{420} of 43.4 was reached and the nitrogen source was limited by changing the base from NH_4OH to NaOH in order to induce the accumulation phase. The fermentation was ended after 72 hours when the OD_{420} values decreased. The broth was pasteurized (70 °C, 1h) and centrifuged afterwards for 20 min at 5 000 rpm (Sorvall RC-5B, F10S-6x500, *Thermo Scientific*). The supernatant was discarded, the pellet lyophilised and used for PHA isolation.

6.4.3. Discussion and results

The fermentation was started with an OD_{420} of 5.75. During the growth phase no distinct lag phase, exponentional phase and stationary phase were visible. Between 24 and 33 hours the

OD_{420} was constant about 28 and decreased afterwards to 18 after 36 hours. It could be assumed that *Ps. putida* GPo1 had an stationary phase but the significant aberration after 45 hours indicates that the alternating values were resulting from light scatering during OD_{420} measurements due to the biodiesel droplets present in the broth. The maximum value was reached after 69 hours at 66.65. After 72 hours the fermentation was ended after a slight decrease of the OD_{420} to 63.95 and depeltion of the fermentation broth volume in the reactor. Since the calculated doubling time of 40.77 hours (Eq. (11)) and a reactor volume of 2 litres the fermenation was limited by the volume in the reactor after 72 hours. Furthermore, due to the depeltion, no reliable oxygen and pH-value measurement was possible anymore. The maximum specific growth rate was 0.017 h^{-1}.

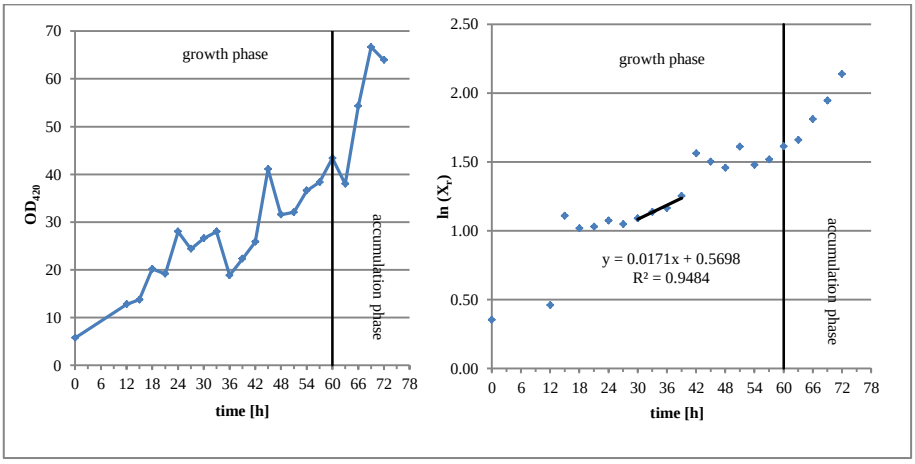

Figure 52. Growth scheme of *Ps. putida* GPo1.

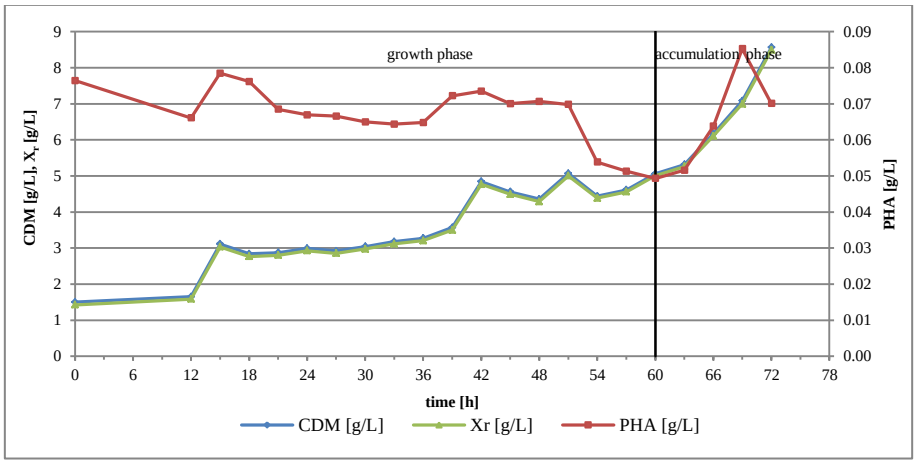

Figure 53. Correlation of CDM, X_r and PHA of *Ps. putida* GPo1.

Cell dry mass and X_r showed an increasing trend over the entire process. Both graphs had a nearly equal course and reached their maximum value after 72 hours with 8.56 g/L and 8.49 g/L (Figure 53). Although the PHA accumulation increased after nitrogen restriction no

obvious accumulation phase was achieved. Because in contrast to *a priori* expectation no nitrogen limitation was accomplished (Figure 54) and further growth occurred. The PHA concentration remained constant until 54 hours between 0.06 and 0.08 g/L and decreased afterwards to 0.05 g/L. It remained constant again until an increase after 63 hours and reached a maximum at 0.085 g/L at 69 hours. During fermentation shutdown the concentration decreased again to 0.07 g/L. The reported CDM of 18 to 53 g/L during growth on sodium octanoate could not be reached (Elbahloul & Steinbüchel, 2009).

The ammonium supply (Figure 54) varied with the changes in the pH value. At 15 hours the pH value was set from 7.0 to 7.1 for ammonium addition for growth acceleration. After 30 hours the pH-value was set to 7.2 for further growth acceleration. This pH value set up was done because *Ps. putida* GPo1 showed insufficient growth to enable an automatically controlled ammonium supply *via* the pH control. In comparison with Figure 53 the ammonium consumption correlated with X_r and CDM. The ammonium concentration decreased slightly after 12 hours and X_r and CDM increased. After 36 hours, the ammonium concentration reached 0.73 g/L. This high concentration led to an increment of CDM and X_r values after 42 hours. As expected, the ammonium concentration decreased after ammonium limitation after 60 hours. No complete depletion of nitrogen source was achieved because the fermentation was shut down before.

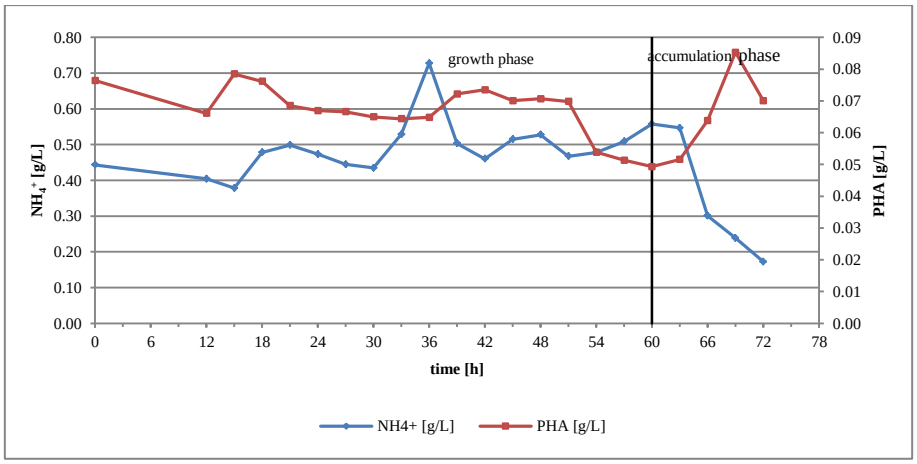

Figure 54. Depletion of nitrogen source of *Ps. putida* GPo1.

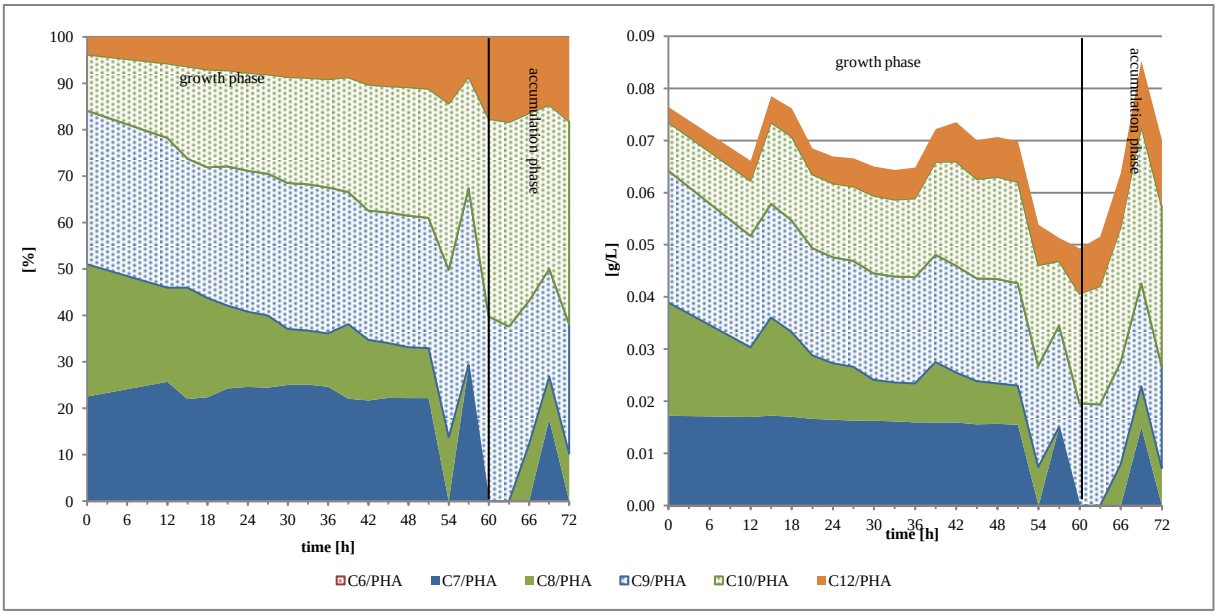

Figure 55. Concentration, composition and shares of *mcl*-PHA content of *Ps. putida* GPo1.

The composition of *mcl*-PHA (Figure 55) remained constant through 51 hours. No C6 was detected. The percentage of C7 of total PHA was between 22 and 25 %, decreasing after 51 hours to 0 % at 54 hours. During the further process C7 was detected twice: after 57 hours with 29.41 % (0.015 g/L) and after 69 hours with 17.66 % (0.015 g/L). The amount of C8 decreased from 28.51 % (0.22 g/L) to 0 % within 57 hours. After 66 hours until 72 hours C8 was detected with a percentage of 9 to 12 % (about 0.007 g/L). The amount of C9 was 28 and 40 % (about 0.02 g/L) over the entire process. The percentage of C10 increased form 12.10 % (0.009 g/L) in the beginning to 42.56 % (0.02 g/L) at the end of the fermentation. C12 increased from 3.77 % (0.003 g/L) to 17.63 % (0.009 g/L).

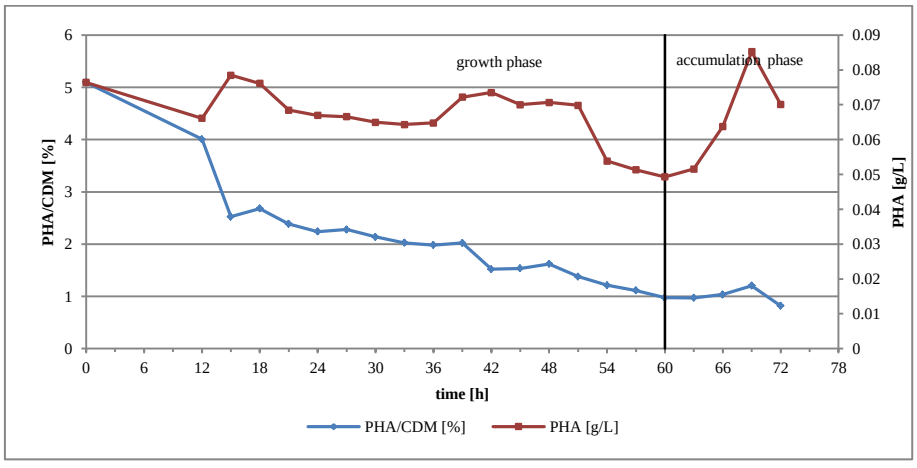

Figure 56. Percentage scheme of PHA from total CDM of *Ps. putida* GPo1.

The content of PHA from total CDM (Figure 56) decreased over the entire process; the yield of PHA remained at a constant level with 0.065 g/L to 0.085 g/L. In general biomass production did not cease for the benefit of PHA accumulation because no nitrogen depletion was accomplished.

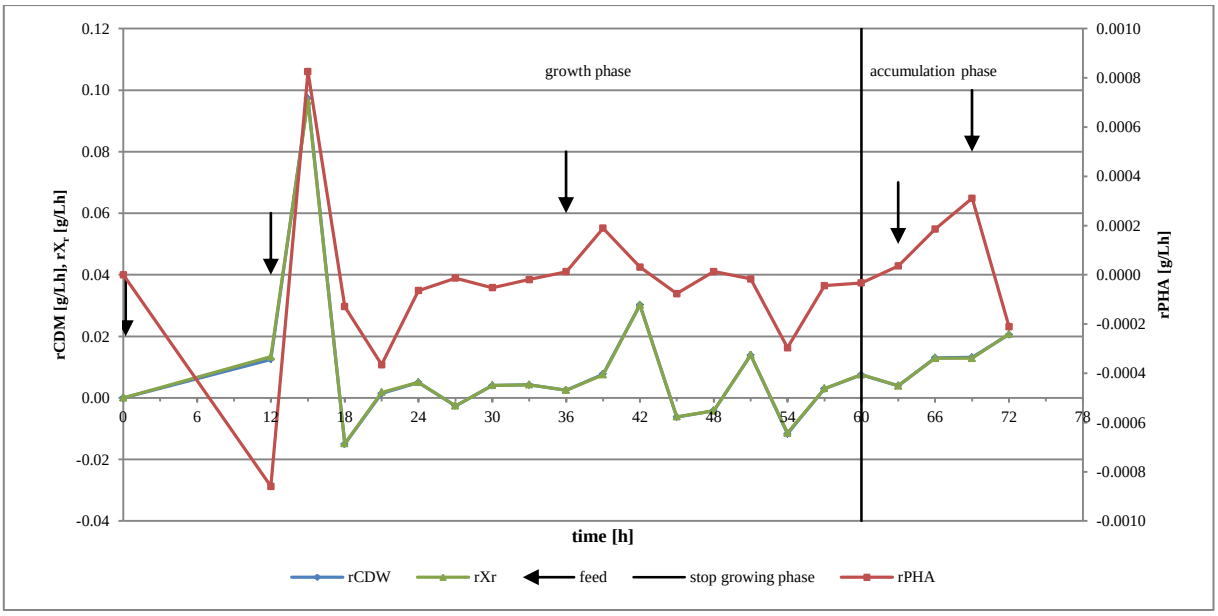

Figure 57. Production rates of CDM, X_r and PHA

The production rates of CDM, X_r and PHA (Figure 57) increased after feeding, providing the digestible carbon source. During the first 12 hours PHA was degraded in favour of biomass accumulation. The PHA degradation could have been prevented with a higher biodiesel concentration in the beginning. During the following process the production rates showed a similar trend.

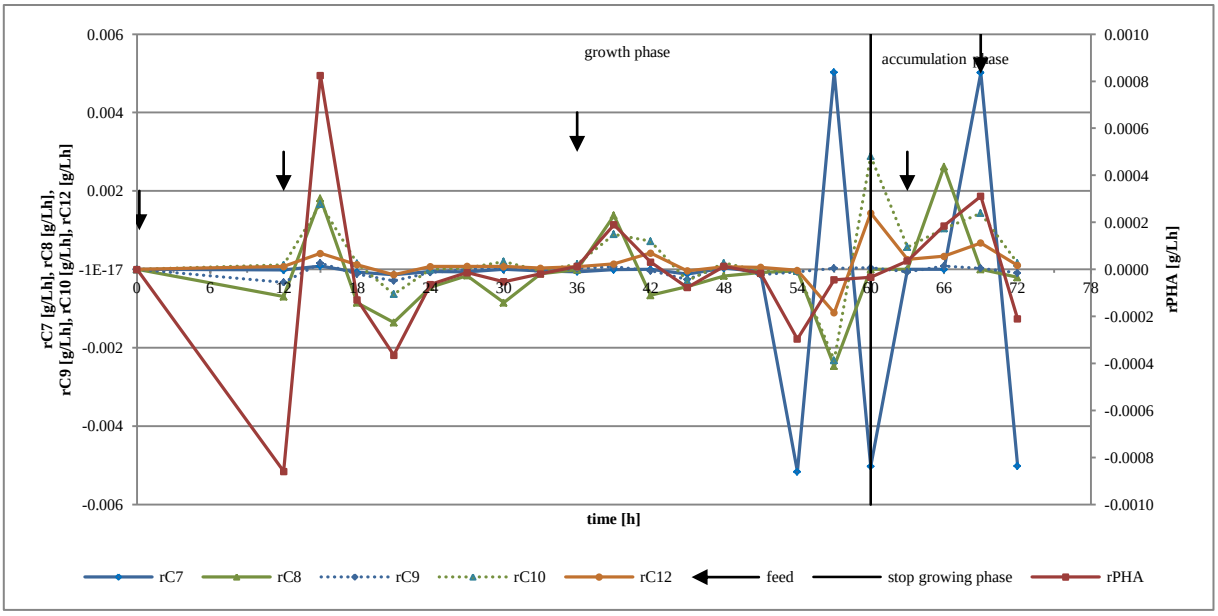

Figure 58. Production rates of C7, C8, C9, C10, C12 and PHA

The production rates of the PHA components (Figure 58 and Figure 59) showed similar trends to the PHA content during the first 51 hours. After each feeding, the rates showed a significant increase. The aberrations at 51 hours showed a lack of carbon source resulting in a significant decrease of C7. Depletion in C7 chains seemed to cause further degradation of higher carbon chains like C8 and C12. The lack of carbon source at 51 hours was also confirmed by the slight increase of CDM and X_r (see Figure 53), the decreasing PHA formation and the constant PHA concentration. At the last measurement point, too less carbon source seemed to have been supplied and PHA was degraded in favour of biomass accumulation.

The specific production rates (Figure 59 and Figure 60) were calculated using the mean catalytically active biomass and seemed to be more stable than the production rates.

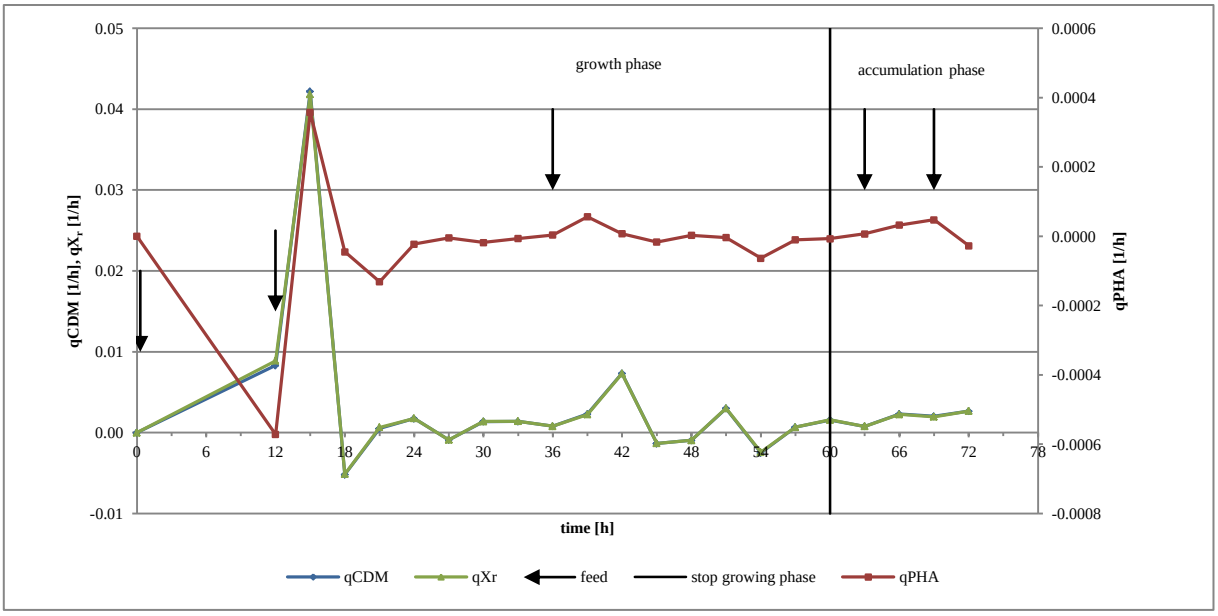

Figure 59. Specific production rates of CDM, X_r and PHA.

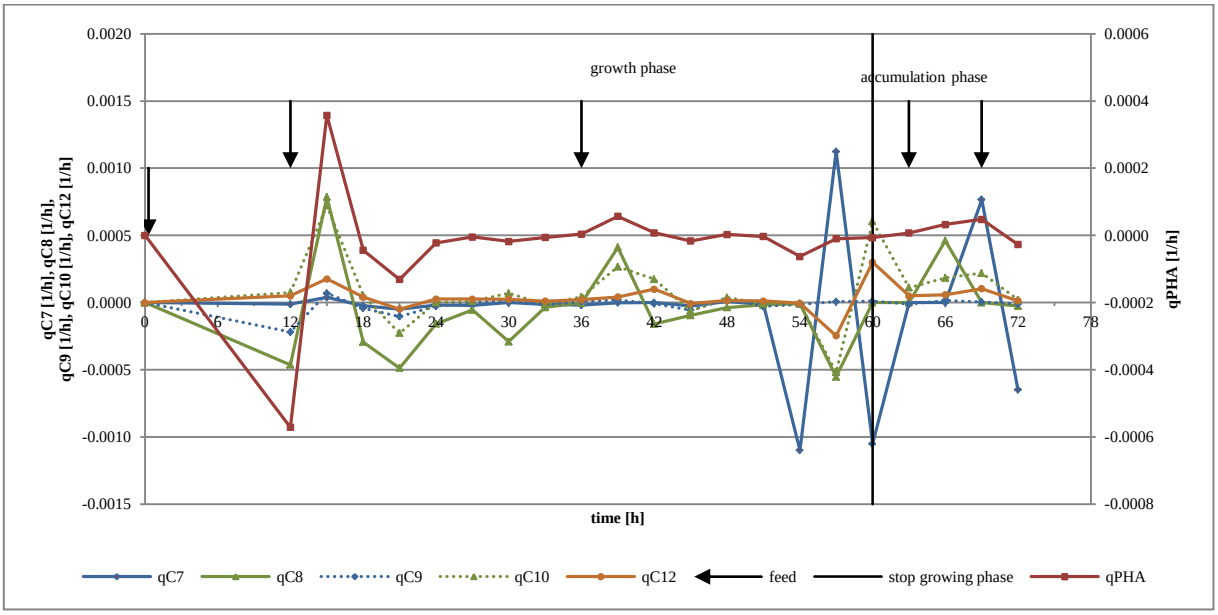

Figure 60. Specific production rates of C7, C8, C9, C10, C12 and PHA.

After the shutdown of the fermentation the fermentation broth was pasteurised and lyophilised. The lyophilised biomass was used for the PHA isolation, described in chapter 4.9, but no PHA at all could have been observed.

6.5. Comparison of the accomplished fermentations

Ps. citronellolis and *chlororaphis* are promising strains for *mcl*-PHA production. *Ps. citronellolis* accumulates PHA non growth associated whereas *Ps. chlororaphis* seemed to accumulate PHA growth associated. The composition of the accumulated PHA differs with the strain. However the differences are minor, and, as reported in literature (Kim *et al.*, 2007),

the composition of *mcl*-PHA should be more depending on the used substrate than on the organism.

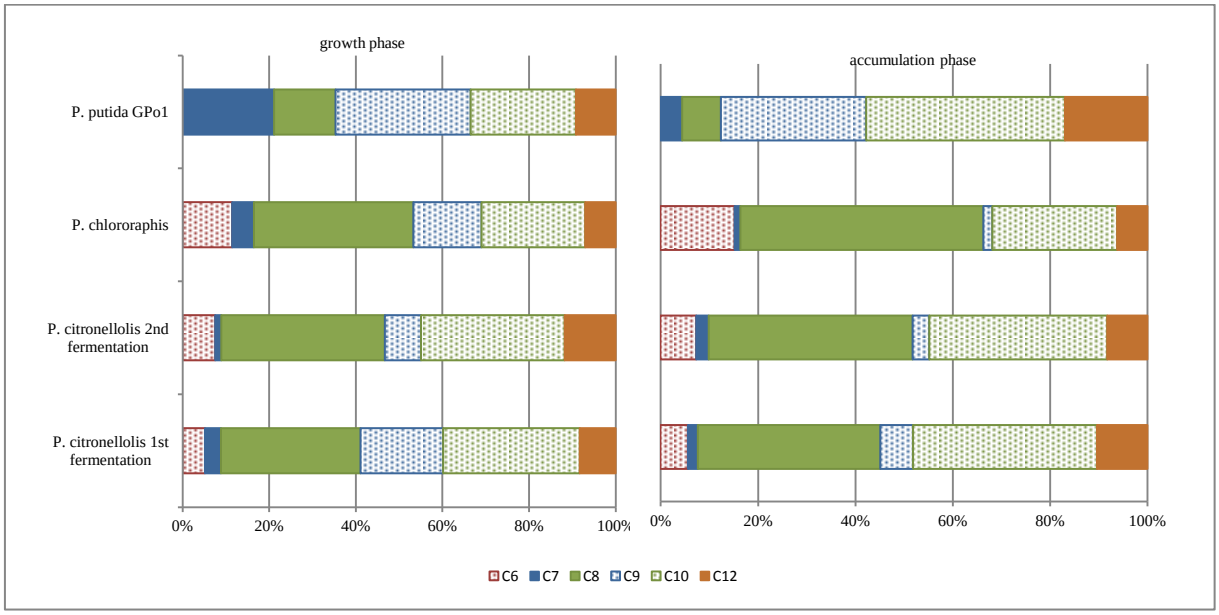

Figure 61. Comparison of the PHA composition in average.

A comparison of the average composition of all three fermentations (Figure 61) confirmed C8 (3-hydroxyoctonoate) and C10 (3-hydroxydecanoate) as the major components of PHA produced by *Ps. citronellolis* (see Figure 27 and Figure 37) and *Ps. chlororaphis* (see Figure 46), during the growing phase as well as during the accumulation phase. Whereas C7 (3-hydroxyheptanoate), C8 (3-hydroxyoctanoate), C9 (3-hydroxynonaoate) and C10 (3-hydroxydecanoate) are the main components of PHA accumulated by *Ps. putida* GPo1 during the growth phase. Although, no obvious accumulation phase was achieved the share of the components changed. In this rudimentary accumulation phase, C9 and C10 are the main components.

The fermentation parameters are displayed in Table 8. The second fermentation with *Ps. citronellolis* achieved a specific maximum growth rate of 0.10 h^{-1} and a doubling time of 6.73 hours, thus growing faster than during the first fermentation (0.08 h^{-1}; 8.45 hours). Although, the biodiesel concentration was higher at the second fermentation, the PHA per BF yield was lower (0.03 g/g) than observed in the first fermentation (0.05 g/g). The PHA yield, determined by the GC-FID analysis, was similar but the actual yield was lower for the second fermentation, whereby the actual yield is influenced

by the performance of the degreasing and isolation steps (see chapter 4.9). It is possible that biomass gets lost during the degreasing step or *mcl*-PHA during the extraction step.

Ps. chlororaphis showed the fastest max. specific growth rate (0.13 h^{-1}) and PHA yield, determined by the GC-FID analysis, was expected to be 3.59 g/L. However the actual yield of 1.02 g/L was lower. Concerning the PHA production rates and specific production rates and the yield, *Ps. chlororaphis* performs similar to *Ps. citronellolis*. *Ps. putida* GPo1 grew about 5 times slower than the other strains. Regarding this growth behaviour and the minor yield of PHA, *Ps. putida* GPo1 is not comparable with the other tested strains. Because it is a well investigated strain, the fermentation should be repeated to get comparable data. Although, no reference data are available for *Ps. citronellolis* and *Ps. chlororaphis* with growth on biodiesel, they seem to be well promising and eligible for further experiments.

Table 8. Fermentation parameters and yields

		Ps. citronellolis 1st fermentation	*Ps. citronellolis* 2nd fermentation	*Ps. chlororaphis*	*Ps. putida* GPo1
μ_{max}	[1/h]	0.08	0.10	0.13	0.02
t_d	[h]	8.45	6.73	5.29	40.77
rPHA	[g/Lh]	0.04	0.05	0.07	-8.80E-05
$rPHA_{acc}$	[g/Lh]	0.07	0.10	0.07	-0.02
qPHA	[1/h]	0.00	0.00	0.00	0.00
$qPHA_{acc}$	[1/h]	0.00	0.00	0.00	0.00
$Y_{CDM/BF}$	[g/g]	0.54	0.59	0.58	0.21
$Y_{PHA/BF}$	[g/g]	0.05	0.03	0.03	0.00
CDM max	[g/L]	32.19	50.12	30.45	8.56
PHA yield GC-FID	[g/L]	2.90	2.84	3.59	0.07
PHA yield indeed	[g/L]	4.27	2.99	1.02	no data

Part D: Outlook

As already mentioned in the introduction, *mcl*-PHAs are becoming an important alternative to fossil based plastics. Nevertheless, the focus is still on the production of *scl*-PHAs.

Sun *et al.* (2007) proposed a price of *mcl*-PHA produced by large-scale fermentation and octane as carbon source with US$ 5-10 per kg, whereby, the costs of the carbon source, the fermentation and downstream costs are reflected in equal shares.

To engage in price-competition with synthetic plastic mainly the downstream processing should be improved. Mostly, organic solvents are used for isolation of PHA. Unfortunately such solvents are expensive and are not environmental friendly. Not to harm the environment, organic solvents has to be recovered, which is again an expensive process.

Utilization of substrate is another major point in reducing process costs for PHA. To contrive this cheap substrates are needed. Cheap substrates are mainly received from by-products like whey from chees manufactures. Glycerol and low quality biodiesel, by-products from the biodiesel production, are also promising cheap carbon sources. In the case of the Animpol project, biodiesel is produced by slaughterhouse wastes and is therefore not in competition with edible resources. Although biodiesel is a good carbon source, the main focus was on biodiesel degradation in regard to environmental pollution. During the Animpol project a scientific breakthrough happened. Two new strains were detected, which are able to accumulate *mcl*-PHA during growth on biodiesel. These new strains, *Ps. citronellolis* and *Ps. chlororaphis,* seem to have a promising industrial relevance and investigations with these strains are going to be continued. One focus is devoted to the prolongation of the accumulation time, respectively to reduce the growth phase, and therefore to increase the PHA yield. The results obtained by *Ps. citronellolis* during this thesis are going to be published in the Journal “Reactive and Functional Polymers” in the near future (Muhr *et al.*, unpublished).

List of figures

References

De Almeida, P. & Silva, P. D. (2009). The peak of oil production—Timings and market recognition. *Energy Policy* **37**, 1267–1276.

Baptist, J. N., Gholson, R. K. & Coon, M. J. (1963). Hydrocarbon oxidation by a bacterial enzyme system. *Biochimica et Biophysica Acta* **69**, 40–47.

Bear, M. M., Mallarde, D., Langlois, V., Randriamahefa, S., Bouvet, O. & Guerin, P. (1999). Natural and artificial functionalized biopolyesters. II. Medium-chain length polyhydroxyoctanoates from *Pseudomonas strains*. *Journal of Environmental Polymer Degradation* **7**, 179–184.

Van Beilen, J. B., Wubbolts, M. G. & Witholt, B. (1994). Genetics of alkane oxidation by *Pseudomonas oleovorans*. *Biodegradation* **5**, 161–74.

Van Beilen, J. B., Panke, S., Lucchini, S., Franchini, A. G., Röthlisberger, M. & Witholt, B. (2001). Analysis of *Pseudomonas putida* alkane-degradation gene clusters and flanking insertion sequences: evolution and regulation of the *alk* genes. *Microbiology* **147**, 1621–1630.

Brandl, H., Gross, R. A., Lenz, R. W. & Fuller, R. C. (1988). *Pseudomonas oleovorans* as a source of poly(ß-Hydroxyalkanoates) for potential applications as biodegradable polyesters. *Applied and Environmental Microbiology* **54**, 1977–1982.

Braunegg, G., Sonnleitner, B. & Lafferty, R. M. (1978). A rapid gas chromatographic method for the determination of poly-ß-hydroxy-butyric acid in microbial biomass. *European Journal of Applied Microbiology and Biotechnology* **6**, 29–37.

Chen, J.-Y., Song, G. & Chen, G.-Q. (2006). A lower specificity PhaC2 synthase from *Pseudomonas stutzeri* catalyses the production of copolyesters consisting of short-chain-length and medium-chain-length 3-hydroxyalkanoates. *Antonie van Leeuwenhoek* **89**, 157–67.

Choi, M. H. & Yoon, S. C. (1994). Polyester biosynthesis characteristics of *Pseudomonas citronellolis* grown on various carbon sources, including 3-methyl-branched substrates. *Applied and Environmental Microbiology* **60**, 3245–3254.

Conte, E., Catara, V., Greco, S., Russo, M., Alicata, R., Strano, L., Lombardo, A., Di Silvestro, S. & Catara, A. (2006). Regulation of polyhydroxyalkanoate synthases (*phaC1* and *phaC2*) gene expression in *Pseudomonas corrugata*. *Applied microbiology and biotechnology* **72**, 1054–62.

DeSmet, M. J., Eggink, G., Witholt, B., Kingma, J. & Wynberg, H. (1983). Characterization of intracellular inclusions formed by *Pseudomonas oleovorans* during growth on octane. *Journal of Bacteriology* **154**, 870–878.

Doran, P. M. (2012). *Bioprocess Engineering Principles*, 2nd ed. London: Academic Press.

Durner, R., Zinn, M., Witholt, B. & Egli, T. (2001). Accumulation of poly[(R)-3-hydroxyalkanoates] in *Pseudomonas oleovorans* during growth in batch and chemostat culture with different carbon sources. *Biotechnology and Bioengineering* **72**, 278–88.

Durner, R., Witholt, B. & Egli, T. (2000). Accumulation of Poly [(R)-3-hydroxyalkanoates] in *Pseudomonas oleovorans* during growth with octanoate in continuous culture at different dilution rates. *Applied and Environmental Microbiology* **66**, 3408–3414.

Déziel, E., Lépine, F., Dennie, D., Boismenu, D., Mamer, O. a & Villemur, R. (1999). Liquid chromatography/mass spectrometry analysis of mixtures of rhamnolipids produced by *Pseudomonas aeruginosa* strain 57RP grown on mannitol or naphthalene. *Biochimica et Biophysica Acta* **1440**, 244–52.

Elbahloul, Y. & Steinbüchel, A. (2009). Large-scale production of poly(3-hydroxyoctanoic acid) by *Pseudomonas putida* GPo1 and a simplified downstream process. *Applied and Environmental Microbiology* **75**, 643–651.

Endres, H.-J. & Sieberts-Raths, A. (2009). *Technische Biopolymere*. München: Carl Hanser Verlag.

De Eugenio, L. I., García, P., Luengo, J. M., Sanz, J. M., Román, J. S., García, J. L. & Prieto, M. a. **(2007).** Biochemical evidence that *phaZ* gene encodes a specific intracellular medium chain length polyhydroxyalkanoate depolymerase in *Pseudomonas putida* KT2442: Characterization of a paradigmatic enzyme. *The Journal of Biological Chemistry* **282**, 4951–62.

European Commission: Bio-Economy Press Release. **(2012).** *Green plastics from the slaughterhouse. Bio-Economy Press Release*. http://ec.europa.eu/research/bioeconomy/press/press_release/index_en.htm [2012/12/04]

European Commission: Research and Innovation. **(n.d.).** ANIMPOL: Polymers and fuels from animal residues. http://ec.europa.eu/research/bioeconomy/biotechnology/projects/animpol_en.htm [2012/12/04]

European commission. **(2010).** *Animpol: Sustainable Plastics - Courtesy of the Slaughterhouse*. http://ec.europa.eu/research/bioeconomy/press/countries_projects/index_en.htm [2012/12/04]

Fiedler, S., Steinbüchel, A. & Rehm, B. H. a. **(2002).** The role of the fatty acid beta-oxidation multienzyme complex from *Pseudomonas oleovorans* in polyhydroxyalkanoate biosynthesis: Molecular characterization of the *fadBA* operon from *P. oleovorans* and of the enoyl-CoA hydratase genes *phaJ* from *P. oleovorans* and *Pseudomonas putida*. *Archives of microbiology* **178**, 149–60.

Fuhrer, T., Fischer, E. & Sauer, U. (2005). Experimental identification and quantification of glucose metabolism in seven bacterial species. *Journal of Bacteriology* **187**, 1581–1590.

Furrer, P., Panke, S. & Zinn, M. (2007). Efficient recovery of low endotoxin medium-chain-length poly([R]-3-hydroxyalkanoate) from bacterial biomass. *Journal of Microbiological Methods* **69**, 206–13.

Förster-Fromme, K. & Jendrossek, D. (2010). Catabolism of citronellol and related acyclic terpenoids in pseudomonads. *Applied Microbiology and Biotechnology* **87**, 859–69.

Gross, R. A., Demello, C. & Lenz, R. W. (1989). Biosynthesis and characterization of poly(ß-hydroxyalkanoates) produced by *Pseudomonas oleovorans*. *Macromolecules* **22**, 1106–1115.

Haynes, W. C. & Rhodes, L. J. (1962). Comparative taxonomy of crystallogenic strains of *Pseudomonas aeruginosa* and *Pseudomonas chlororaphis*. *Journal of Bacteriology* **84**, 1080–1084.

Hazer, B. & Steinbüchel, A. (2007). Increased diversification of polyhydroxyalkanoates by modification reactions for industrial and medical applications. *Applied Microbiology and Biotechnology* **74**, 1–12.

Hoffmann, N., Steinbüchel, A. & Rehm, B. H. (2000). The *Pseudomonas aeruginosa phaG* gene product is involved in the synthesis of polyhydroxyalkanoic acid consisting of medium-chain-length constituents from non-related carbon sources. *FEMS Microbiology Letters* **184**, 253–9.

Huijberts, G. N., Eggink, G., de Waard, P., Huisman, G. W. & Witholt, B. (1992). *Pseudomonas putida* KT2442 cultivated on glucose accumulates poly(3-hydroxyalkanoates) consisting of saturated and unsaturated monomers. *Applied and environmental microbiology* **58**, 536–44.

Huijberts, G. N., de Rijk, T. C., de Waard, P. & Eggink, G. (1994). 13C nuclear magnetic resonance studies of *Pseudomonas putida* fatty acid metabolic routes involved in poly(3-hydroxyalkanoate) synthesis. *Journal of Bacteriology* **176**, 1661–6.

Huisman, G. W., de Leeuw, O., Eggink, G. & Witholt, B. (1989). Synthesis of poly-3-hydroxyalkanoates is a common feature of fluorescent *Pseudomonads*. *Applied and Environmental Microbiology* **55**, 1949–54.

Huisman, G. W., Wonink, E., Meima, R., Kazemier, B. & Terpstra, P. (1991). Metabolism of poly(3-hydroxyalkanoates) (PHAs) by *Pseudomonas oleovorans*. *The Journal of Biological Chemistry* **266**, 2191–2198.

Jacques, R. J. S., Santos, E. C., Bento, F. M., Peralba, M. C. R., Selbach, P. A., Sá, E. L. S. & Camargo, F. A. O. (2005). Anthracene biodegradation by *Pseudomonas* sp. isolated from a petrochemical sludge landfarming site. *International Biodeterioration & Biodegradation* **56**, 143–150.

Jacques, R. J. S., Santos, E. C., Haddad, R., Catharino, R. R., Eberlin, M. N., Bento, F. M. & Oliveira Camargo, F. A. de. **(2008).** Mass spectrometry analysis of surface tension reducing substances produced by a PAH-degrading *Pseudomonas citronellolis* strain. *Brazilian Journal of Microbiology* **39**, 353–356.

Jendrossek, D., Schirmer, A. & Schlegel, H. G. (1996). Biodegradation of polyhydroxyalkanoic acids. *Applied Microbiology and Biotechnology1* **46**, 451–463.

Kanner, D., Gerber, N. N. & Bartha, R. (1978). Pattern of phenanzine pigment production by a strain of *Pseudomonas aeruginosa*. *Journal of Bacteriology* **134**, 690–692.

Kersters, K., Ludwig, W., Vancanneyt, M., De Vos, P., Gillis, M. & Schleifer, K.-H. (1996). Recent changes in the classification of the *Pseudomonads*: An overview. *Systematic and Applied Microbiology* **19**, 465–477.

Kessler, B. & Witholt, B. (2001). Factors involved in the regulatory network of polyhydroxyalkanoate metabolism. *Journal of Biotechnology* **86**, 97–104.

Kessler, B. & Palleroni, N. J. (2000). Taxonomic implications of synthesis of poly-beta-hydroxybutyrate and other poly-beta-hydroxyalkanoates by aerobic *pseudomonads*. *International Journal of Systematic and Evolutionary Microbiology* **50**, 711–713.

Khanna, S. & Srivastava, A. K. (2005). Recent advances in microbial polyhydroxyalkanoates. *Process Biochemistry* **40**, 607–619.

Kim, D. Y., Kim, H. W., Chung, M. G. & Rhee, Y. H. (2007). Biosynthesis , modification , and biodegradation of bacterial medium-chain-length polyhydroxyalkanoates. *The Journal of Microbiology* **45**, 87–97.

Kobayashi, T., Shiraki, M., Abe, T., Sugiyama, A. & Saito, T. (2003). Purification and properties of an intracellular 3-hydroxybutyrate-oligomer hydrolase (PhaZ2) in *Ralstonia eutropha* H16 and its identification as a novel intracellular poly(3-hydroxybutyrate) depolymerase. *Journal of Bacteriology* **185**, 3485–3490.

Koller, M. (2001). Polyhydroxyalkanoates: Fermentation strategies for quality improvement and new isolation methods. *Diploma Thesis.* Graz University of Technology.

Koller, M., Salerno, A. & Dias, M. (2010). Modern biotechnological polymer synthesis: A review. *Food Technol Biotechnol* **48**, 255–269.

Kranz, R. G., Gabbert, K. K. & Madigan, M. T. (1997). Positive selection systems for discovery of novel polyester biosynthesis genes based on fatty acid detoxification. *Applied and Environmental Microbiology* **63**, 3010–3013.

Kueng Walter. **(1982).** Wachstum und Poly-D(-)-3-Hydroxy-Buttersaeure-Akkumulation bei *Alcaligenes latus*. *Diploma Thesis*. Graz University of Technology.

Kögl, F. & Postowshy, J. J. (1930). Über das grüne Stoffwechselprodukt des *Bacillus chlororaphis*. *Justus Liebigs Annalen der Chemie* **480**, 280–297.

Lageveen, R. G., Huisman, G. W., Preusting, H., Ketelaar, P., Eggink, G. & Witholt, B. (1988). Formation of polyesters by *Pseudomonas oleovorans*: Effect of substrates on formation and composition of poly-(R)-3-hydroxyalkanoates and poly-(R)-3-hydroxyalkenoates. *Applied and Environmental Microbiology* **54**, 2924–2932.

Laursen, J. B. & Nielsen, J. (2004). Phenazine natural products: Biosynthesis, synthetic analogues, and biological activity. *Chemical Reviews* **104**, 1663–86.

Lemoigne, M. (1926). Produits de deshydration et de polymerisation de l'acide b-oxybutyric. *Bull Soc Chem Biol* **8**, 770–782.

Ma, F. & Hanna, M. A. (1999). Biodiesel production : A review. *Bioresource Technology* **70**, 1–15.

Marsalek Lukas. **(2011).** Production of polyhydroxyalkanoates by *Pseudomonas putida* strains using alternative raw materials. *Diploma Thesis*. Masaryk University.

Martin, D. P. & Williams, S. F. (2003). Medical applications of poly-4-hydroxybutyrate: a strong flexible absorbable biomaterial. *Biochemical Engineering Journal* **16**, 97–105.

Mavrodi, D. V., Peever, T. L., Mavrodi, O. V., Parejko, J. a, Raaijmakers, J. M., Lemanceau, P., Mazurier, S., Heide, L., Blankenfeldt, W. & other authors. **(2010).** Diversity and evolution of the phenazine biosynthesis pathway. *Applied and Environmental Microbiology* **76**, 866–79.

Merrick, J. M. & Doudoroff, M. (1964). Depolymerization of poly-ß-hydroxybutyrate by an intracellular enzyme system. *Journal of Bacteriology* **88**, 60–71.

Migula, W. (1894). Über ein neues System der Bakterien. *Arbeit Bakteriol Inst Karlsruhe* **1**, 235–328.

Mittelbach, M. (unpublished data). Renewable Resources Group, Institute of Chemistry, Karl-Franzen-University Graz.

Mittelbach, M. & Remschmidt, C. (2004). *Biodiesel the comprehensive handbook*, 1st ed. Martin Mittelbach.

Moore, E. R. B., Mau, M., Arnscheidt, A., Böttger, E. C., Hutson, R. a., Collins, M. D., Van De Peer, Y., De Wachter, R. & Timmis, K. N. (1996). The determination and comparison of the 16S rRNA gene sequences of species of the genus *Pseudomonas* (sensu stricto) and estimation of the natural intrageneric relationships. *Systematic and Applied Microbiology* **19**, 478–492.

Muhr, A., Rechberger, E. M., Salerno, A., Reiterer, A., Schiller, M., Kwiecien, M., Adamus, G., Kowalczuk, M., Strohmeier, K. & other authors. **(n.d.).** Biodegradable latexes from animal-derived waste: Biosynthesis and characterization of *mcl*-PHA accumulated by *Ps. citronellolis*. *Reactive and Functional Polymers*.

Palleroni, N. J., Kunisawa, R., Contopoulou, R. & Doudoroff, M. (1973). Nucleic acid homologies in the genus Pseudomonas. *International Journal of Systematic Bacteriology* **23**, 333–339.

Palleroni, N. J. (2010). The *Pseudomonas* story. *Environmental Microbiology* **12**, 1377–83.

Peix, A., Valverde, A., Rivas, R., Igual, J. M., Ramirez-Bahena, M.-H., Mateos, P. F., Santa-Regina, I., Rodriguez-Barrueco, C., Martinez-Molina, E. & Velazquez, E. (2007). Reclassification of *Pseudomonas aurantiaca* as a synonym of P*seudomonas chlororaphis* and proposal of three subspecies, *P. chlororaphis* subsp. *chlororaphis* subsp. nov., *P. chlororaphis* subsp. *aureofaciens* subsp. nov., comb. nov. and *P. chlororaphis* subsp. *aurantiaca* subsp. nov., comb. nov. *International Journal of Systematic and Evolutionary Microbiology* **57**, 1286–1290.

Philip, S., Keshavarz, T. & Roy, I. (2007). Polyhydroxyalkanoates : biodegradable polymers with a range of applications. *Journal of Chemical Technology and Biotechnology* **82**, 233–247.

Pierson, L. S. & Pierson, E. A. (2010). Metabolism and function of phenazines in bacteria: Impacts on the behavior of bacteria in the environment and biotechnological processes. *Applied Microbiology and Biotechnology* **86**, 1659–1670.

Rai, R., Keshavarz, T., Roether, J. A., Boccaccini, A. R. & Roy, I. (2011). Medium chain length polyhydroxyalkanoates, promising new biomedical materials for the future. *Materials Science and Engineering R* **72**, 29–47.

Rehm, B. H. A., Krüger, N. & Steinbüchel, A. (1998). A new metabolic link between fatty acid *de novo* synthesis and polyhydroxyalkanoic acid synthesis. *Journal of Biological Chemistry* **273**, 24044–24051.

Rehm, B. H. a. **(2003).** Polyester synthases: Natural catalysts for plastics. *The Biochemical Journal* **376**, 15–33.

Ruth, K., de Roo, G., Egli, T. & Ren, Q. (2008). Identification of two acyl-CoA synthetases from *Pseudomonas putida* GPo1: One is located at the surface of polyhydroxyalkanoates granules. *Biomacromolecules* **9**, 1652–9.

Sadouk, Z., Tazerouti, A. & Hacene, H. (2009). Biodegradation of diesel oil and production of fatty acid esters by a newly isolated *Pseudomonas citronellolis* KHA. *World Journal of Microbiology and Biotechnology* **25**, 65–70.

Schwartz, R. D. (1973). Octene epoxidation by a cold-stable alkane-oxidizing isolate of Pseudomonas oleovorans. *Applied Microbiology* **25**, 574–7.

Schwartz, R. D. & Mccoy, C. J. (1976). Synthesis of enzymatic epoxidation: Synthesis of 7,8-epoxy-1-octene, 1,2-7,8-diepoxyoctane, and 1,2-epoxyoctane by *Pseudomonas oleovorans*. *Applied and Environmental Microbiology* **31**, 2–7.

Schwartz, R. D. & McCoy, C. J. (1973). *Pseudomonas oleovorans* hydroxylation-epoxidation system: Additional strain improvements. *Applied Microbiology* **26**, 217–218.

Seubert, W. (1960). Degradation of isoprenoid compounds by microorganisms I., *Pseudomonas citronellolis* n. sp: Isolation and characterization of an isoprenoid-degrading bacterium. *Journal of Bacteriology* **79**, 426–434.

Singh, A. K. & Mallick, N. (2008). Enhanced production of *scl-lcl*-PHA co-polymer by sludge-isolated *Pseudomonas aeruginosa* MTCC 7925. *Letters in Applied Microbiology* **46**, 350–357.

Smits, T. H., Röthlisberger, M., Witholt, B. & van Beilen, J. B. (1999). Molecular screening for alkane hydroxylase genes in Gram-negative and Gram-positive strains. *Environmental microbiology* **1**, 307–17.

Stanier, R. Y., Palleroni, N. J. & Doudoroff, M. (1966). The aerobic *Pseudomonas*: A taxonomic study. *Journal of General Microbiology* **43**, 159–271.

Steinbüchel, A. & Valentin, H. E. (1995). Diversity of bacterial polyhydroxyalkanoic acids. *FEMS Microbiology Letters* **128**, 219–228.

Sudesh, K., Abe, H. & Doi, Y. (2000). Synthesis, structure and properties of polyhydroxyalkanoates: Biological polyesters. *Progress in Polymer Science* **25**, 1503–1555.

Sun, Z., Ramsay, J. a, Guay, M. & Ramsay, B. a. **(2007).** Fermentation process development for the production of medium-chain-length poly-3-hyroxyalkanoates. *Applied microbiology and biotechnology* **75**, 475–85.

Timm, A. & Steinbüchel, A. (1990). Formation of polyesters consisting of medium-chain-length 3-hydroxyalkanoic acids from gluconate by *Pseudomonas aeruginosa* and other fluorescent *Pseudomonads*. *Applied and Environmental Microbiology* **56**, 3360–3367.

Tobie, W. C. (1945). A proposed biochemical basis for the genus *Pseudomonas*. *Journal of Bacteriology* **49**, 459–62.

Uchino, K., Saito, T., Gebauer, B. & Jendrossek, D. (2007). Isolated poly(3-hydroxybutyrate) (PHB) granules are complex bacterial organelles catalyzing formation of PHB from acetyl coenzyme A (CoA) and degradation of PHB to acetyl-CoA. *Journal of Bacteriology* **189**, 8250–6.

York, G. M., Lupberger, J., Tian, J., Adam, G., Stubbe, J., Sinskey, A. J. & Lawrence, A. G. (2003). *Ralstonia eutropha* H16 encodes two and possibly three intracellular poly[d-(−)-3-hydroxybutyrate] depolymerase genes. *Journal of Bacteriology* **185**, 3788–3794.

Zinn, M., Witholt, B. & Egli, T. (2001). Occurrence, synthesis and medical application of bacterial polyhydroxyalkanoate. *Advanced Drug Delivery Reviews* **53**, 5–21.

Zinn, M., Durner, R., Zinn, H., Ren, Q., Egli, T. & Witholt, B. (2011). Growth and accumulation dynamics of poly(3-hydroxyalkanoate) (PHA) in *Pseudomonas putida* GPo1 cultivated in continuous culture under transient feed conditions. *Biotechnology Journal* **6**, 1240–1252.